Doctoral thesis for a doctoral degree at the faculty of medicine,

Julius-Maximilians-Universität Würzburg,

Department of Internal Medicine I, Section Cardiology/Immunology

Director: Professor Dr. med. Stefan Frantz

Cardiac Antigens and T cell Specificity after Experimental Myocardial Infarction in Mice

-

Kardiale Antigene und T-Zell Spezifität nach experimentellem Myokardinfarkt in Mäusen

submitted by

Chiara Claudia Gaal

from

Bonn

Würzburg 2021

Submitted on:

12.11.2021

First Reviewer: Prof Dr. med. Stefan Frantz

Second Reviewer: PD Dr. med. Niklas Beyersdorf

Dean: Prof. Dr. med. Matthias Frosch

Date of Public Defence:

08.03.2022

Date of Receipt of Certificates:

The doctoral candidate is an approbated physician.

For my family

TABLE OF CONTENTS

1. INTRODUCTION

1.1. Myocardial infarction

1.1.1. Overview

Cardiovascular diseases (CVD) are the leading cause of death in the European Union (over 4 million deaths annually), with devastating individual and economic consequences.[1-3] The most common within the various pathologies subsumed as CVD are atherosclerosis of the coronary arteries and subsequent myocardial infarction (MI).

In the majority of cases MI presents itself with acute pain in the chest and possible radiation to the left arm, neck or epigastrium, shortness of breath and other vegetative symptoms. Electrocardiography, blood work and coronary angiography are the main pillars for diagnosis.

As repeatedly described, MI occurs as the result of insufficient supply of oxygen. A mismatch between the blood supply to the heart over the coronary arteries and the actual demand of the myocardium can be observed. This ischemia can be objectified using electrocardiography. With this tool two different forms can be distinguished, the ST- (STEMI) and non-ST-elevation myocardial infarction (NSTEMI). As opposed to Angina pectoris, both are characterized by rapid cell death and loss of contractile tissue.

The most common reason for MI is the instability and consecutive rupture of atherosclerotic plaques, followed by the release of inflammatory and thrombogenic cytokines, thromboembolic superposition and finally complete coronary insufficiency by endothelial obstruction.

90% of all MI's originate in an unhealthy lifestyle.[4] Primarily the change of this lifestyle shows the highest impact within primary and secondary prevention, resulting in the decrease of the most important risk factors, such as smoking, high blood pressure, high cholesterol, high BMI, low body activity and high stress levels.

Today's medicine focuses on two major aspects: prevention of MI by treating risk factors and treatment of heart failure due to poor healing years after MI.

The adult mammalian heart shows negligible regenerative ability. Therefore, ischemic myocardial injury leads to irreversible loss of contractile tissue, leading to the formation of a collagenous scar and progressive remodeling. [5] It seems crucial that the focus of therapy should shift to the healing phase after MI and foster cardiac repair in order to prevent long term damage.

It is clear that there is a huge potential for researchers of finding more than beneficial ways of treatment. Very early in the 1990s research started indicating an important involvement of the immune system in MI in the course peaking in the notion that T cells are a major player within the cardiac healing process and that there may be a way to influence them.

1.1.2. Progress in treatment

Over the last decades enormous steps towards a better treatment of MI have been made. Focused on the statistical distribution of the mortality rates over time, the first wave occurs during or shortly after MI. Fast diagnosis within the preclinical sector has been optimized over time and therefore the "diagnosis to treatment time" minimized, which has had an imminent consequence on the mortality rate.[6,7] Moreover, the establishment of a standard procedure of treatment with clear instructions concerning the administration of drugs as well as further diagnostical and therapeutical steps has also been important.[3] With the help of electrocardiography and percutaneous intervention methods diagnosis and treatment have been improved drastically resulting in a lowered mortality. [7,8]

The second wave of mortality peaks years later, when patients develop progressive heart failure as a result of the initial infarction.[9] The methods of treatment in this sector have also been improved over time, though not as significantly as monitored for the first wave. To this day the therapy of congestive heart failure turns out to be a very challenging task.

1.1.3. Myocardial infarction triggers heart failure due to poor healing

MI is not only an acute life-threatening condition but proves to be a long-term regenerative challenge for the whole organism. Survivors of the initial ischemic event can develop chronic heart failure due to poor myocardial healing.[9] T cell reactivity may advance myocardial healing by stimulating a reparative fibrosis within the infarcted tissue. Nonetheless a prolonged or augmented reaction can lead to adverse remodeling and therefore the induction of consecutive chronic heart failure.[10] In 2014 in the United States 6.5 million people suffered from heart failure.[11] Statistically MI imposes the most frequent cause of heart failure. Reduction of acute infarct mortality through progress in acute care combined with treatment insufficiency of infarct survivors chronically lead to an increasing heart failure prevalence (**Figure 1**).

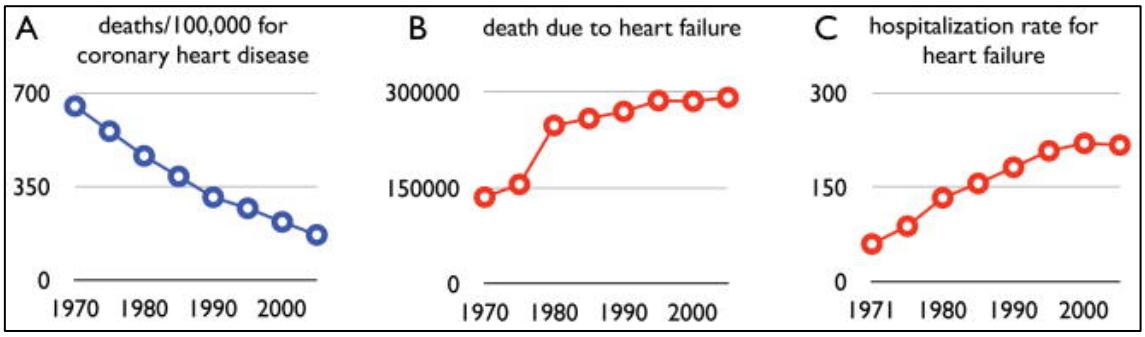

Figure 1 Disease statistics
(**A**) Deaths/100,000 population for coronary heart disease in men, ages 35–74, U.S., 1970–2005.
(**B**) Deaths due to heart failure, U.S., 1970–2005.
(**C**) Hospitalizations/100,000 population for heart failure, age 65 and older, U.S., 1971–2006.
Initially adapted from NHLBI Fact Book 2008; Figure from Nahrendorf et al. [12]

Since MI still constitutes the biggest cause of death in the western world the underlying question here is: How can we identify and subsequently support the group of poor healers in order to support myocardial repair and prevent long term heart failure?

1.1.4. The unmet need in cardiology: Improving scar formation after myocardial infarction

The main concern of our modern medicine is wound healing. A damaged area demands repair. Clinicians are well aware that an open wound needs to be cleansed, closed and treated accordingly. With MI this system seems to be out of order. Today, after MI and the completion of the acute treatment, the patient is left alone in dealing with the "wound". The notion of the "ischemic myocardial wound" as a potential therapeutic target has only recently been developing. This is where the standard of procedure should be changed. In order to do that, the healing process after MI must be further investigated to fully understand and possibly manipulate the underlying immune-inflammatory mechanisms.

During and shortly after MI the infarcted area shows a dynamic character. The myocardial infarct size can be progressive for several hours after initial coronary artery occlusion, which is called infarct extension. Thrombolysis and reperfusion techniques can here limit and reduce the damaged area. Within the first weeks, after the initial loss of contractile tissue has stopped, infarct expansion or contraction occurs. This proves to have a tremendous contributing factor on remodeling and therefore overall prognosis.[13] Ventricular dilatation may occur and infarct expansion can find its peak in subacute cardiac rupture and death.

Speaking in the long-term, filling pressure, wall stress and left ventricular volume can increase mediating adverse remodeling, resulting in heart failure and poor prognosis.[14-16] The scar formation, where cardiomyocyte deficiency and an increase of fibroblasts can be observed, consists of the loss of contractile functional myocardial tissue and can lead to geometrical changes that have an adverse effect on cardiac energy consumption and cardiac output.[17] Furthermore, not only the infarcted area of the heart shows structural changes, also border and non-infarcted areas. These adverse structural changes impair cardiac function and can lead to heart failure.[15] MI also leads to increased short- and long-term compensatory regulatory mechanisms. Initially these pose to have a beneficial character, if prolonged, the adverse effects on cardiac function prevail.[18] Conversely, preservation of left ventricular geometry and prevention of heart failure could result from

a sufficient healing. Hence, the quality of infarct healing shortly after myocardial injury is thought to determine the outcome for a patient for years to come.[12] Inhibitors of the angiotensin converting enzyme (ACE) have been shown to have beneficial effects on cardiac function in long-term treatment after MI.[19] The SAVE trial was indeed able to show a mortality reduction from 25 to 20% with ACE inhibitor treatment.[20]
Nevertheless, as of today there is still too little known about the exact processes of cardiac scar formation. Therefore, it is most imperative to fully understand the underlying mechanisms to avoid adverse remodelling and long-term heart failure.

1.1.5. Role of inflammation and immune system

The infarcted myocardium is increasingly being perceived in the aspect of wound healing.[5] In addition to the classic concerns about the hemodynamic condition, the immune-inflammatory phenomena underlying the myocardial healing process have now received attention.[21-24] Though the exact character of their influence being beneficial or destructive is still being discussed.[25,26] This new perspective on the early healing processes after MI shows us new starting points for the treatment of infarction patients.

1.1.5.1. Neutrophils and monocytes/macrophages

The involvement of the innate immune system via neutrophils and monocytes/macrophages in the recovery after MI has already been discussed for some time.[12,27] One of the very first reactions to myocardial injury is the invasion of the cardiac tissue by monocytes/macrophages. They originate from the bone marrow and spleen, where the release has been triggered by chemokine signals or respectively angiotensin originating in the spleen.[28] They support the repair of the myocardium by stimulating the ongoing cardiomyocyte proliferation and neovascularisation.[29] Here the mobilization occurs sequentially with two different monocyte subsets showing divergent and complementary functions. In the first few days after MI in the murine model inflammatory Ly-6C(high) monocytes/macrophages dominate in the infarcted tissue and promote the digestion of damaged tissue by phagocytosis, proteolysis and inflammation.

Afterwards a modulation in chemokine secretion mobilizes rather reparative Ly-6C(low) monocytes/macrophages. Conversely, they show an attenuated inflammatory function, express vascular-endothelial growth factor, promote healing via myofibroblast accumulation, angiogenesis and deposition of collagen.[30-33] Mechanisms similar to that may also apply in humans.[34] Recently is has also been discovered that T cell activity influences monocyte recruitment and macrophage activation.[35]

Overall neutrophils and monocytes/macrophages depict a various field of detrimental as well as favourable effects on the healing myocardium. There have been several attempts in manipulating these effects in order to find methods for fostering the myocardial healing process.[36-38] In the end a controlled inflammation with a certain balance between the different influences is the path to protection against intraventricular thrombi after acute infarction[27], a sufficient scar formation[31] and a suppression of pathological remodelling[33].

1.1.5.2. Recently discovered specific arm in the form of adaptive immune responses

Apart from the innate immune system, increasing amounts of studies have shown an involvement of the adaptive immune system in healing after MI. Especially T-lymphocytes have been observed to facilitate tissue repair in various fields including cardiac healing.[39-42] They are thought to play a key role in the modulation of post-MI, inflammation, healing and remodeling.[22,43-49] This contribution has been investigated in different organism, from zebrafish[42] to mammals[10,44,45,47,50], implying that it is a phenomenon maintained over the course of evolution.

Numerous populations of T-Lymphocytes for instance $CD4^+$ T cells[47], $Foxp3^+$ regulatory T cells (T_{regs})[45], $Foxp3^-$ conventional T-helper cells (T_{conv})[51] and invariant natural killer T (iNKT) cells[52] have been named in their relevance for inflammatory responses after MI and their effect on myocardial healing and remodeling. $Foxp3^+$ regulatory T-cells accelerate the resolution of inflammation and promote extracellular matrix deposition in the myocardial scar. $Foxp3^-$ conventional T-helper cells positively influence the infarcted

myocardial tissue by mechanisms that depend on the extracellular purinergic metabolism.[51]

It is known that cardiac antigens released from necrotic cardiomyocytes are drained to the mediastinal lymph nodes where they are presented to T cells. After priming, they proliferate and in turn migrate into the damaged myocardial tissue and promote tissue repair.[45,47,49,53,54] Accordingly, it has been observed that animals lacking $CD4^+$ T cells show impaired myocardial repair.[45-47] In addition, induction of polyclonal expansion of regulatory T cells [45] or adaptive transfer of myosin-specific $CD4^+$ T cells prior to MI was also found to improve post-MI healing success.

In summary, both salutary effects on early cardiac healing by modulation of macrophage polarization[45], fibroblast activity[53] and extracellular purinergic metabbolism[54] as well as detrimental effects by chronic myocardial T cell activation have been attributed to T cells. A chronic activation has been shown to facilitate the development of adverse remodelling in models of ischemic and stress overload–induced HF[10,55-57].

Finally, the currently available knowledge and research status concerning the effect of T cells after MI shows a broad spectrum of possible outcomes in mice. A meticulous balance and order must be sustained to ensure the best cardiac healing and scar development possible. The manipulation of these processes shows tremendous promise, though must be conducted very carefully i1n order to prevent tipping the scale towards myocardial fibrosis or rupture.

1.2. The antigenic world from a T cell perspective

1.2.1 T cell maturation and development

T cells are part of the adaptive immune system, making them a crucial element within the organism to react to the pathogens in the surrounding world and adapt the immune response accordingly. $CD4^+$ T cells exert a critical function in both cellular and humoral immunity through helper and non-helper cell functions.

Multipotent hematopoietic stem cells that are residing in the bone marrow, are the origin of T cells. After developing to lymphoid progenitor cells, they leave the bone marrow and migrate to the thymus, where the majority of T cell differentiation and maturation takes place. Anatomically speaking, the thymus is divided into an outer cortex and an inner medulla. The thymus contains many dendritic cells, which present a vast variety of peptides to the T cells. T cell progenitors or also referred to as thymocytes, follow different maturation steps to become immune competent T cells.[58] Those express a T cell receptor on their surface. Due to the ability to distinguish between self and foreign antigens, the TCR can induce through its signalling pathway changes in gene expression, leading to proliferation, cytokine secretion, development of other stimulating factors and differentiation into effector and memory T cells. The binding is characterised by two aspects: Low affinity, increasing the probability of activating encounters, and degeneracy. Structurally the TCR complex consists of two protein chains. Mostly alpha (α) and beta (β) chain, though 5% of the cells have a gamma γ and delta δ chain. Those respectively contain a constant domain C, proximal to the cell membrane and a variable domain V, interacting with the antigen. Furthermore, a transmembrane domain and a c terminal cytoplasmic part. The variable domain again consists of V and J segments for the alpha (α) chain or V, D, and J segments for the beta (β) chain. With even more variable compounds leading to an enormous amount of possible combinations, creating the variability in the T cell repertoire (**Figure 2**).[59]

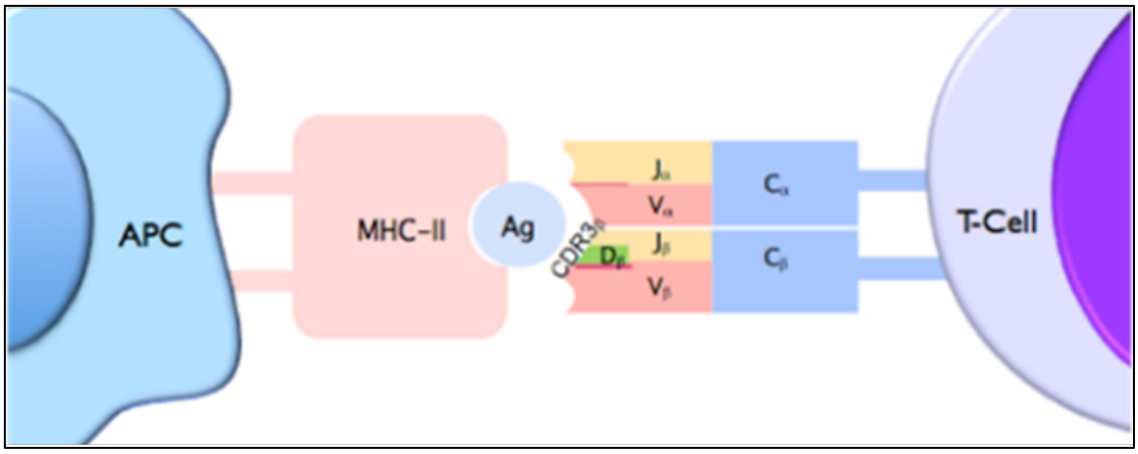

Figure 2 Antigen Presentation

This figure illustrates the antigen presentation of the antigen presenting cell (APC) by MHC-II to the T cell and its T cell receptor (TCR). The TCR is characterized by different sets of subelements: C, J, V, D. During maturation these TCRs are developed to identify a single specific antigen.

The development of T cell receptors can roughly be divided into three stages. First, they neither express CD4 nor CD8 on their surface, double negative (DN) thymocytes, then they express both. The double positive (DP) thymocytes undergo positive and negative selection resulting in the commitment to either the $CD4^+$ or $CD8^+$ lineage.[60] The amount of available T cell receptors is drastically decimated by the thymic selection process. Roughly fifty million double positive thymocytes start this process in the murine thymus[61], whereas already 90% of those are neglected and degrade due to a useless TCR. Contingent for positive selection are permissive interactions with an APC type called cortical thymic epithelial cells (cTECs). These cells build an improved three-dimensional microenvironment in the cortex enabling intimate interactions with DN and DP thymocytes and have a unique capability of processing antigens.[60] Most likely this is bestowed upon the proteolytic pathway resulting in a distinct peptide-MHC (pMHC) ligandome unlike those of any other thymic or peripheral APC.[62] A peptide-MHC ligandome is the repertoire of peptides that are bound by MHC molecules. Concerning MHC-II antigen presentation a special lysosomal protease cathepsin L and thymus-specific serine protease (TSSP) are expressed by the cTECs, crucial for the process of positive selection. The $CD4^+$ T cell thymic repertoire is significantly reduced in cathepsin L-deficient mice.[63] TSSP-deficient mice on the other hand display a faulty positive selection of certain transgenic TCRs and show altered antigen specific CD4+ T cell

responses although their polyclonal CD4+ T cell numbers are normal.[64] Furthermore cTECs characteristically show an unusually high rate of constitutive macroautophagy, the endogenous way of loading of MHC-II with peptides.[65] This process is the key shaping factor of the cTECs MHC-II ligandome.[66] In the cortex the receptors with the highest affinity and therefore efficiency are selected and amplified. Positive and negative selection both result from the strength of the TCRs interaction with self-peptideMHC expressed in the thymic medulla. Weak self-interactions are supported by fostering cell amplification and development into either $CD4^+$ or $CD8^+$ cells, marking the positive selection process.

The last differentiation step of negative selection includes the now single positive (CD4 or CD8) thymocytes to enter the thymic medulla, although a substantial fraction of negative selection is to be found to occur in the cortex as well. The presentation of autoantigens by medullary thymic epithelial cells (mTECs), dendritic cells or macrophages to the thymocytes, marks this step and leads conversely to cell apoptosis by clonal deletion, if a strong interaction of the TCR with autoantigens presented by self-pMHC is noted.[60,67] The thymic medulla is essential due to two characteristics: expression of normally rigorously tissue-restricted antigens (TRA) by mTECs and hematopoetic APCs.[60] mTECs show a dual role in the tolerization process of the T cell repertoire, as antigen providers and also as presenters. Both DCs and mTECs have been shown to contribute to negative selection without redundancy giving the single positive (SP) thymocytes possibility to engage in multiple contacts. After the negative selection process some very few cells with a moderate autoantigenic affinity survive and develop to be $Foxp3^+$, $CD4^+$ regulatory T cells (T_{regs}).[68] The rest with higher affinity is sorted out, whereas the TCRs with no or low to none reaction to self-pMHC are selected and further proliferated.

Finally, after successful recombination the T cells exhibit an antigen specific T cell receptor (TCR).[69] This TCR is comprised of an α and a β chain (TRA and TRB), each chain in turn consisting of several gene segments. Further selection and rearrangement follow. If this course is disturbed at any given point or cannot be successfully finished, T cell apoptosis is induced in order to develop only functional T cells. This thymic selection process contributes to a highly differentiated and diverse TCR repertoire. Nevertheless,

it can still contain minimal amounts of nonfunctional or autoreactive receptors. The majority of thymocytes die in the course of T cell maturation, though if passed embody immune competent, mature T cells, ready to target specific antigens.[70]

1.2.2. Antigen processing and presentation

For the key elements of the adaptive immune system to properly function, a previous antigen processing and presentation has to have taken place. Antigen processing and presentation occurs all over the body in every tissue and organ. Antigen presenting cells, on contact with proteins, bacteria or other cells and their molecules, phagocyte those and present them with the help of protein complexes on their surface to the immune system. In general, two major histocompatibility complexes are important for antigen presentation. The major-histocompatibility-complex I (MHC-I) for endogenous, MHC-II for presentation of exogenous antigens uptaken by phagocytosis or pinocytosis.

CD4+ T cells show an interaction of the T cell receptors (TCRs) recognizing epitopes presented on MHC-II complexes. Engaging simultaneously with protein fragment and MHC is called MHC restriction and was first described by Zinkernagel and Doherty in 1974.[71] $CD8^+$ T cells are restricted to MHC-I and $CD4^+$ T cells to MHC-II. Only antigen presenting cells (APCs), which include dendritic cells (DC), macrophages and B Cells, express MHC-II. They process peptides originating from extracellular sources or from proteins degraded by the endocytic pathway.[72,73] These proteins are processed in the proteasome into small peptide fragments and bound to MHC-II in the endoplasmic reticulum (ER). Those are transported to the cell membrane and present their peptide fragments to $CD4^+$ T cells and consequently activate them. This succeeds only if the T cell Receptor (TCR) of the corresponding $CD4^+$ T cell matches the peptide being presented. T cells generally circulate within the organism, but the process of antigen presentation and activation occurs mainly in the secondary lymphoid organs.

On the surface of all nucleated cells MHC-I molecules are present. Peptides within the cytosol of the cell are being processed in the proteasome and in the endoplasmic reticulum (ER), moved through the Golgi apparatus to the cell surface and presented as

short peptides bound to MHC-I. Here mainly endogenous peptides are presented for the immune system to distinguish between endogenous and healthy and exogenous and therefore potentially dangerous cells that need to be eliminated. Since viral proteins or other extracellular antigens are found in the cytosol as well, they are also presented on MHC-I. This process called cross-presentation enables the $CD8^+$ T cells to examine the intracellular proteome of the cell for any signs of infection or even malignancy. The presentation occurs between the antigen presenting cell (APC) and $CD8^+$ T cell.

In the human organism MHC molecules are termed human leukocyte antigen (HLA) and are subdivided into classes corresponding the MHC-I (HLA-A, -B, -C) and MHC-II (HLA-DP, -DM, -DQ, -DR). The genes encoding for these proteins are found on chromosome 6 of the human genome.[67] Since this study is based on a murine model further emphasis is kept on MHC.

1.2.3 T cell priming and phenotypic plasticity

T cells generally circulate, but the process of antigen presentation and activation occurs mainly in the secondary lymphoid organs. The T cell priming marks an essential step within the preparation for an adequate immunological response. After T cell generation in the bone marrow and maturation within the thymus, T cells constantly circulate through blood and lymphatic system. They enter from the vascular system into the lymph nodes via high endothelial venules, circulate within the lymph node between T-Zone and B-Zone to facilitate antigen presentation and leave the lymph node via efferent lymph vessels, which all join in the thoracic duct and lead to a reentry into the vascular system. The circle closes on return to the lymph nodes. Without yet encountering their antigen (Ag) circulating T cells are called naïve T cells. This recirculation process is essential to increase the number of possible encounters of rare antigen specific, naive T cells with new antigens. “T cell priming” marks the first activation of T cells with their corresponding antigen. Dendritic cells (DCs) are the main antigen presenting cells involved in $CD4^+$ T cell priming. During an infection or inflammation DCs phagocyte, process and present involved antigens mainly on MHC-II molecules. Three key signals are required for the T

cell priming process: The TCR-peptide/MHC-II (pMHC-II) interaction provides the first signals resulting in the downstream signaling pathway activation of the TCR complex.[74] The second signal is mediated by co-stimulatory molecules like B7 (CD80/CD86) on APCs and their interaction with their respective ligands, like CD28, on T cells.[67,75] Finally, the third signal is predominantly relying on APC's secreting cytokines like interferons (IFNs) or interleukin (IL)-12.[76,77] Multiple possibilities of specific transcription factor and cytokine expression generate a great heterogeneity, hallmark of $CD4^+$ T cell pools (See **Figure 3**). Generally speaking, the priming itself also occurs in three stages: During the initial activation phase numerous transient encounters between naïve T cells and dendritic cells happen transitioning into a secondary phase of more stable and long-lasting contacts adding up to an increased cytokine production of interleukin-2 and interferon-gamma. Finally, a phase of high motility and rapid proliferation follows.[78] The activation and differentiation happen into different forms of T effector cells or T helper cells. Those are, in contrast to naïve T cells, able to invade inflamed tissue and modulate the immunological on-site response. Autoreactive T cells are eliminated as well as the ones with low affinity binding T cell receptors (TCR). All resulting in a high number of largely differentiated T cell receptors, primed to recognize specific antigens, therefore leading to large pools of antigen-specific effector and memory T cell subsets.[67]

1.2.4. T cell subsets

In response to TCR engagement $CD4^+$ and $CD8^+$ T cells become activated in secondary lymphoid organs and develop into different subsets, which has been illustrated in **Figure 3**. By conventional T cells (T_{conv}) a group of T cell subsets with pro inflammatory function, such as $CD8^+$ cells but also $CD4^+$ Th_1, Th_2, Th_9, Th_{17} and T_{FH} cells are subsumed. As elaborated before, $CD8^+$ cells interact with peptides presented on MHC-I and differentiate into cytotoxic T cells, that secret perforin, granzymes and granulysin in order to induce the apoptosis of target cells and lead the defence against intracellular pathogens, viruses and malignant cells. Conversely, $CD4^+$ cells interact with peptides presented on MHC-II and develop depending on the polarizing cytokine milieu into

different subsets with individual effector molecules and functions. The differences are not surprising since the differentiation inducing cytokines can range e.g. from the proinflammatory cytokine IFN-γ to TGF-ß an anti-inflammatory cytokine (**Figure 3**). Towards a Th_1 differentiation IL-12 and IFN-γ are required. IFN-γ secretion modulates the activation of macrophages and their differentiation and thereby leads the defence against intracellular pathogens. Th_2 cells can on the other hand secret IL-4, IL-5 and IL-13 and induce B cell activation and proliferation by secretion of growth factors as well as stimulate a class switch of B cells towards IgE. They are prone to develop on stimulation with IL-4. Furthermore, Th_{17} cells can be characterized by a polarization through IL-6 and TGF-β leading to a secretion of IL-17, which promotes neutrophil production and recruitment and therefore an increased defence against extracellular bacteria and fungi.[67,79]

Th_9 cells develop by stimulation through IL-4 and TGF-β and in turn promote responses mediated by eosinophils, mast cells and basophils e.g. against helminth infections by IL-9 secretion.

Continuing with T_{FH} cells, which are produced in the presence of IL-6 and IL-21 and help in B cell differentiation, affinity maturation and isotype switching through IL-4, IL-21 and IFN-γ secretion.[67,79]

Apart from conventional T cells another class of $CD4^+$ T cells called regulatory T cells (T_{regs}) can be distinguished, which exhibit mainly immunoregulatory features. Characteristically the surface protein CD25 can be found on T_{regs}[80] and their foremost expressed transcription factor is forkhead box protein 3 (Foxp3). Foxp3 is a crucial factor in modulating the developmental and suppressive function of T_{regs}.[81,82] Two different regulatory T cells can be differentiated: thymus derived, naturally occurring regulatory T cells (tT_{regs}) and peripheral regulatory T cells (pT_{regs}).[83] Differentiation towards pT_{regs} occurs through activation by TGF-β and retinoid acid combined with the absence of pro inflammatory cytokines e.g. IL-6.[84]

Regulatory T cells are the main protagonist in the controlling and suppression of the immune system. This is stressed by the development of autoimmune disease in T_{reg} depleted mice.[85] Secreted IL-10, TGF-β, IL-35 and galectin-3 by T_{regs} exert mediatory

function towards many cells within the immune system including dendritic cells and interfere with a sufficient T cell activation.[86,87]

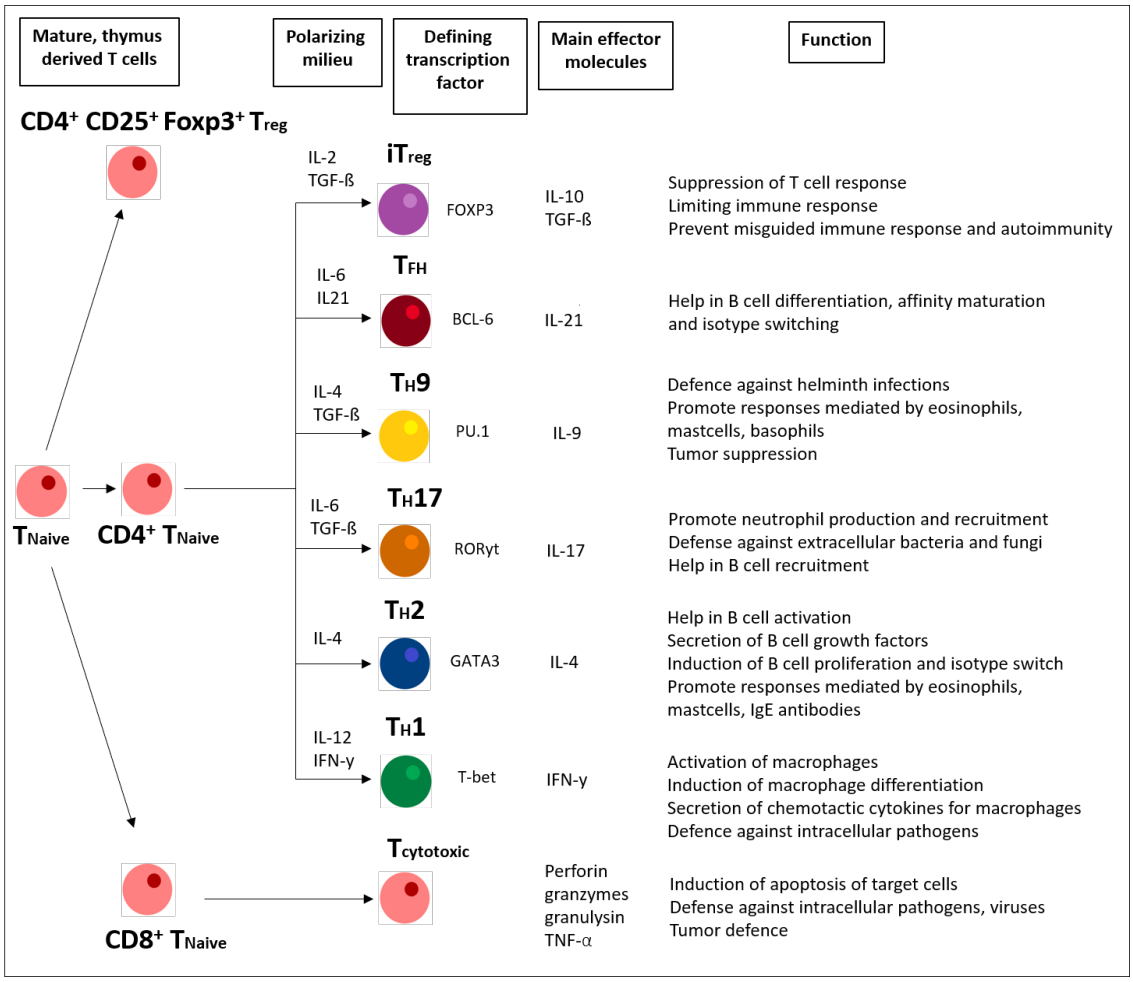

Figure 3 T cell subset maturation and differentiation
In the thymus naïve T cells develop into both naïve $CD8^+$ and $CD4^+$ T cells as well as naturally occurring $Foxp3^+$ regulatory $CD4^+$ T cells. After T cell priming the differentiation depends substantially on the polarizing cytokine milieu. Naive $CD4^+$ T cells can differentiate into effector T cells such as T helper type 1 (Th1) cells,Th2 cells, Th9 cells, Th17 cells, and follicular helper T (TFH) cells, or develop into regulatory T cells such as peripherally induced $Foxp3^+$ Treg cells. All cell types show a distinct set of functions. The figure content is based on [67,79]

Antigen specific T cells after MI could be represented by e.g. regulatory T cells or Th_{17} cells, which would imply completely different functions. The exact identification and further characterization of these antigen specific T cell subsets in the future would be essential in trying to modulate the induced responses accordingly.

1.2.5. MHC-restriction, isogenic mouse strains and disease susceptibility

Considering that $CD4^+$ T cell priming is critically dependent on antigen presentation of antigenic peptides in the context of MHC-II molecules, it is important to note that polymorphisms on the MHC-II genes have major impact in defining which antigens turn out to get accessible to T cell priming. The varying expression of haplotypes through different mouse strains presents us with the possibility of a diverse data acquisition and validation. The most commonly used mouse strains in research are Balb/c and C57BL/6J with a corresponding genotype $I\text{-}A^d$ and $I\text{-}A^b$. Since more data can be found on these two strains, a further investigation of their antigen expression can be analyzed against a broader background. On a closer look the different mouse strains show a different disease susceptibility. Immunization with cardiac myosin induces T cell mediated myocarditis in genetically predisposed mice. [88] Balb/c mice are more susceptible to develop experimental autoimmune myocarditis, whereas C57BL/6J mice are not.[89] Furthermore it could be shown that autoimmune myocarditis could be transferred by adoptive cell transfer.[50] All this data suggests some mouse strains to be more susceptible to certain diseases than others. The vast field of different isogenic mouse strains and their corresponding and sometimes contradictory experimental findings impose a big challenge for research, but also display promising new focusing points for further investigation and understanding. Nevertheless, since isogenic mouse strains by definition have the same genotype, the translational meaning of these findings to the human organism and population, exhibiting millions of different genotypes, is still somewhat limited.

1.3. Current predicament

1.3.1. What triggers $CD4^+$ T cell activation after myocardial infarction?

The importance of the immunological response after MI, especially in the context of healing, has recently gained more and more attention. T cells migrate to the heart after infarction. Antigen specificity is a hallmark of T cell responses, but the specificity of T cell

responses caused by myocardial damage remains largely unknown. Do we search for a general inflammatory cytokine mediated phenomenon? Or could the T cell response after MI be antigen-specific, even heart-specific? And what would this cardiac specificity mean? What do cardiac antigens entail? Are there antigens that are solely present in the heart and nowhere else? What could be putative candidates? So far, no study could clearly provide answers to these questions. In particular, it is unclear whether lymphocytes respond to specific cardiomyocyte components (e.g. myosin, troponin).[49]
All in all, the combination of a hypothesis driven approach and a broad unbiased screening should lead to a definitive mapping of cardiac antigens that trigger post-MI $CD4^+$ T cell responses for the first time. We expect this approach to help us:

1) develop new tools to monitor heart-specific T cell responses in infected mice, and
2) identify new targets for specific immunotherapies to improve myocardial repair.

The results obtained from the planned mouse experiments may then be transferred to humans in a further step and verified or adapted. These experiments are a prerequisite to better understand cardiac healing, to develop new diagnostic and therapeutic approaches and clarify the overarching question: Are post-MI T cell responses directed to heart antigens and if yes, which exactly?

1.4. Aims

The first objective is to perform extensive cardiac epitope mapping of two different mouse strains, expressing different MHC haplotype ($I\text{-}A^d$, $I\text{-}A^b$) via in silico predictions. Resulting in the design of a comprehensive panel of MHC-II restricted cardiac epitopes that could be putative antigens, relevant in the immune inflammatory processes after MI.
The second objective is consecutively to test this panel of both haplotypes ($I\text{-}A^d$, $I\text{-}A^b$) by in vitro T cell proliferation and antigen recall assays to identify those antigens that trigger T cell activation in an experimental myocardial infarction (EMI) model ex vivo.
The third objective is to develop new tools in the form of T cell hybridomas to monitor the activity of heart-specific T cells in vivo and thereby analyze their functional relevance in post-MI.

2. MATERIAL

2.1. Fine chemicals, drugs and reagents

The chemicals and reagents listed below were used in the experiments of this thesis. All substances were acquired from:
Bayer AG (Leverkusen, Germany), B.Braun Melsungen AG (Melsungen, Germany), Carl Roth GmbH (Karlsruhe, Germany), Merck (Darmstadt, Germany), Morphisto GmbH (Frankfurt am Main, Germany), Ratiopharm (Ulm, Germany), Sakura Finetek (Torrance, USA), Sigma-Aldrich (Steinheim, Germany), VWR International (Radnor,USA)

Aqua ad iniectabilia	2-Methyl-butan
Aqua destillata	Mowiol
BSA (Bovine serum albumin)	2-Propanol
Buprenorphin	PSR-staining solution
DMSO	Rotihistol A+B
Ethanol	Siriusred (Direct Red 80)
Ethanol denatured >99,6%	Trypan blue
Formalin solution, buffered10%	Tween 20
Heparin-Natrium 25000	Xylol
Isoflurane	

2.2. Buffers, solutions, liquids

BSS/(BSA)	KCl	5.33 mM
	$KH_2 PO_4$	0.44 mM
	NaCl	138.0 mM
	$NaHCO_3$	4.0 mM
	Na_2HPO_4	0.3 mM
	(BSA)	(5%)
Erythrocyte-Lysis Buffer	Aqua ad inj.	90%
	Ery. Lysis	10%
Ethanol 70%	Aqua ad inj.	30%
	Ethanol	70%

FACS buffer	NaCl (pH 7.4)	137.0 mM
	Na_2HPO_4	10.0 mM
	KCl	2.6 mM
	$KH_2\ PO_4$	1.8 mM
	BSA	0.1%
	NaN_3	0.1%
Dulbecco's PBS	NaCl (pH 7.4)	137.0 mM
	Na_2HPO_4	10.0 mM
	KCl	2.6 mM
	$KH_2\ PO_4$	10.0 mM
Picro-sirius red	Picric acid	1.5%
	Sirius red	0.1%
Tween-PBS	Tween 20	0,05%
	PBS	99,95%

2.3. Ready to use kits and solutions

Kit/Solution	Supplier
CTL Wash Buffer	CTL Europe (Bonn, Germany)
CTL Test Buffer	CTL Europe (Bonn, Germany)
Elispot Kit	CTL Europe (Bonn, Germany)
Freezing Media Kit (Cryo ABC)	CTL Europe (Bonn, Germany)
Legendplex Mouse Th1/Th2 panel Kit (8-plex)	BioLegend (San Diego, USA)
PBS Dulbecco w/o Ca2+ w/o Mg2+	Sigma-Aldrich (Steinheim, Germany)
RPMI	Gibco/Life Technologies (Carlsbad, USA)

2.4. Antibodies, biomolecules and compounds

Single Peptides (see Antigen atlas)	Jpt peptide technologies (Berlin, Germany)
Peptide Pools (see Antigen atlas)	Jpt peptide technologies (Berlin, Germany)
CD3/28 beads	ThermoFisher Scientific (Waltham, USA)
$Myhca_{614-628}$ peptide	ThermoFisher Scientific (Waltham, USA)
$Ovalbumin_{323-339}$ peptide	Sigma-Aldrich (Steinheim, Germany)
anti-CD4 (clone RM4-5)	Biolegend (San Diego, USA)
anti-CD45 (clone 30F11)	Biolegend (San Diego, USA)
anti-TCRβ (clone H57-597)	Biolegend (San Diego, USA)

2.5. Consumables

Centrifuge tubes (50ml, 15ml)	Greiner (Frickenhausen, Germany)
Combitips (5 ml, 2.5 ml, 1ml)	Eppendorf (Hamburg, Germany)
CPT-tubes	BD Bioscience (Franklin Lakes, USA)
Cryo tube (1.8ml)	ThermoFisher Scientific (Waltham, USA)
Entellan	Merck (Darmstadt, Germany)
FACS tubes	BD Bioscience (Franklin Lakes, USA)
Filter pipette tips (10µl, 100µl, 200µl, 1000µl)	Sarstedt AG & Co. KG (Nümbrecht, Germany)
Needles (25G and 19G)	B.Braun Melsungen AG (Melsungen, Germany)
Nitrile gloves	Paul Hartmann AG (Heidenheim an der Brenz, Germany)

Parafilm	American National Can (Greenwich, USA)
PCR tubes (0.2 ml)	Eppendorf (Hamburg, Germany)
Platesealer Easyseal	Greiner (Frickenhausen, Germany)
Pipette tips (20µl, 300µl, 1000µl)	Eppendorf (Hamburg, Germany)
Pipette (5ml, 10ml, 25ml)	Greiner (Frickenhausen, Germany)
Pre-Separation mesh Filters (30µm)	Miltenyi Biotec (Bergisch Gladbach, Germany)
Reagent Reservoir (25 ml)	ThermoFisher Scientific (Waltham, USA)
Scalpel	Hartenstein (Würzburg, Germany)
Sterillium	Bode Chemie (Hamburg, Germany)
Suture Silk Black 6/0	FSSB GmbH (Jestetten, Germany)
Syringe (2ml)	BD Bioscience (Erembodegem, Belgium)
Terralin®	Schülke (Norderstedt, Germany)
TissueTek®	Sakura Finetek (Torrance, USA)
96-well Maxisorp Nunc-Immuno-plate	ThermoFisher Scientific (Waltham, USA)
96-well plates (V-bottom, U-bottom)	Greiner (Frickenhausen, Germany)

2.6. Devices and instruments

Analytical balance	Kern&Sohn (Balingen, Germany)
Attune NxT Flow Cytometer	BD Biosciences (Erembodegem, Belgium)
BD FACS Aria III	BD Biosciences (Erembodegem, Belgium)
Calculator	Casio (Tokyo-Shibuya, Japan)
Centrifuge Mikro 200	Hettich (Tuttlingen, Germany)
Centrifuge 420R	Hettich (Tuttlingen, Germany)
Cryotom CM1850	Leica (Wetzlar, Germany)
Cryo 1°C Freezing Container, Nalgene	Sigma-Aldrich (Steinheim, Germany)
Incubator, Hera cell 240i	ThermoFisher Scientific (Waltham, USA)
Isoflurane Vaporizer	Harvard Apparatus (Holliston, USA)
Laminar flow hood	Steril S.p.A.
Magnetic stirrer	IKA®-Werke (Staufen-Germany)
Manual Counter	Sport Thieme (Grasleben, Germany)
Microscope DMi1	Leica (Wetzlar, Germany)
Multichannel pipette (300 µl)	Eppendorf (Hamburg, Germany)
Multipette stream	Eppendorf (Hamburg, Germany)
Neubauer Chamber	Optik Labor (Lancing, UK)
Pipettes	Eppendorf (Hamburg, Germany)
Pipette controller	Brand (Wertheim, Germany)
Plate shaker	Heidolph (Schwabach, Germany)
Refrigerators	Liebherr (Bulle, Switzerland)
Surgical instruments	B.Braun Melsungen AG (Melsungen, Germany)
Vortex Mixer	IKA®-Werke (Staufen-Germany)

2.7. Software and electronic data processing

For data acquisition, analysis and presentation the following software was used:

Software	Supplier
BD FACS DivaTM	BD Bioscience (Franklin Lakes, USA)
Elispot, Immunospot Software	CTL Europe (Bonn, Germany)
Legendplex V8.0	Biolegend (San Diego, USA)
Flow Jo V10	Tree Star (Ashland, USA)
Graph Pad Prism 7	GraphPad software (San Diego, USA)
Image J	NIH Softwares (Bethesda, USA)
Legendplex software	BioLegend (San Diego, USA)
Microsoft Office 2016	Microsoft Corporation (Redmond, USA)
PowerPoint Figure Pattern	Motifolio Illustration Toolkit (Maryland, USA)
Thomson EndNote X8	Clarivate Analytics (Philadelphia, USA)

Databases	
Human Protein Atlas	Prosper
IEDB	Uniprot

3. METHODS

3.1. Defining an in-silico cardiac antigen atlas

3.1.1. Cardiac antigens

As of today, a proper definition of the term “cardiac antigen” does not exist. After MI we deem two main groups as sources for cardiac antigens very promising: heart specific proteins and stress-related proteins.

When talking about heart specific proteins, the focus lies on those, released after cardiomyocyte necrosis or apoptosis within the cell loss in the course of MI - mainly motor proteins. A closer look at the cardiac proteome is of essential interest here. All in silico numbers and data were acquired in 11/2017. These numbers are under constant development and change as the field progresses. The analysis of the cardiac transcriptome (**Figure 4**) demonstrates a 63% expression of all human proteins(n=19628) in the heart. On a closer look, 201 of these genes have compared to other tissue types an elevated expression in the heart. They mostly consist of genes coding for proteins of cytoplasm and various regions of the sarcomeres, all related to muscle contraction, ion transport and ATPase activity. Further analyses showed that 82% of the mRNA molecules derived from heart tissue correspond to housekeeping genes and only 13% of the mRNA pool corresponds to genes categorized to be either heart enriched, group enriched or heart enhanced.[90-92] The highest level of enriched expression in the heart can be found in 12 genes. These are most likely expected to be the source for cardiac antigens. Heart-specific proteins, which are released after cardiomyocyte necrosis, that could be relevant within the antigen presentation and therefore the priming of T cells.

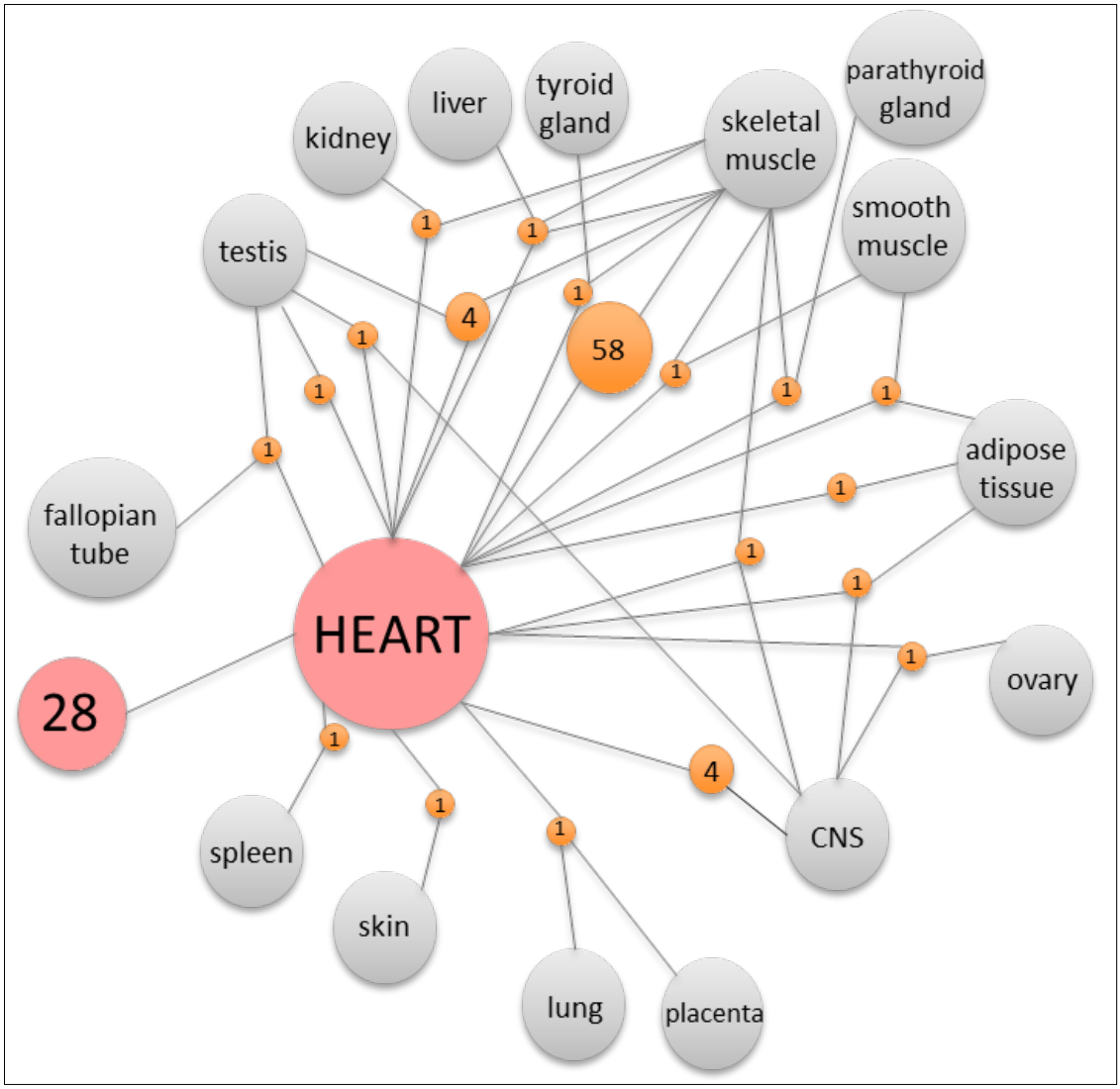

Figure 4 The cardiac transcriptome

An interactive network plot of the heart muscle enriched and group enriched genes connected to their respective enriched tissues (grey circles). Red nodes represent the number of heart muscle enriched genes and orange nodes represent the number of genes that are group enriched. The sizes of the red and orange nodes are related to the number of genes displayed within the node. (Figure adapted from the Human Protein Atlas, 11/2017)

The transformation of arginine residues in proteins into their polar equivalent citrulline is catalyzed by a set of enzymes labelled as peptidyl arginine deiminase (PAD). In patients with rheumatoid arthritis autoreactive T and B cells have been shown to selectively target joint-associated proteins, after enhancement of immune recognition by protein citrullination.[93] PAD enzyme expression mainly occurs by neutrophils, which are the dominant cell type infiltrating the myocardium after infarction. Additionally in some MI patients that show a higher mortality, anti-citrulline antibodies could be found.[94]

Furthermore a relevance of citrullinated fibrinogen as an antigen in the process of rheumatoid arthritis has been shown.[95] For this reason, we believe that these modified proteins can be an important source of MHC-II restricted antigens.

The third group consists of stress-related proteins, which are related to tissue injury in general. Heat-shock proteins (HSP) have an important role controlling immune responses. They are the target for HSP specific T cells, antibodies in healthy subjects and also within autoimmune disorders. Injured myocardial tissue up-regulates the expression of Hsp72, which is targeted by the corresponding Hsp72-specific antibodies. Finally, the pathogenesis of atherosclerosis is also influenced by Hsp60 and Hsp70 specific immune responses. Therefore Hsp-specific T cell responses could be also triggered by MI.

Taking every aspect into account, the group of cardiac antigens originates from a broad mixture of different proteins, all involved in the inflammatory processes during and shortly after MI. Nevertheless, their exact relevance still has to be identified.[90-92,96]

3.1.2. The human protein atlas

The human protein atlas supplied information on every protein of interest about tissue distribution and expression levels in the heart, leading to the selecting of those with the highest tissue specificity to the heart.

3.1.3. Uniprot

For further analysis on epitope presentation we required the FASTA sequence of the putative proteins, which were gathered from www.uniprot.org in 11/2017.[97]

3.1.4. IEDB (Immune epitope database and analysis resource)

The IEDB website (www.iedb.org)[98-101] provided us with a huge database on human and mouse epitopes. It contains information on immune epitopes and the molecular targets of adaptive immune responses, all curated from the available published literature submitted by the National Institutes of Health funded epitope discovery efforts. The IEDB

curation of journal articles has caught up to the present day, starting with articles of 1960, with >95% of relevant published literature manually curated. Together these amount to more than 15 000 journal articles and more than 704 000 experiments to date. With their T cell prediction tools we were able to collect data on peptide binding to MHC-II molecules, focusing on H2-IA^{d} for the Balb/c mouse strain and H2-IA^{b} for the C57BL/6J strain.

The FASTA sequence of our chosen candidate proteins was inserted into the prediction tool and the amino acid sequences were selected that had a high affinity to MHC-II and a high probability of presentation. The 10. percentile was chosen as threshold for the epitope selection. The peptides presented were 15 amino acids long with a central core. Epitopes with a low percentile and low Ic_{50} implicating a high affinity towards MHC-II were selected and in case of overlapping cores combined. Finally, a list of epitopes was obtained from all the different peptides for either the alleles I-A^{b} or I-A^{d}.

The MHC-II binding predictions were made in 11/2017 using the IEDB analysis resource Consensus tool.[102,103]

3.1.5. Prosper - Protease specificity prediction server

Ideally the putative peptide sequence is not targeted by proteases in the myocardium, eliminating any chance of actual presentation by degradation. Thus, all identified sequences were investigated for possible cleaving sites with the prosper database, a protease specificity prediction server. Inserting the FASTA sequence, the program demonstrated the in vivo cleaving sites of numerous proteases. This approach indicated whether other proteases present in the infarcted myocardium (e.g. MMP2, MMP9) can cleave an epitope of interest. Despite the consultation we did not exclude any peptides based on the data we acquired in 11/2017.

3.2. Animal experimentation

3.2.1. Animals

The mice for experimentation were ordered at Charles River. In specific male Balb/c mice and C57BL/6J mice at the age of 7 weeks. The experiments were conducted at the age of 8-10 weeks.

3.2.2. Study approval

All animal procedures have been approved by the local authorities (Regierung von Unterfranken, Germany) and were according to the guidelines of the Federation for Laboratory Animal Science Associations (FELASA). [104,105]

Some experiments were conducted using spleens available from other ongoing experiments in the lab, for the sake of R3.

BALB/C TVA: RUF-55.2.2-2532-2-648

C57BL/6J TVA: RUF-55.2.2-2532-2-1016

3.2.3. Animal facility and keeping

The animals were kept in the animal facility of the DZHI in Würzburg, Germany. The housing conditions correspond to the standards set out in the permits for the facility and are documented using SOPs. The animal facility at the DZHI is an access-controlled rodent husbandry using Type IIL-FilterTop-Makrolon cages. The mice were permanently housed under specific pathogen free conditions (SPF) with a controlled 12-hours light-dark cycle. The cages contain common, low-dust rodent bedding, nesting material and retreat options for the animals. A maximum of 5 animals are kept in a type IIL cage. Special rodent feed for experimental animals is offered ad libitum, as is water in watering bottles.
After delivery, the animals go through an adaptation period of at least one week before any experimental use. They are subjected to a thorough inspection upon delivery and immediately before use. Only animals free of signs of disease are used for experiments.

3.2.4. Experimental myocardial infarction

As described in many publications before, the model of experimental myocardial infarction (EMI) is a well-established laboratory procedure. It is based on the ligation of the left anterior descending (LAD) artery in order to induce permanent ischemia in the heart.

After a short inhalation of isoflurane in a so-called anaesthetic box (5% isoflurane mixed with oxygen), the test animals of both MI and Sham group were intubated and ventilated with a ventilator with isoflurane supply (2% isoflurane mixed with oxygen). The animals were always positioned on a hot plate to avoid dropping of the body temperature and the eyes were protected with an eye protection ointment containing dexpanthenol during the entire procedure. Thoracotomy and ligation of the LAD artery were performed under deep anaesthesia. Without injuring the muscle fibres, the connective tissue between the pectoral and serratus muscle was carefully separated. In-between the 3rd and 4th rib the intercostal muscles were incised, and a tissue tensioner was placed without injuring the ribs to ensure proper vision on the heart. A ligature was then placed around the left coronary artery, the tissue tensioner was removed and the intercostal space between the 3rd and 4th rib was closed with a suture. The muscles were placed in their original anatomical place and reattached with a suture. With surgical sutures the skin was closed and the extubation followed. In the sham group, the animals were operated in an analogous manner, with no coronary artery ligation.

The procedures were carried out under general anaesthesia (2% isoflurane mixed with oxygen) and pre-emptive buprenorphine analgesia (0,1 mg/kg i.p.). Due to its delayed onset of action, buprenorphine was administered 30 minutes before the actual surgical procedure. Up to three days after surgery, the animals were treated with buprenorphine twice a day (0,1 mg/kg i.p.) in accordance with the recommendations of pain therapy in laboratory animals (GV SOLAS, 2015) to ensure optimal pain management. While administering pain medication the animals were scored concerning behaviour and pain. All surgeries were performed by an experienced experimenter, were performed according to the provisions of the Animal Welfare Act and approved by the local authorities (Regierung von Unterfranken).

3.2.5. Endpoint analysis

Endpoints in our experimentation were set at seven days or correspondingly 56 days after EMI. As determined in the TVA, the mice were sedated in a glass jar with dry ice. In the unconscious state the spinal cord was severed at the neck by manual dislocation.
After disinfecting the body, the skin across the chest was cut with sterile scissors in a Y shape to expose the thorax as well as the abdomen. After cutting through the rib cage on either side, the heart was extracted at the stem. A small part of the apex was removed and with that side facing downwards placed on a small amount of Tissue-Tek. The whole heart was then covered in more Tissue-Tek and fixated by pouring 2-Methylbutan on top until fully covered. In a next step, the mediastinal lymph nodes were extracted very carefully, while trying to avoid the removal of any thymus tissue. The mediastinal lymph nodes were placed in a 15 ml Falcon tube with 2 ml of CTL Wash Medium. Last but not least, the spleen was located in the upper left abdomen and cautiously removed, without rupturing the capsule, and placed in a 15 ml falcon tube with 2 ml of CTL Wash Medium as well. After the organ harvest, the remains of the mice were being disposed in a central collection of the facility.

3.3. Cell biology and molecular biology methods

3.3.1. Conventional histology

3.3.1.1. Histological slicing

After the harvesting of the heart and its embedment and fixation in Tissue-Tek, the samples were stored in cryo tubes in -80 °C until final processing.
To slowly increase the temperature the embedded hearts were placed in the Cryotom for 45 min at ~ -23 °C. A cutting thickness of 12 µm was chosen. Per sampled heart two different areas within the infarct zone were sampled each with again 3 cuts to ensure proper analysis. The heart slices were placed on slides and left to dry for about 60-120 min. Finally, they were stored at -20°C until PSR staining several days later.

The remaining heart samples were sealed with more Tissue-Tek and stored at -80°C for later examination.

3.3.1.2. PSR staining

First, the cryo preserved slices were thawed. For that purpose, they were taken out of the -20°C storage and directly placed in buffered formalin for 30 min. Simultaneously, the differently concentrated ethanol solutions were prepared and filled into the corresponding cuvette holders. The cuts were placed for 2 min in Ethanol 50% afterwards for 2 min in Ethanol 75% and finally for 2 min in Ethanol 99% to dry the cut out. 5 min in Xylol/Ethanol 1:1 and 5 min in pure Xylol follow. Subsequently the cuts were placed in Rotihistol for 5 min and then again in another Rotihistol filled cut holder without Xylol contamination. As a final step they were covered with a drop of Entellan and the glass lid was positioned on top of it. The sample is now stained, fixated and ready for analysis. As for Picrosiriusred-Staining, collagen appears red under light microscopy and muscle fibres, cytoplasm and background as yellow. Whereas in polarization microscopy collagen fibres type I (thick fibres) have a yellow-orange and collagen fibres of type III (thin fibres) a green birefringence. The staining solution consists of Siriusred in a saturated aqueous solution of picric acid.

Sirius red is a comparatively large dye molecule that causes an increase in birefringence when it attaches along collagen fibres (optical anisotropy). As a large dye molecule, it diffuses only slowly into denser tissue structures, this enables a short staining time of 1 to 2 h. The staining solution is stable for over a month. Dried picric acid is explosive. [106]

3.3.2. Determination of infarct size

An immediate assessment of the infarct size occurred during the organ extraction (Figure 5).

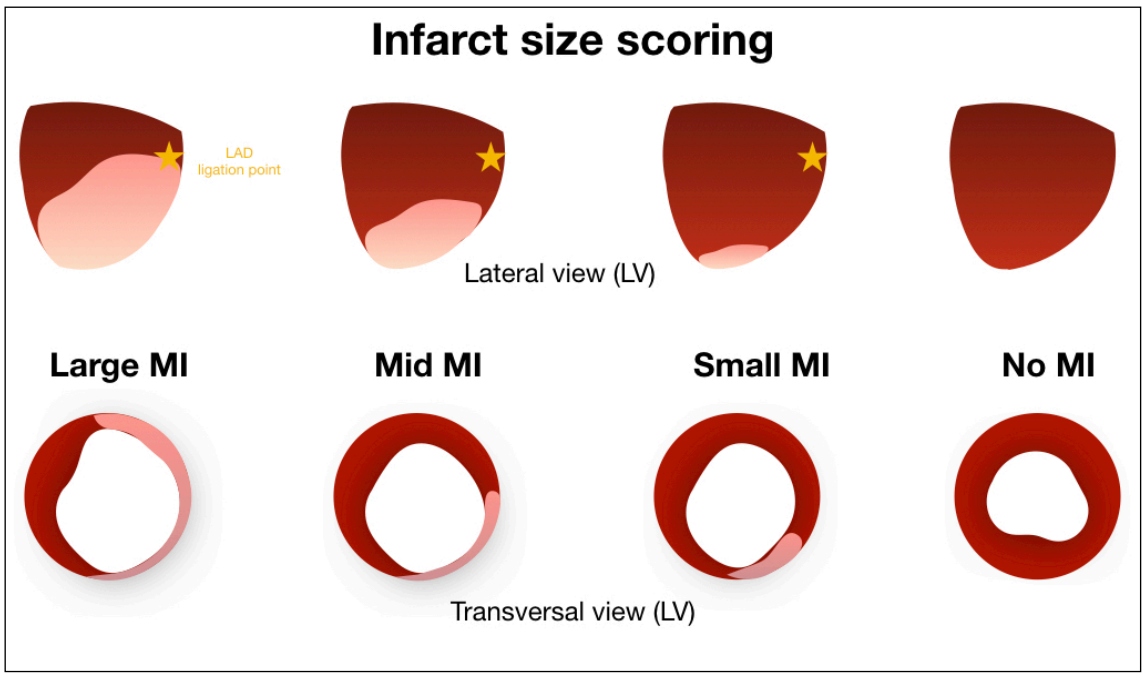

Figure 5 Guide to assessing infarct size at gross morphology level
Lateral and transversal view of the varying infarct size morphologies. This figure was used from the internal lab SOP for Organ harvesting.

Since the exact measurement of the infarct size is of crucial importance for the proper analysis of the infarcted hearts and the generated data of those animals, a more precise method was used at a later stage. After a picture of the histological cut of the infarcted area was taken under microscope, the analysis was conducted with ImageJ. The inside and outside borders as well as the border to the myocardium on both sides were marked. With the help of Excel, we calculated the infarcted area.

3.3.3. T cell purification

After the organ harvesting, the spleens were individually ground against a 30 µm mesh filter with the help of a syringe plunger into 15 ml falcon tubes. Afterwards the filter was washed additionally with CTL wash medium for a maximum yield of cells. Only the fibrous capsule remained in the filter. The cells were then diluted into 15 ml of CTL wash and

centrifuged at 550 G for 15 min with rapid acceleration and brake on high. Subsequently the supernatant was removed, and the remaining pellet resuspended in 2ml Erythrocyte-Lysis Buffer, which was previously diluted 1:10. 2 min after resuspension the falcon was filled up to 15 ml with more CTL Wash Medium and centrifuged again as seen above. The supernatant was removed again and the pellet, now mostly free of erythrocytes was resuspended in 1 ml CTL Test and ready for counting.

3.3.4. Cell counting

For cell counting we used the widely recognised method of manual counting via Neubauer chamber and microscope. The cell suspension was diluted in trypan blue to a suitable amount (around 100 cells per small quadrant). 10 µl were added under the correctly fixated glass slide and the cells were counted within the nine designated small quadrants. To improve accuracy, this counting process was repeated in three other big quadrants and a mean was used for further calculations.

3.3.5. Elispot assay

The ELISPOT (enzyme-linked immune absorbent spot) is a type of assay used to detect cytokines or antibodies that are secreted by individual immune cells after stimulation with antigens and immobilized on a membrane. Currently it displays the most sensitive tool available to quantify cytokine secretion.

Adapted protocol by CTL

Day 0: After the preparation of the capture solution, in this case with IFN-γ and IL-2 capture antibodies, for the membrane coting, the membranes in each well were activated by 70% ethanol. The prompt greying of the membrane showed its activation and immediately PBS had to be added to each well and incubated for less than one minute. Subsequently two washing steps with more PBS followed. Once washed for the last time, the PBS was discarded, and the capture solution was pipetted in each well. Finally, the plate was sealed with a parafilm and incubated for 24h at 4°C.

Day 1: The single cell solutions of lymphocytes were adjusted to the corresponding cell concentration to match the amount of 500.000 cells per well. Since the cells were plated in 100 µl of solution, the desired concentration was 5 mio/ml. During the preparation of the well plates, the cells were placed in a 37°C incubator to prevent any loss of function. First, the capture solution in the plates had to be discarded and the wells were washed twice with PBS. Then, before plating the cells, the antigens were pipetted into the wells. Leading to an antigen concentration, after adding of the cells, of 1 µl/ml. With previous experiments this antigen concentration was deemed enough for a maximum T cell response. For a straightforward process, the antigens were pre-prepared in 96-well v-bottom plates, could be thawed and easily transferred to the elispot plate with a multi-channel pipette. The elispot plates with the cell solution as well as the antigen solution were placed carefully in a 37°C CO_2 incubator for 24h.

Day 2: The first step of the second day was the preparation of the anti-murine IFN-γ/IL-2 detection solution. Subsequently the elispot plates were washed twice with PBS and twice with 0,05% Tween. The detection solution was added to each well and incubated for two hours. Shortly before the end of incubation, the tertiary solution was prepared. After all fluids in the plate were discarded, they were washed three times with 0,05% Tween and the tertiary solution was added to each well. Following an incubation time of 1h, the preparation of the blue developer solution as well as washing of the plates twice with 0,05% Tween and twice with distilled water followed. Now the blue developer solution was added to each well. The solution had to be plated within 10 min after mixing. The plates were incubated for 15 min, the remaining fluid discarded and the membrane gently rinsed with tap water to stop the reaction. This washing step was repeated three times and once again in the end with distilled water. As a final step, the freshly prepared red developer solution was added to each well and incubated for 10 min. Again, the reaction was stopped by rinsing four times with tap water and once with distilled water. During all those steps, especially between washing and adding the solutions, the membranes had to stay wet to prevent them from drying. Finally, the plates were dried at room temperature face down overnight or within two hours under the laminar flow.

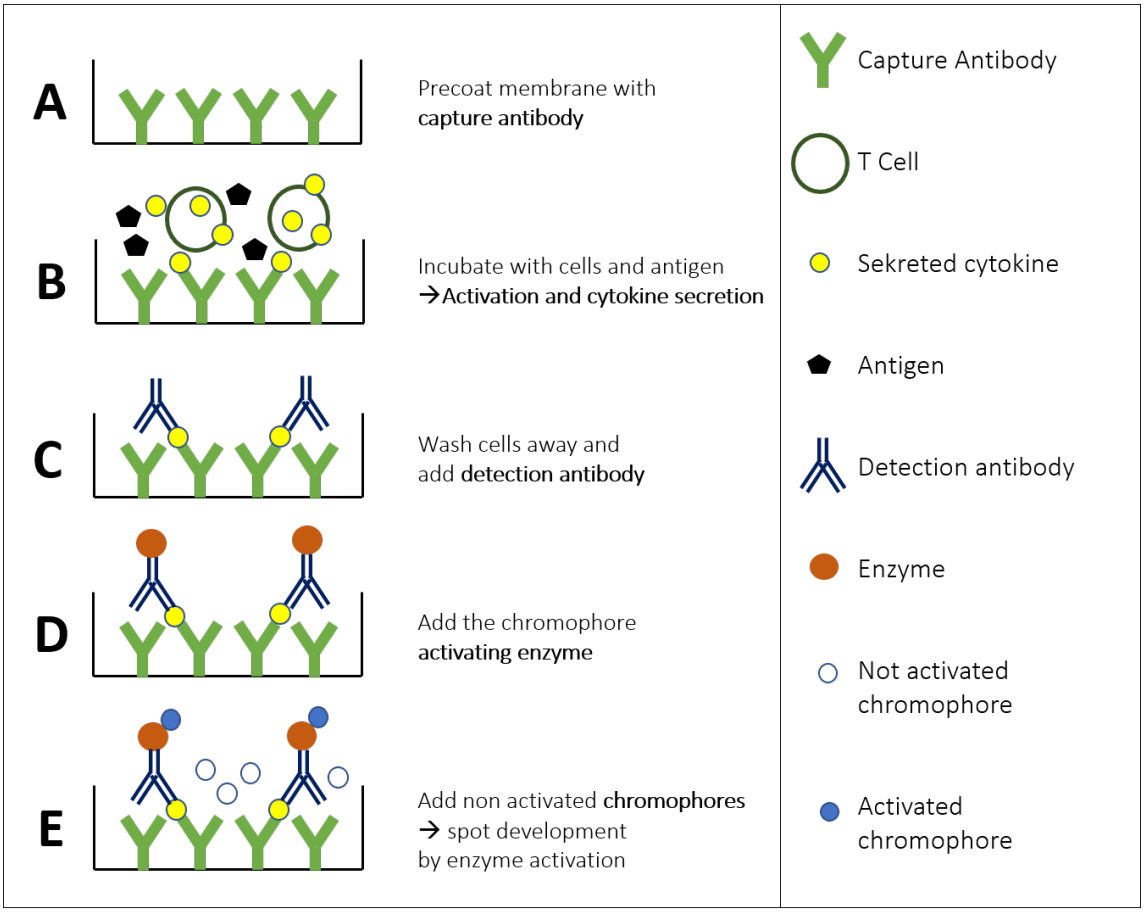

Figure 6 Elispot assay

(A) Day 0: Well membrane is coated with capture antibodies for IL-2 and IFN-γ **(B)** Day 1: Incubate cells with predefined putative antigens. Secreted cytokines (IL-2+IFN-γ) are captured by capture antibodies. **(C)** Supernatant is discarded, and detection antibodies are added to bind to the captured cytokines. **(D)** A tertiary solution is added with a chromophore activating enzyme that binds to the detection antibodies. **(E)** Finally, blue chromophores for IL-2 and red chromophores for IFN-γ are added and activated by the previously bound chromophore activating enzyme, which leads to a distinct spot formation.

3.3.6. Cell freezing

For optimal cell recovery when thawing, the CTL freezing kit was used. First, the cells were centrifuged at 550 G for 5 min with rapid acceleration and brake on high and the supernatant removed. Afterwards the pellet was resuspended in the cryo C solution with a maximum concentration of 30 mio/ml. Then, under constant twirling of the tube, cryo A and cryo B were mixed together in a relation of 80% to 20%. Slowly the cryo AB mixture was added to the cryo C cell solution 1:1, therefore obtaining a solution with a maximum cell concentration of 15 mio/ml. Afterwards the cryo vials may be stored limitlessly in a nitrogen tank until thawing.

3.3.7. Cell thawing

The cryo vials were brought from the nitrogen tank (-80 °C) covered in dry ice to the bench. During that process the cryo vials already started thawing. They were left in a 37°C water bath for 10 min to thaw the vial completely. After the vial was turned slowly over 180 °C, all cell suspensions from one animal were pooled in a 50 ml falcon tube and filled up with CTL wash. Then the new cell suspension was centrifuged at 550 G for 5 min with rapid acceleration and brake on high. This washing step was repeated once and afterwards the cell yield was determined by counting via Neubauer chamber. The cells were then diluted to the desired concentration.

3.3.8. Hybridoma

The experiments for this part were performed together with Elena Vogel. Main incentive behind the production of hybridomas is the fusion of ($CD4^+$) T cells with thymoma cells (cancer cells) in order to create an unlimited source of nearly immortal hybrid cells for experimentation. Because the T cells have a limited lifespan, efficient cultivation under laboratory conditions is not possible. Thymoma cells, e.g. the lineage BW 5147gal, kindly provided by Prof. Thomas Herrmann, Immunobiology Würzburg Germany, on the other hand are immortal. The fusion of both cell types allows the combination of their properties in the form of so-called hybridoma cells. These are now able to divide

themselves without any restriction and still maintain their T cell specificity. **Figure 7** illustrates the exact process of hybridoma synthesis.

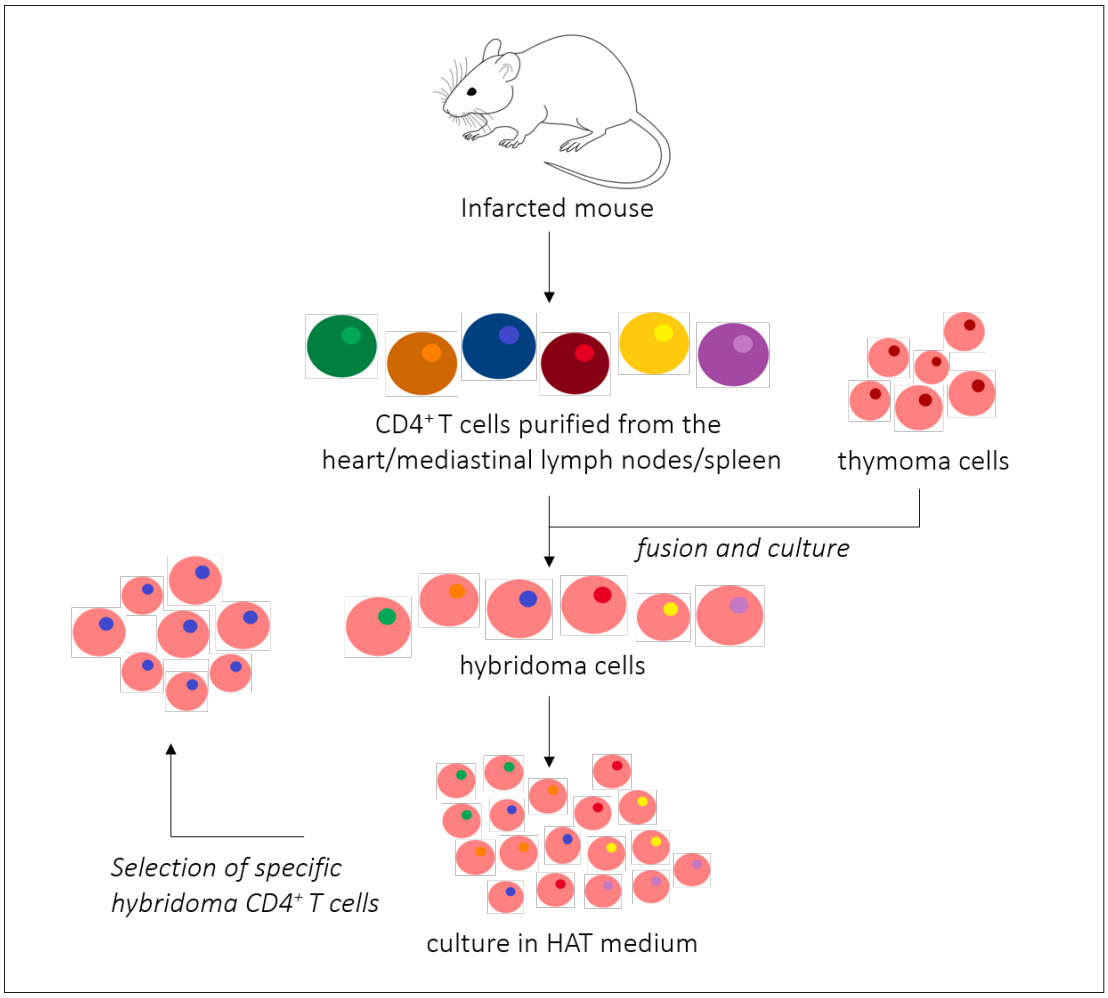

Figure 7 Synthetizing process of hybridomas from CD4⁺ T cells
CD4⁺ T cells purified from the heart, mediastinal lymph nodes or spleen of infarcted Balb/c mice were fused with thymoma cells, cultured in HAT medium and then selected for specific CD4⁺ hybridoma cells.

The T cells as well as the thymoma cells were added to the fusion solution and centrifuged under the influence of polyethylene glycol (PEG). Since most of the water is bound by polyethylene glycol, the cell membranes were brought into close contact with one another, whereby a spontaneous fusion of the cell membranes was achieved. Because PEG has a toxic effect on cells, the concentration and exposure time of the PEG solution were critical to the success of the fusion. After the fusion, cells were formed that had two or more cell nuclei, called heterokaryon. To finalise the development to a mature

hybridoma cell, these nuclei had to fuse spontaneously. Since chromosomes are often rejected in this process, only a very small part of the hybridoma cells remained stable. After cell fusion, five cell types were present in the solution: hybridoma cells, unfused T cells, unfused thymoma cells, fused T cells and fused thymoma cells. In order to select the hybridoma cells, a selective medium was used in which only hybridoma cells can survive. A suitable medium was the so-called HAT medium, which contains the chemical substances hypoxanthine, aminopterin and thymidine. Hypoxanthine is a precursor for purines required for the construction of the DNA. However, the enzyme hypoxanthine guanine phosphoribosyl transferase (HGPRT) is necessary for its conversion. As a thymoma cell line was used in the fusion, which lacks this enzyme or is only present in its inactive form, individual thymoma cells could not survive in this medium. T cells, on the other hand, have HGPRT, but cannot survive by themselves and die quickly in the culture medium. Only hybridoma cells can be cultured due to the immortality of the thymoma cells and the HGPRT genes of the T cells. Aminopterin serves only to block other purinergic synthetic pathways. Since this includes the de novo synthesis of essential thymine, it must be added to the medium. From the hybridoma cells selected by this process, the clones with the desired properties were still to be isolated.

This screening was preferably done by an ELISA assay, flow cytometry and immunofluorescence. After a HAT selection it is not uncommon to get tens of thousands of clones, with only a few hundred cells among these with the desired characteristics. After further cultivation, only a few dozen hybridoma cells remained stable. A portion of the positive clones was kept in liquid nitrogen for later use while the remaining cells were cultured further.

3.3.9. Fluorescence-activated cell sorting (FACS)

Fluorescence activated cell sorting (FACS) is a technique commonly used for an individual characterization of cells or particles in a heterogeneous group concerning purity, cell size and volume. Simultaneously single cells can be examined for multiple parameters. The antigens on the surface as well as intracellular ones can be used to distinguish different cell subpopulations.

The intensity of fluorescent-label is a readout for the expression of the antigen. This antigen is detected by specific antibodies. For that purpose, a single cell solution has to be prepared. The cells are incubated with fluorochrome-labelled or unlabelled antibodies in tubes or microtiter plates. The FACS can separate populations of interest from another. Depending on size and their internal fluorescence intensities, the cells, when exposed to the lasers, give different feedbacks, which enable the cell sorter to count and sort the cells into predesigned groups.

The sample cell suspension is directed through a very thin capillary past lasers in the cell sorter to assemble all individual cells consecutively with space in between them corresponding to their diameter. An incorporated vibrating mechanism induces breaking within this flow and leads to a separation of droplets containing single cells. Shortly before the droplet formation the individual fluorescence and light scattered from each cell is detected. Cells are then sorted by an electrostatic deflection system. This recorded information can be used for subsequent analysis.

This method was utilized for the hybridoma experiments. To sort the cells the FACS Aria II machine was used in the following configuration: 488nm (blue argon laser), 633nm (red HeNe laser), 405nm (violet laser) and 561nm (yellow laser). The mouse $CD4^+$ T cells were analysed with the following antibody panel: anti-CD4 (clone RM4-5), anti-CD45 (clone 30F11) and anti-TCRβ (clone H57-597). In addition, AmCyan Zombie Aqua was used for live/dead discrimination. $CD4^+$ T cells were sorted as singlets live $CD45^+$ $TCR\beta^+$ $CD4^+$ events. From the heart a total of $1{,}0x10^5$ cells were sorted for the MI group and $2{,}6x10^4$ for the Sham group. After sorting sample purity was reassessed by FACS: over 95% purity. The sorted CD4+ T cells were employed in further fusion experimentation with the BW 5147gal murine T cell line, kindly provided by Prof. Thomas Herrmann (Institute for Virology and Immunology, Würzburg). To set up the cell sorter, unstained cells and single colour controls were used.

3.3.10. Legendplex assay

For quantifying cytokines of interest, the ELISA assay, though especially the elispot assay are the most sensitive tools available. Nevertheless, the multiplex assay displays an

opportunity to measure multiple analytes in the same sample. The legend plex assay from Biolegend is a bead-based assay (Luminex and flow cytometry cytokine bead array, CBA), measuring the following cytokines: (IL-2, IL-4, IL-5, IL-6, IL-10, IL-13, IFN-γ, TNF-α). The concept of the legend plex assay is similar to a capture sandwich ELISA. The main difference is though that the capture antibody is coated onto beads in suspension instead of being directly coated to the well. The beads used in this assay were precoated with a capture monoclonal antibody, specific to a corresponding cytokine and an internal labelling with a unique combination of fluorescent dyes. Simultaneously up to 100 different cytokines can be detected that way.

Before the beginning of the experiment all reagents were brought up to room temperature. During the entire procedure the plate had to be kept in an upright position to avoid any loss of beads and the plate had to be wrapped in aluminium foil for all incubation steps. The controls, eight duplicates in total (C0-C7), were the mouse Th panel standard cocktail mix with all beads (C7), a consecutive dilution of 1:4 repeated for each standard (C6-C1) and finally a standard with only assay buffer and no beads (C0). Standard controls and samples were run with three technical replicates to improve the statistical analysis and were arranged in a vertical configuration for a more convenient data acquisition. To measure the cell culture supernatant samples assay buffer was added to all wells. Each standard was added to the standard wells and each sample to the sample wells. The mixed beads were vortexed for 30 s and added to each well. After these steps the plate was sealed with a plate sealer covered with aluminium foil for light protection and shaken at 800rpm on a plate shaker for two hours at room temperature. Finally, the plate was centrifuged at 250 G for 5 min in a swinging bucket rotor with microplate adaptor. Centrifugation should not be exceeded as it can affect bead resuspension in later steps. Immediately after centrifugation the supernatant was discarded by quickly inverting and flicking the plate in one continuous and forceful motion. The plate was then blotted on a stack of clean paper towel to drain the remaining liquid inside the well as much as possible. The plate was then washed once by dispensing washing buffer into each well and shaken at 800 rpm for 1 min. The supernatant was again discarded as mentioned above. After detection antibodies were added to each well, the plate was

sealed and covered with aluminium foil again. At 800 rpm the plate was shaken for 1 h. Consecutively, SA-PE was added to each well directly. The plate was again sealed and wrapped in aluminium and shaken for 30 min at 800 rpm. The supernatant was again discarded as mentioned, 1X wash buffer was added to each well and resuspended by pipetting.

Finally, the samples were analysed on the same day with the Attune NxT Flow Cytometer, using the following lasers: 488nm (blue argon laser), 633nm (red HeNe laser), 405nm and 561nm (yellow laser). The analysis was conducted with the Legendplex V8.0 software. Briefly, each bead was identified according to its size and complexity with the forward scatter (FSC) and side scatter (SSC), distinguishing into beads A and beads B. Each cytokine can be further differentiated based on the APC fluorescence intensity. The signal on the PE chanel was then used to quantify each analyte. Afterwards the PE signal was integrated into the standard curve and each analyte concentration was plotted as pg/ml.

3.4. Statistical analysis

The statistical analysis was conducted by the doctoral candidate with the program Graph Pad Prism (7.0). All graphs show the results in mean ± SEM (standard error of mean) obtained from *n* animals (n is indicated in each figure legend).

For the graphs illustrating one variable in two different groups, 2-tailed unpaired t-tests were conducted, considering that all samples follow normal distribution.

For multiple comparisons, a one-way ANOVA (Analysis of Variance) followed by Dunnett's post hoc test were performed, focusing on the comparison of one independent variable in different groups.

A two-way ANOVA followed by the turkey post hoc test was used for multiple comparisons, containing two independent variables in several groups.

Statistical significance was determined with differences considered significant at $p<0.05$.

3.5 Permissions

Several figures contain results previously published in the Journal of Clinical Investigation Volume 129, Issue 11 on November 1st, 2019.

J Clin Invest. 2019;129(11):4922–4936. https://doi.org/10.1172/JCI123859.
© 2019 American Society for Clinical Investigation

To include published data as part of the dissertation is permitted by the journal.
Other figures were created solely by the author or are marked otherwise.

4. RESULTS

4.1. In silico analysis

With a broad screening of different proteins by in silico predictions we planned on identifying a comprehensive panel of MHC-II restricted cardiac epitopes, relevant in the immune inflammatory processes after MI, while maintaining a largely unbiased view on the selection process. The combination of a hypothesis driven approach and a broad unbiased screening should lead to a definitive mapping of cardiac antigens that trigger post-MI $CD4^+$ T cell responses for the first time.

4.1.1. Putative proteins for epitope search

As of today, the cardiac antigens that could be relevant for T cell responses after MI, have not yet been identified. So far it is not even clear whether this process is a general inflammatory cytokine mediated phenomenon or a specific lymphocyte reaction to antigens being released. When considering proteins that could be significant in this context, we defined three main groups of interest: heart specific proteins, inflammation associated proteins and clot derived proteins. (Table 1)

Table 1 Putative cardiac antigens and their specific expression patterns

Heart-specific Antigens			
Protein	**Cardiac exp. level**	**Tissue distribution**	**Localization**
Actc1 Actin alpha 1, cardiac isoform	High	Heart-enriched	Intracellular (motor)
Adrb1 Adrenoceptor beta 1	High	Heart-enhanced	Membrane
Mybpc3 Myosin binding protein C, cardiac	High	Heart-enriched	Intracellular (motor)
Myh6 Myosin heavy chain 6, cardiac isoform	High	Heart-enriched	Intracellular (motor)
Mhl2 Myosin light chain 2 (Ventricular)	High	Heart-enriched	Intracellular (motor)
Tnni3 Troponin I type3, cardiac isoform	High	Heart-enriched	Intracellular (motor)
Tnnt2 Troponin T type2, cardiac isoform	High	Heart-enriched	Intracellular (motor)
Inflammation-associated-Antigens			
Hspb3 Heat-shock protein 27	High (RNA)	Heart-enriched	Intracellular
Hspa1a Heat-shock protein 72	Medium (steady-state) High upon disease	Mixed, associated with inflammation	Mitochondrial
Clot-derived-Antigens			
Fga Fibrinogen-alpha chain	Not expressed; fibrin deposited in the injured heart	Liver	Secreted (Circulation)
Fgb Fibrinogen-beta chain	Same as Fga	Liver	Secreted (Circulation)
Fgg Fibrinogen-gamma chain	Same as FGa	Liver	Secreted (Circulation)

After cardiomyocyte death during MI cardiomyocyte components are released (mainly motor proteins), which could be possible antigen resources stimulating adaptive immune cells. Hence, we sought to confirm, if $CD4^+$ T cell responses after MI are heart specific, and ultimately identify relevant cardiac epitopes. The selected cardiac proteins involve sarcomere elements such as α actin, cardiac muscle 1 [ACTC1], myosin-binding protein C3 [MYBPC3], myosin heavy chain α [MYHCA], myosin light chain 2 [MYL2], troponin I3, cardiac muscle [TNNI3], and troponin T2, cardiac muscle [TNNT2] , a cardiac receptor in

the form of adrenergic receptor beta 1 [ARB1], and mitochondrial components with heat shock protein family B3 [HSPB3] and [Hspa1a].

Heart specific proteins already imply a preferred expression in the heart and could be essential for the control of a specific immune response in the heart. The human protein atlas lists 28 heart specific proteins. The highest level of enriched expression in the heart can be found in 12 genes. These are most likely expected to be the source for cardiac antigens. For the other proteins with a lower expression we did not anticipate them to reach a significant concentration in the lymph nodes and they were therefore excluded. Further proteins could be excluded such as atrial or brain natriuretic peptide (ANP/BNP), which are expressed in the atrium, or genes related to the electrical or conductive system e.g. HCN4. The list was finally curated down to seven groups, selecting i) heart enriched, ii) ventricular and iii) highly expressed proteins, which appeared to be the most promising: α actin, cardiac muscle 1 (Actc1), myosin heavy chain 6 (Myh6), ventricular myosin light chain 2 (Mhl2), cardiac myosin binding protein C (Mybpc3), troponin T type 2 (Tnnt2), troponin I type 3 (Tnni3) and adrenoreceptor beta 1 (Adrb1).[92]

Stress-related proteins are linked to tissue injury in general and increasingly expressed by the injured myocardium, which endorses the notion of their relevance in the specific immune response in the context of MI. Inflammation associated antigens could be deriving from heat-shock protein 27 (HspB3) and heat-shock protein 72 (Hspa1a).

4.1.2. Identified epitopes

The in silico simulation of the MHC-II binding properties was basis of the selection process of the specific 15 mers peptides.[102] In total we finalised a library of 193 epitopes for the I-A^d haplotype, corresponding to Balb/c mice, and 206 for I-A^b, corresponding the C57BL/6J. Those cover the eight most relevant heart-enriched proteins encoded by mRNAs with more than 5 levels on the heart compared with those in all other tissues, as detailed in the human protein atlas, for in vivo and ex vivo testing.[49,92] (See Table 6, Appendix)

For the selection process a good binding affinity and stability of the epitopes, as well as probability for actual presentation were of major importance. For binding affinity, we chose only peptides with a percentile rank of <10. We sought this to be a sufficient threshold generally used as standard threshold. Furthermore, the threshold for binding affinity was defined at $<IC_{50}$ 5000nM, subdividing in groups of small affinity for $<IC_{50}$ 5000nM + <10 percentile rank, mid-affinity for $<IC_{50}$ 500nM and high affinity for $<IC_{50}$ 50nM. A low number is an indicator of higher affinity. Most epitopes have a high or an intermediate affinity. Rarely epitopes also express a low affinity, though no known T cell epitope has been proven to have an IC_{50} value greater than 5000.

4.1.3. Inter strain differences (Balb/c vs. C57BL/6J)

Looking at the epitopes found for the haplotype I-A^d and I-A^b, a clear difference between Balb/c and C57BL/6J can be noted (**Figure 8**).

Comparing the number of epitopes found per protein, normalized by protein size, more seem to be existent for the Balb/c mouse strain. A deeper magenta colouring signifies a higher normalized number of epitopes per protein (**Figure 8, A**), which we deem as sign for a higher susceptibility. Looking more closely at the binding affinity of these epitopes, those with a Balb/c background show a lower mean percentile - meaning higher binding affinity - than those with a C57BL/6J background (**Figure 8, B**). A higher binding affinity of the proteins is desirable for more stable antigen interactions. The inverted colouring scale was used, since in both cases a deeper magenta colouring should provoke our interest.

The previously mentioned disease susceptibility towards the development of experimental autoimmune myocarditis in Balb/c mice versus C57BL/6J matches these findings.

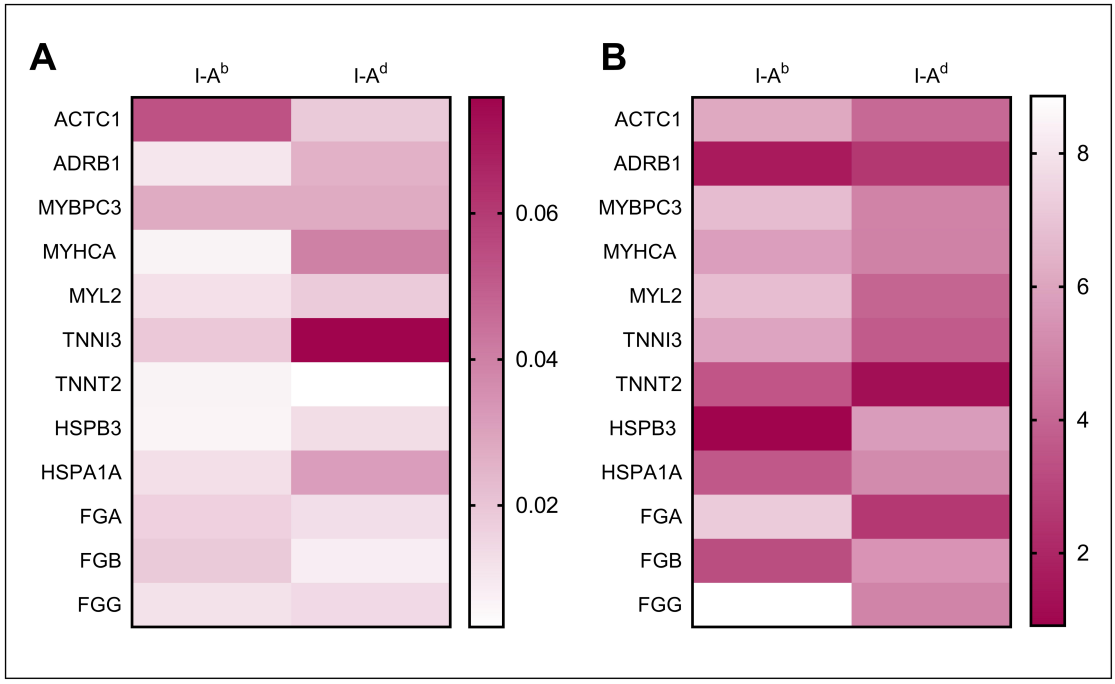

Figure 8 Epitopes from in-silico predictions

(**A**) Heatmap illustrating the number of identified epitopes per protein normalized by the size of the corresponding protein (amino acid) (**B**) Analysis of the overall epitope affinity (percentile) comparing the different proteins to one another. The percentile scale is colored inversely compared to A and darker means lower percentile and therefore higher affinity. (Only epitopes with a percentile of <10 were chosen.)

For that reason, we decided to investigate our putative antigens first of all against a Balb/c background. To understand the whole picture some further analysis on C57BL/6J followed.

4.1.4. Antigen atlas: The example Myh6

Over the course of the in-silico prediction process an "Antigen atlas" with all necessary information on the putative proteins has been gathered. Basic structural facts about the protein are summarized in **Table 2**.

Table 2 Characteristics of the peptide of interest: Myhca
(Source Uniprot and Human Protein Atlas: Proteinatlas.org 11/2017)

Protein name:	**Myhca – Myosin, heavy chain 6, cardiac muscle, alpha**
Species:	*Mus musculus*
Mass/Length	223 kDa/ 1,938 aa (whole protein)
FASTA Sequence Source: Uniprot Date: 05.12.2017	MTDAQMADFGAAAQYLRKSEKERLEAQTRPFDIRTECFVPDDKEEYVKA KVVSREGGKVTAETENGKTVTIKEDQVMQQNPPKFDKIEDMAMLTFLHE PAVLYNLKERYAAWMIYTYSGLFCVTVNPYKWLPVYNAEVVAAYRGKKR SEAPPHIFSISDNAYQYMLTDRENQSILITGESGAGKTVNTKRVIQYFASIA AIGDRSKKENPNANKGTLEDQIIQANPALEAFGNAKTVRNDNSSRFGKFIR IHFGATGKLASADIETYLLEKSRVIFQLKAERNYHIFYQILSNKKPELLDMLL VTNNPYDYAFVSQGEVSVASIDDSEELLATDSAFDVLSFTAEEKAGVYKL TGAIMHYGNMKFKQKQREEQAEPDGTEDADKSAYLMGLNSADLLKGLC HPRVKVGNEYVTKGQSVQQVYYSIGALAKSVYEKMFNWMVTRINATLET KQPRQYFIGVLDIAGFEIFDFNSFEQLCINFTNEKLQQFFNHHMFVLEQEE YKKEGIEWEFIDFGMDLQACIDLIEKPMGIMSILEEECMFPKASDMTFKAK LYDNHLGKSNNFQKPRNVKGKQEAHFSLVHYAGTVDYNIMGWLEKNKD PLNETVVGLYQKSSLKLMATLFSTYASADTGDSGKGKGGKKKGSSFQTV SALHRENLNKLMTNLKTTHPHFVRCIIPNERKAPGVMDNPLVMHQLRCN GVLEGIRICRKGFPNRILYGDFRQRYRILNPAAIPEGQFIDSRKGAEKLLGS LDIDHNQYKFGHTKVFFKAGLLGLLEEMRDERLSRIITRIQAQARGQLMRI EFKKIVERRDALLVIQWNIRAFMGVKNWPWMKLYFKIKPLLKSAETEKEM ANMKEEFGRVKDALEKSEARRKELEEKMVSLLQEKNDLQLQVQAEQDNL NDAEERCDQLIKNKIQLEAKVKEMTERLEDEEEMNAELTAKKRKLEDECS ELKKDIDDLELTLAKVEKEKHATENKVKNLTEEMAGLDEIIAKLTKEKKALQ EAHQQALDDLQAEEDKVNTLTKSKVKLEQQVDDLEGSLEQEKKVRMDLE RAKRKLEGDLKLTQESIMDLENDKLQLEEKLKKKEFDISQQNSKIEDEQAL ALQLQKKLKENQARIEELEEELEAERTARAKVEKLRSDLSRELEEISERLE EAGGATSVQIEMNKKREAEFQKMRRDLEEATLQHEATAAALRKKHADSV AELGEQIDNLQRVKQKLEKEKSEFKLELDDVTSNMEQIIKAKANLEKVSRT LEDQANEYRVKLEEAQRSLNDFTTQRAKLQTENGELARQLEEKEALISQL TRGKLSYTQQMEDLKRQLEEEGKAKNALAHALQSSRHDCDLLREQYEEE MEAKAELQRVLSKANSEVAQWRTKYETDAIQRTEELEEAKKKLAQRLQD AEEAVEAVNAKCSSLEKTKHRLQNEIEDLMVDVERSNAAAAALDKKQRN FDKILAEWKQKYEESQSELESSQKEARSLSTELFKLKNAYEESLEHLETFK RENKNLQEEISDLTEQLGEGGKNVHELEKIRKQLEVEKLELQSALEEAEA SLEHEEGKILRAQLEFNQIKAEIERKLAEKDEEMEQAKRNHLRMVDSLQT SLDAETRSRNEALRVKKKMEGDLNEMEIQLSQANRIASEAQKHLKNSQA HLKDTQLQLDDAVHANDDLKENIAIVERRNNLLQAELEELRAVVEQTERS RKLAEQELIETSERVQLLHSQNTSLINQKKKMESDLTQLQTEVEEAVQEC RNAEEKAKKAITDAAMMAEELKKEQDTSAHLERMKKNMEQTIKDLQHRL DEAEQIALKGGKKQLQKLEARVRELENELEAEQKRNAESVKGMRKSERR IKELTYQTEEDKKNLMRLQDLVDKLQLKVKAYKRQAEEAEEQANTNLSKF RKVQHELDEAEERADIAESQVNKLRAKSRDIGAKKMHDEE
Expression Pattern: Source: Human Protein Atlas Date: 10.11.2017	Selective cytoplasmic expression in heart and skeletal muscle.

The protein expression across all tissues is illustrated in **Figure 9**. **Figure 10** shows the protease cleaving sites provided by prosper. Proteases such as MMP2 or MMP9 would have been candidates to cleave putative epitopes and inactivate them by cleaving. All cleaving sites found within the sequences were corresponding to proteases not resident in the myocardium and thus not participating in the alteration of our putative epitopes. Therefore no modification of our antigen list had to be done.[107]

Table 3 is a summary of all identified epitopes divided by affinity towards MHC-II. The final list of putative epitopes for MYHCA is depicted in **Table 4**.

Figure 9 Protein expression across different tissues
This graph shows the protein expression of the protein Myhca across all tissues in the human body. It could be detected only in two tissues, the heart muscle and the skeletal muscle, with a high expression in the cardiac muscle and therefore an excellent candidate for $CD4^+$ T cell priming after MI. (Source Human Protein Atlas: Proteinatlas.org, 11/2017)

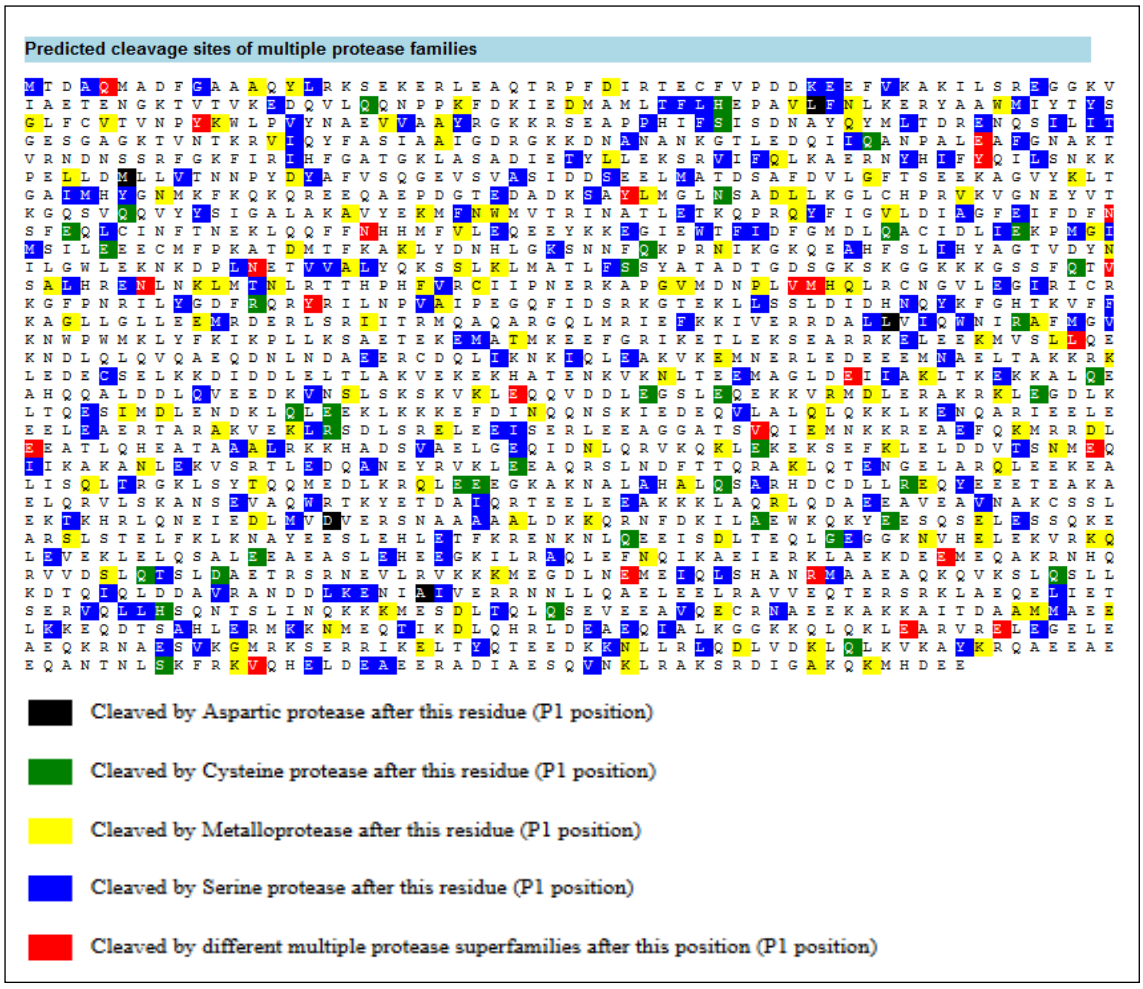

Figure 10 Myhca protease cleaving sites

The FASTA sequence of the Myhca peptide analyzed concerning protease cleaving sites. The above-mentioned proteases, aspartic protease, cysteine protease, metalloprotease, serine protease and different multiple protease superfamilies' are relevant within the heart. Therefore, the named cleaving sites can be neglected. Cleaving sites of proteases present in the heart would lead to protein inactivation and thus also possible epitope inactivation before any antigen presentation. (Source: Prosper: https://prosper.erc.monash.edu.au/ , 11/2017)

Table 3 MHC-II prediction

Summary of all epitopes found for the Myhca peptide with the MHC-II T cell prediction tool from IEDB. Divided in the haplotypes I-A^b and I-A^d with the corresponding groups of epitopes with a percentile < 10 subdivided in peptides with a high-, mid- or low-affinity of the cores. (Source: 11/2017 IEDB: http://tools.immuneepitope.org/mhcii/)

	I-A^b	I-A^d
Number of peptides < 10 percentile rank	13	77
Number of peptide cores with high affinity (< Ic_{50} 50 nM)	0	0
Number of peptide cores with mid-affinity (< Ic_{50} 500 nM)	0	8
Number of peptide cores with low-affinity (< Ic_{50} 5000 nM)	13	69

Table 4 Peptides of interest

All epitopes with a percentile <10 (or [*] indicated by experimental evidence) from the peptide Myhca$_{614-629}$. Peptide amino acid sequence with the bold underlined core. (Data gathered 11/2017)

Haplotype	Peptide Position	Peptide core	Percentile
I-A^b	Myh6$_{109-127}$	AAW**MIYTYSGLFCVTV**NP	6.64
I-A^b	Myh6$_{122-142}$	VTVNP**YKWLPVYNA**EVVAAY	7.45
I-A^b	Myh6$_{186-206}$	VNTKRV**IQYFASIAA**IGDRSK	4.16
I-A^b	Myh6$_{216-233}$	TLED**QIIQANPAL**EAFGN	7.14
I-A^b	Myh6$_{247-265}$	FIRIH**FGATGKLAS**ADIE	5.98
I-A^b	Myh6$_{305-323}$	NNP**YDYAFVSQGEVSV**AS	6.72
I-A^b	Myh6$_{345-369}$	EKA**GVYKLTGAI**MHYGNM	6.79
I-A^b	Myh6$_{416-435}$	SVQQV**YYSIGALAK**SVYEK	3.24
I-A^b	Myh6$_{431-451}$	SVYEKM**FNWMVTRIN**ATLETK	4.47
I-A^b	Myh6$_{718-732}$	GDFR**QRYRILNPA**AI	2.13
I-A^b	Myh6$_{719-738}$	DFRQR**YRILNPAAI**PEGQFI	1.77
I-A^b	Myh6$_{1430-1445}$	LM**VDVERSNAA**AAAL	9.37
I-A^b	Myh6$_{1431-1446}$	MVDV**ERSNAAAAA**LD	9.72
I-A^d	Myh6$_{1-15}$	MTD**AQMADFGAA**AQY	5.60
I-A^d	Myh6$_{41-56}$	DKEE**YVKAKVVSR**EG	1.79
I-A^d	Myh6$_{86-100}$	KIE**DMAMLTFLH**EPA	4.06
I-A^d	Myh6$_{105-119}$	LKER**YAAWMIYTY**SG	6.58
I-A^d	Myh6$_{131-145}$	LP**VYNAEVVAA**YRGK	5.69
I-A^d	Myh6$_{186-201}$	VNT**KRVIQYFAS**IAA	4.25
I-A^d	Myh6$_{190-204}$	RV**IQYFASIAA**IGDRS	3.42
I-A^d	Myh6$_{191-205}$	VIQY**FASIAAIGD**RS	2.73
I-A^d	Myh6$_{216-231}$	LE**DQIIQANPALEA**F	9.18
I-A^d	Myh6$_{420-434}$	Q**VYYSIGALAK**SVYE	2.46
I-A^d	Myh6$_{605-619}$	TVVG**LYQKSSLKL**MA	9.10
I-A^d	Myh6$_{608-622}$	GL**YQKSSLKLM**ATLF	1.55
I-A^d	Myh6$_{609-623}$	LYQ**KSSLKLMAT**LFS	0.98
I-A^d	Myh6$_{610-624}$	YQKSS**LKLMATLFS**T	1.20
I-A^d	*Myh6$_{614-628}$	SLK**LMATLFSTY**ASA	9.04
I-A^d	Myh6$_{641-655}$	KK**GSSFQTVSA**LHRE	5.64
I-A^d	Myh6$_{642-656}$	KGS**SFQTVSALH**REN	7.20
I-A^d	Myh6$_{720-734}$	FR**QRYRILNPA**AIPE	2.13
I-A^d	Myh6$_{721-735}$	RQ**RYRILNPAA**IPEG	4.00
I-A^d	Myh6$_{722-736}$	**QRYRILNPA**AIPEGQ	2.13
I-A^d	Myh6$_{776-790}$	EE**MRDERLSRI**ITRI	9.91
I-A^d	Myh6$_{777-791}$	EMRD**ERLSRIITR**IQ	7.57
I-A^d	Myh6$_{778-792}$	MRDER**LSRIITRIQ**A	5.05
I-A^d	Myh6$_{781-795}$	ERL**SRIITRIQA**QAR	7.80
I-A^d	Myh6$_{786-801}$	IITRI**QAQARGQLM**RI	7.08
I-A^d	Myh6$_{793-807}$	QARGQ**LMRIEFKKI**V	9.50
I-A^d	Myh6$_{810-824}$	RDAL**LVIQWNIRA**FM	8.21
I-A^d	Myh6$_{814-828}$	LV**IQWNIRAFM**GVKN	4.57
I-A^d	Myh6$_{815-829}$	VIQWN**IRAFMGVKN**W	3.38
I-A^d	Myh6$_{833-847}$	KL**YFKIKPLLK**SAET	9.13

I-A^d	Myh6$_{910-924}$	**LIKNKIQLE**AKVKEM	8.97
I-A^d	Myh6$_{911-925}$	IKNKI**QLEAKVKEM**T	7.40
I-A^d	Myh6$_{994-1008}$	**LTKEKKALQ**EAHQQA	5.89
I-A^d	Myh6$_{996-1010}$	KEKK**ALQEAHQQA**LD	5.26
I-A^d	Myh6$_{1000-1014}$	AL**QEAHQQALD**DLQA	4.42
I-A^d	Myh6$_{1003-1017}$	EAH**QQALDDLQA**EED	2.63
I-A^d	Myh6$_{1039-1053}$	S**LEQEKKVRM**DLERA	4.18
I-A^d	Myh6$_{1040-1054}$	LEQEK**KVRMDLERA**K	2.54
I-A^d	Myh6$_{1044-1058}$	KK**VRMDLERAK**RKLE	4.45
I-A^d	Myh6$_{1124-1138}$	**LEAERTARA**KVEKLR	2.40
I-A^d	Myh6$_{1126-1140}$	AERT**ARAKVEKLR**SD	2.55
I-A^d	Myh6$_{1183-1197}$	AT**LQHEATAAA**LRKK	3.04
I-A^d	Myh6$_{1185-1199}$	LQ**HEATAAALR**KKHA	2.21
I-A^d	Myh6$_{1231-1245}$	DDVT**SNMEQIIKA**KA	3.20
I-A^d	Myh6$_{1235-1249}$	SN**MEQIIKAKA**NLEK	1.18
I-A^d	Myh6$_{1238-1252}$	EQ**IIKAKANLE**KVSR	7.20
I-A^d	Myh6$_{1258-1272}$	ANE**YRVKLEEAQ**RSL	3.96
I-A^d	Myh6$_{1259-1273}$	NEYR**VKLEEAQRS**LN	3.67
I-A^d	Myh6$_{1290-1304}$	ARQ**LEEKEALIS**QLT	7.55
I-A^d	Myh6$_{1293-1307}$	LEE**KEALISQLT**RGK	8.74
I-A^d	Myh6$_{1326-1340}$	KAK**NALAHALQS**SRH	7.27
I-A^d	Myh6$_{1327-1341}$	AKNAL**AHALQSSRH**D	9.00
I-A^d	Myh6$_{1350-1364}$	EE**EMEAKAELQ**RVLS	2.52
I-A^d	Myh6$_{1351-1365}$	EEMEA**KAELQRVLS**K	2.48
I-A^d	Myh6$_{1388-1402}$	**LEEAKKKLA**QRLQDA	5.96
I-A^d	Myh6$_{1391-1405}$	AKK**KLAQRLQDA**EEA	3.10
I-A^d	Myh6$_{1394-1408}$	KLA**QRLQDAEEA**VEA	5.32
I-A^d	Myh6$_{1397-1411}$	QRL**QDAEEAVEA**VNA	2.09
I-A^d	Myh6$_{1401-1415}$	DA**EEAVEAVNA**KCSS	5.43
I-A^d	Myh6$_{1435-1449}$	**ERSNAAAAA**LDKKQR	2.00
I-A^d	Myh6$_{1470-1484}$	ESS**QKEARSLST**ELF	7.68
I-A^d	Myh6$_{1471-1485}$	SSQKE**ARSLSTELF**K	4.21
I-A^d	Myh6$_{1528-1542}$	EKI**RKQLEVEKL**ELQ	2.97
I-A^d	Myh6$_{1530-1544}$	IRKQ**LEVEKLELQ**SA	4.42
I-A^d	Myh6$_{1539-1553}$	VEKLE**LQSALEEAEA**	4.75
I-A^d	Myh6$_{1567-1582}$	NQ**IKAEIERKLA**EKD	6.53
I-A^d	Myh6$_{1589-1605}$	RNH**LRMVDSLQT**SLD	4.31
I-A^d	Myh6$_{1621-1635}$	GD**LNEMEIQLS**QANR	0.80
I-A^d	Myh6$_{1623-1637}$	LN**EMEIQLSQA**NRIA	0.59
I-A^d	Myh6$_{1651-1688}$	HLK**DTQLQLDDA**VHA	7.48
I-A^d	Myh6$_{1652-1686}$	LKDTQ**LQLDDAVHA**N	6.67
I-A^d	Myh6$_{1752-1766}$	NAEEK**AKKAITDAA**M	2.63
I-A^d	Myh6$_{1782-1796}$	ERMK**KNMEQTIKD**LQ	7.74
I-A^d	Myh6$_{1783-1797}$	RMKKN**MEQTIKDLQ**H	6.04
I-A^d	Myh6$_{1808-1823}$	GG**KKQLQKLEA**RVRE	2.62
I-A^d	Myh6$_{1809-1824}$	GKKQ**LQKLEARVR**EL	5.02
I-A^d	Myh6$_{1868-1882}$	LVDKL**QLKVKAYKR**Q	1.15

4.2. In vivo testing

After creating the antigen atlas containing a panel of many putative antigens possibly relevant for the specific immune response after MI, we sought to consecutively test it by in vitro T cell proliferation and antigen recall assays ex vivo. The method of choice was the ELISPOT assay, currently the most sensitive approach available to detect even small counts of antigen producing cells.

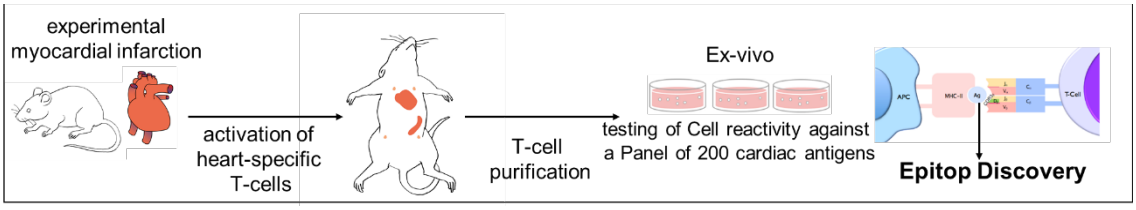

Figure 11 Model of experimental design
The experimental model illustrated, starting with Balb/c mice getting exposed to EMI and leading subsequently to an activation of heart specific T cells. Heart, mediastinal lymph nodes and spleen are extracted seven days after MI and purified for T cells. Ex-vivo these cells are tested for cell reactivity against a panel of ~200 cardiac antigens leading ideally to an epitope discovery.

4.2.1. T cell specificity in Balb/c

Balb/c mice have predominantly been used in the context of autoimmune myocarditis[108] for experimentation, especially concerning the effect of myosin. Moreover, our in-silico screening suggested that a higher number of cardiac antigens concerning several proteins, such as MYHCA, can be presented on the Balb/c MHC-II haplotype (I-A^d) compared to I-A^b. Therefore, we decided to primarily focus our in vivo antigen mapping experiments on the Balb/c strain. Nevertheless, further analysis on a C57BL/6J background followed.

4.2.1.1. Early T cell responses after myocardial infarction

Splenocytes as well as lymphocytes from mediastinal lymph nodes were purified from animals seven days (**Figure 12, 13, 16, 17, 18**) or 56 days (**Figure 14** and **15**) after EMI conducted by ligation of the left anterior descending artery or as a negative control group from sham thoracotomized mice. These cells were cultured in the presence of

denominated peptide pools (mostly 15 mers, MHC-II–restricted), as well as single incubation with $MYHCA_{614-628}$ peptide. Furthermore, two negative controls were implemented. Stimulation with the $OVA_{323-339}$ peptide as an irrelevant antigen, without any expression in the heart, as well as an incubation without any antigens at all and thus without any applied activation. These controls were crucial for acquiring information about general background cell activation, since all of the obtained data was normalized by the no-activation background and further compared to the values of activation by $OVA_{323-339}$. The ELISPOT Assay was used as a readout for antigen-specific stimulation by measurement of IL-2 and IFN-γ production. The number of activated, cytokine secreting cells detected in each well is indicated next to the corresponding representative well picture (**D** and **E**). The bar graphs display the group mean values, the SEM, and the distribution of each individual value. With a 2-tailed, unpaired *t*-test the statistical analysis was determined (**B** and **C**). $*P < 0.05$. This data was acquired from 3 independent experiments.

Figure 12, A-E, indicates that lymphocytes purified from the spleen of infarcted mice show a significant IL-2 response to MYHCA-derived epitopes, which is considered a readout for antigen-specific stimulation. On the contrary, sham-operated, non-infarcted mice did not show a similar response, but remained inactivated. When incubated with other, beforehand putatively relevant identified antigen pools, no IL-2 response was observed, illustrating the fact that MYHCA is a dominant cardiac antigen in the context of MI. This explicit heart-specific cardiac isoform has been shown to be relevant in the pathogenesis of experimental autoimmune myocarditis and this explicit MHC-II-restricted epitope, $MYHCA_{614–628}$, was deemed relevant in that disease model.[88,109] Confirming this role, our data, shown in **Figure 12, A, C,** and **E**, reveals similar T cell responses to the single $MYHCA_{614–628}$ peptide in infarcted Balb/c mice.

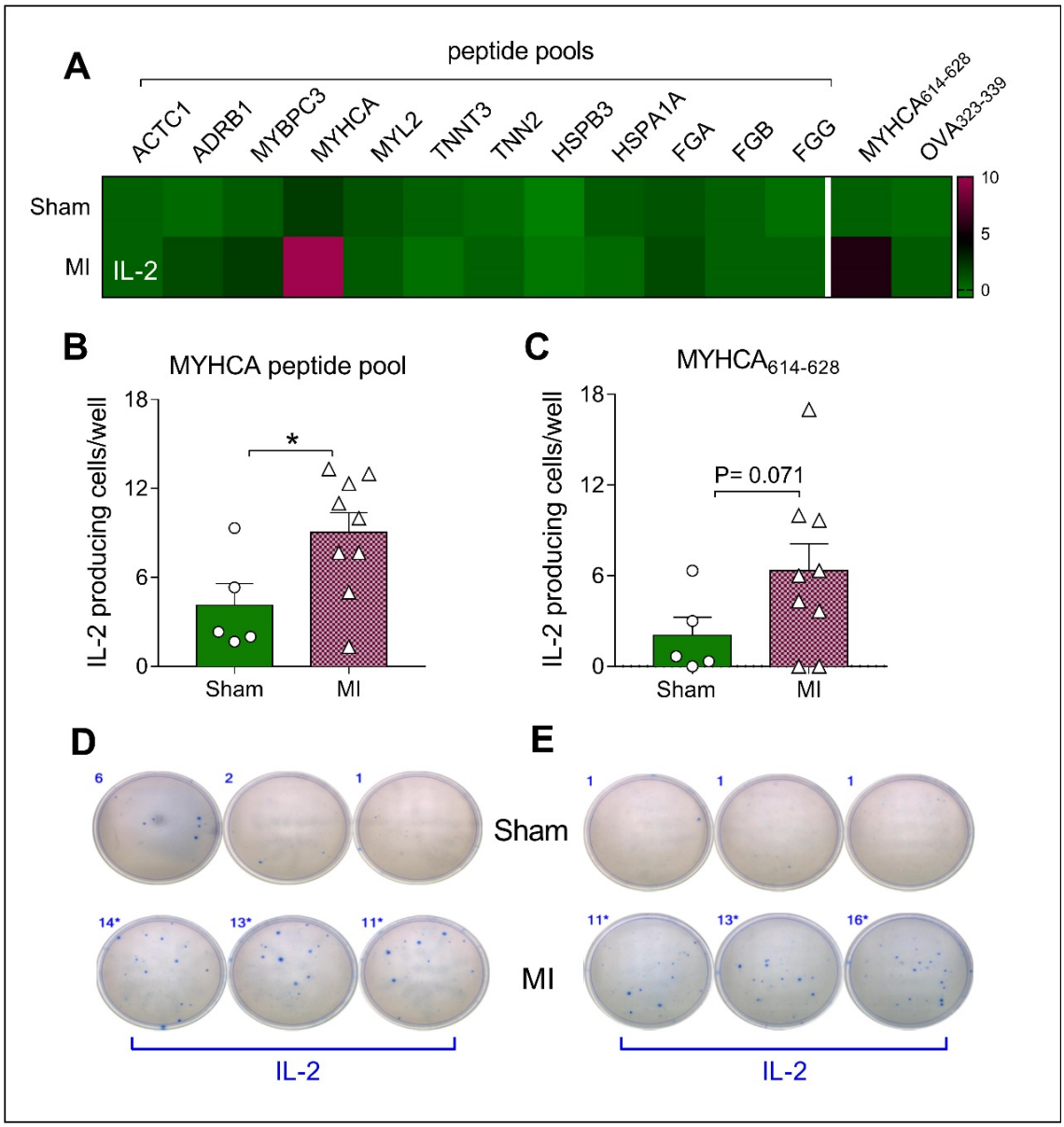

Figure 12 IL-2 response of splenocytes to antigens 7 days after MI

(**A**) Heatmap illustrating specific T cell responses to predefined putative antigens of interest quantified with elispot assays. (**B** and **C**) Quantification of IL-2–producing cells per well corresponding to the reaction towards (**B**) the MYHCA peptide pool and (**C**) $MYHCA_{614–628}$. (**D** and **E**) Examples of representative elispot well images of the corresponding antigens.

When comparing the results to those of the negative controls, it can be further noted that no cell activation by neither ovalbumin ($OVA_{323–339}$) nor the complete no activation group was observed.

Nevertheless, the obtained data on the IFN-γ response shows a different picture. No sign of activation to any of the peptide pools, including $MYHCA_{614–628}$, could be observed.

No significance was found for neither the comparison of the infarcted mice versus sham operated, nor $MYHCA_{614–628}$ versus $OVA_{323–339}$. (**Figure 13**).

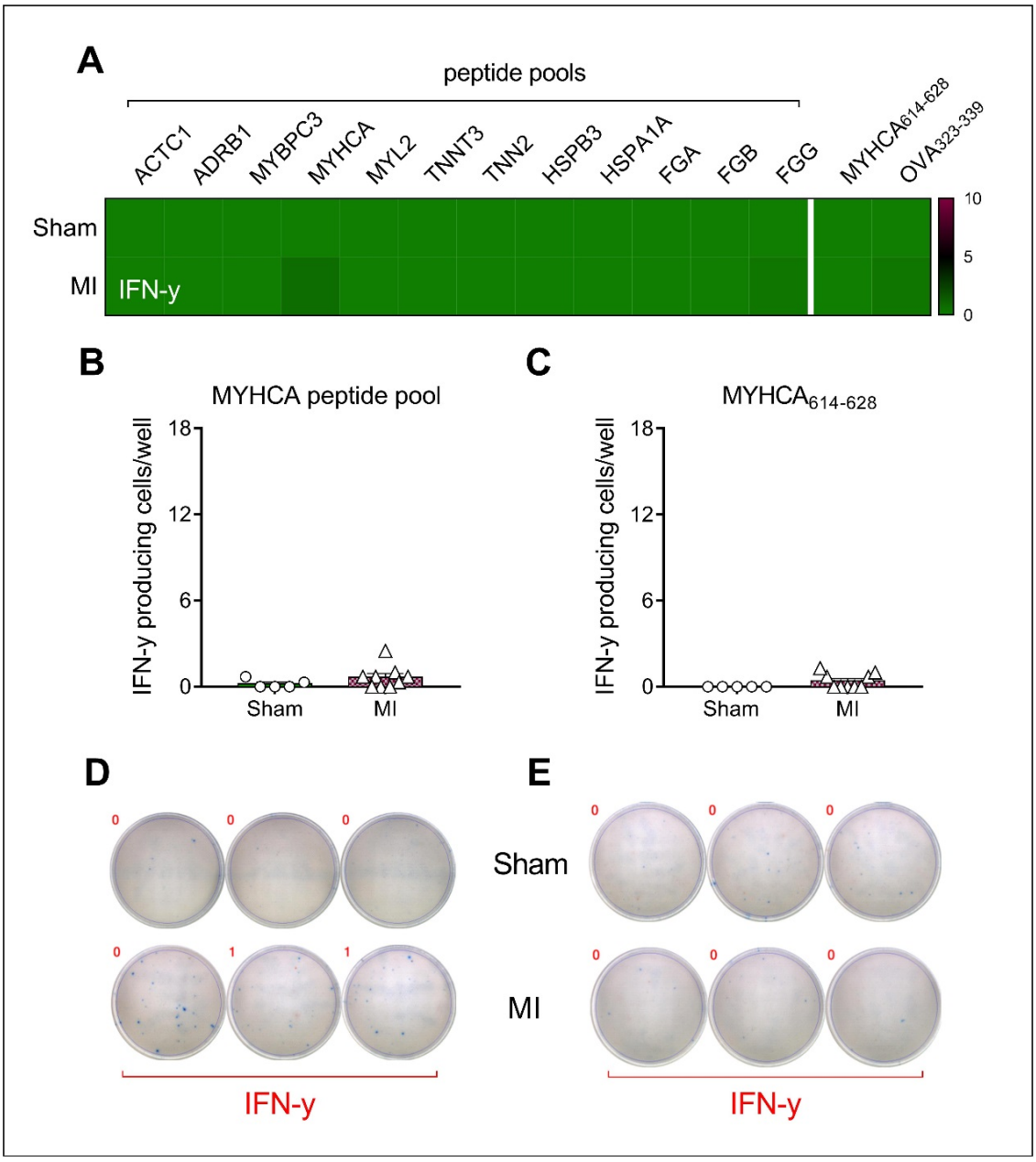

Figure 13 IFN-γ response of splenocytes to antigens 7 days after MI

(**A**) Heatmap illustrating specific T cell responses to predefined putative antigens of interest quantified with elispot assays. (**B** and **C**) Quantification of IFN-γ–producing cells per well corresponding to the reaction towards (**B**) the MYHCA peptide pool and (**C**) $MYHCA_{614–628}$. (**D** and **E**) Examples of representative elispot well images of the corresponding antigens.

4.2.1.2. Late T cell responses after myocardial infarction

In further experiments we focused on the reaction of splenocytes, purified from animals 56 days after EMI, to our antigen panel. Whereas 7 days mark the peak of the healing phase after myocardial injury, 56 days mark the chronic remodelling phase.

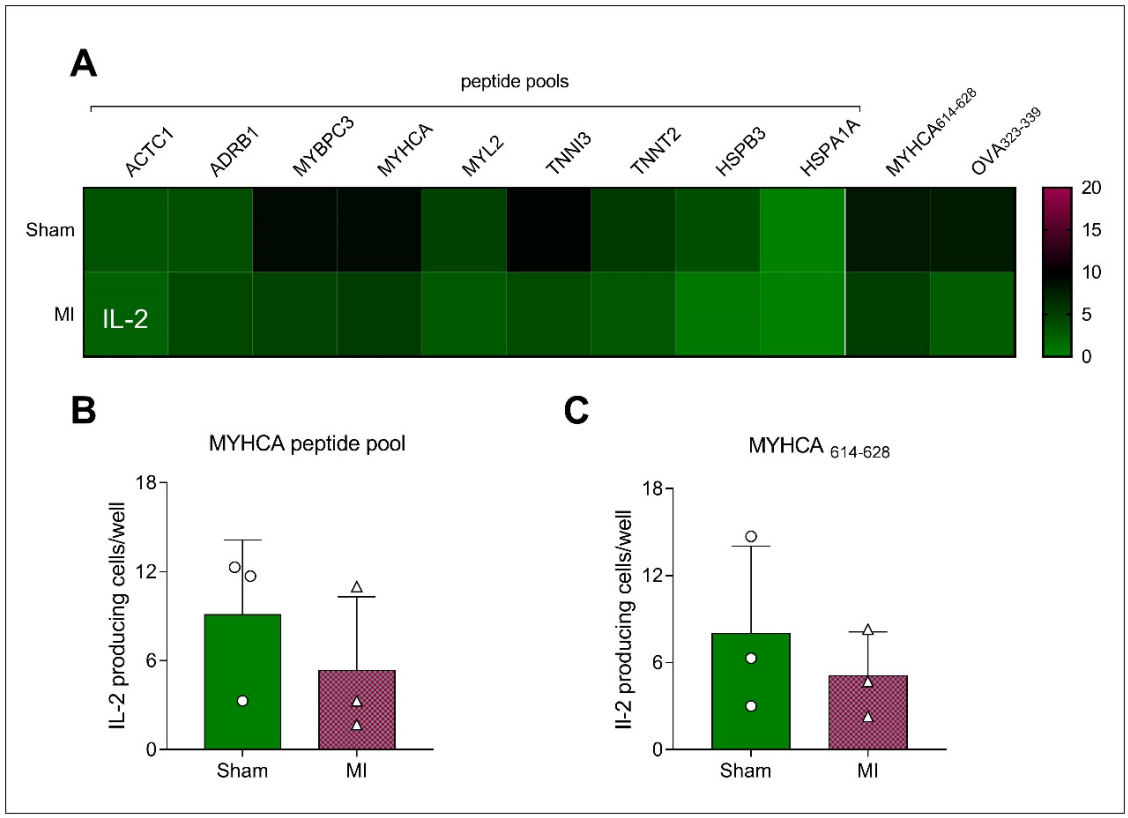

Figure 14 IL-2 response of splenocytes to antigens 56 days after MI
(**A**) Heatmaps illustrating specific T cell responses to predefined putative antigens of interest quantified with elispot assays. (**B** and **C**) Quantification of IL-2–producing cells per well corresponding to the reaction towards (**B**) the MYHCA peptide pool and (**C**) $MYHCA_{614–628}$.

When focusing on the IL-2 response of splenocytes towards the different antigen pools (**Figure 14**) 56 days after MI, a clear elevation of the amount of activated T cells by the MYHCA pool or the single $MYHCA_{614–628}$ in the infarcted animals, as observed seven days after MI, was not evident anymore. This could be indicating that the early post-MI specific T cell response is self-limiting and completely resolved at chronic stages. The corresponding data was acquired from one round of experiments and the bar graphs display again the group mean values, the SEM, and the distribution of each individual

value. With a 2-tailed, unpaired *t* test the statistical analysis was determined (**B** and **C**). $*P < 0.05$.

The IFN-γ response of splenocytes 56 days after MI matches the one after seven days. No apparent activation of IFN-γ producing T cells can be observed here either (**Figure 15**).

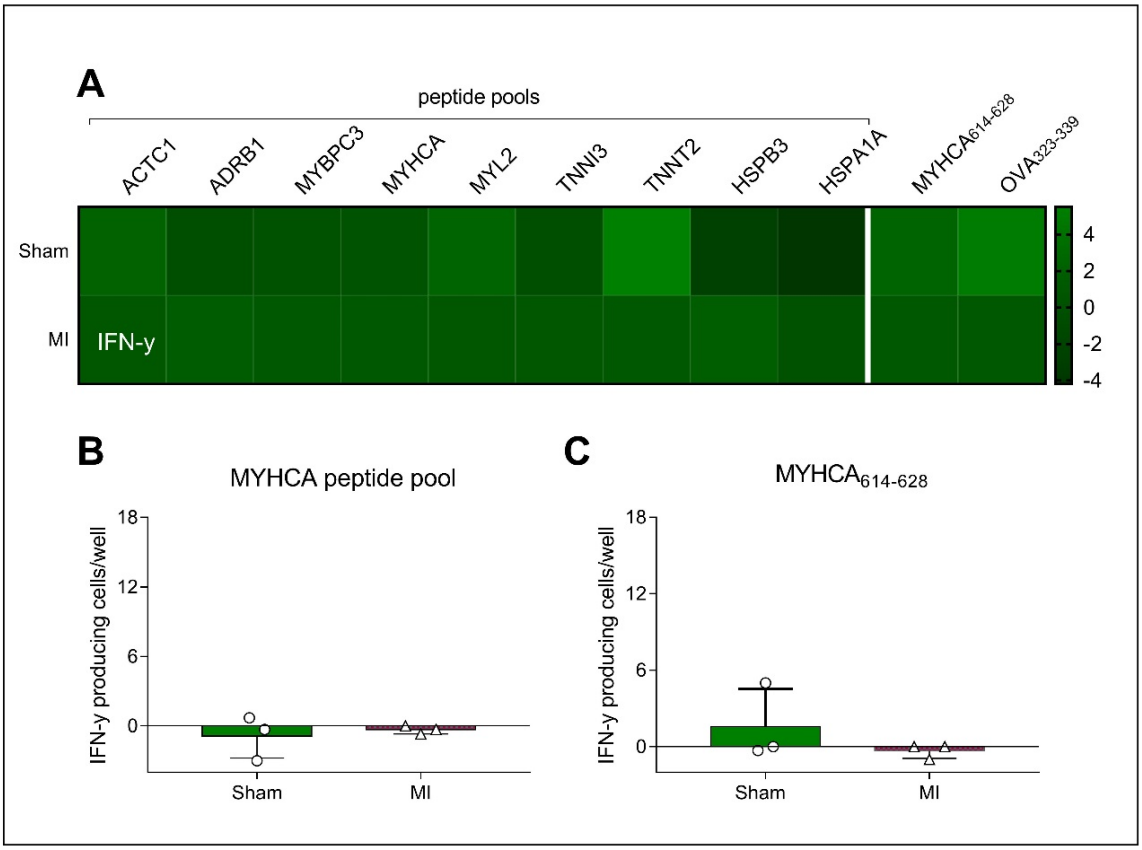

Figure 15 IFN-γ response of splenocytes to antigens 56 days after MI
(**A**) Heatmap illustrating specific T cell responses to predefined putative antigens of interest quantified with elispot assays. (**B** and **C**) Quantification of IFN-γ–producing cells per well corresponding to the reaction towards (**B**) the MYHCA peptide pool and (**C**) $MYHCA_{614–628}$.

4.2.1.3. Med-LN T cell responses after myocardial infarction

Due to a relatively small cell count within the mediastinal lymph nodes, all biological replicates from sham operated mice as well as separately from the infarcted ones were pooled into one metamouse. Only animals with a clear macroscopic infarction were pooled, nevertheless small along with middle and big MI's were mixed. A general enlargement of the mediastinal lymph nodes within the infarcted group, as widely

observed by our group[49], lead to a correspondingly higher cell yield of lymphocytes . The cell amount purified in the sham operated group was not enough to complete the elispot assay with our full panel, resulting in the testing of only the MYHCA pool and the single peptide $MYHCA_{614–628}$. This should be considered in the evaluation. A statistical analysis is due to the single figure comparison not possible, even though a clear difference can be observed.

The IL-2 response of lymphocytes from the mediastinal lymph nodes seven days after MI (**Figure 16**) matches the response of lymphocytes purified from the spleen (**Figure 12**). The activation in the T cells within the MI group relatively to the sham-operated group is at an even higher level in the mediastinal LNs compared to the spleen. This elevation was to be expected since the local heart draining LNs have a higher probability for specific $CD4^+$ T cells originating from the heart than e.g. the locally much more distant spleen.

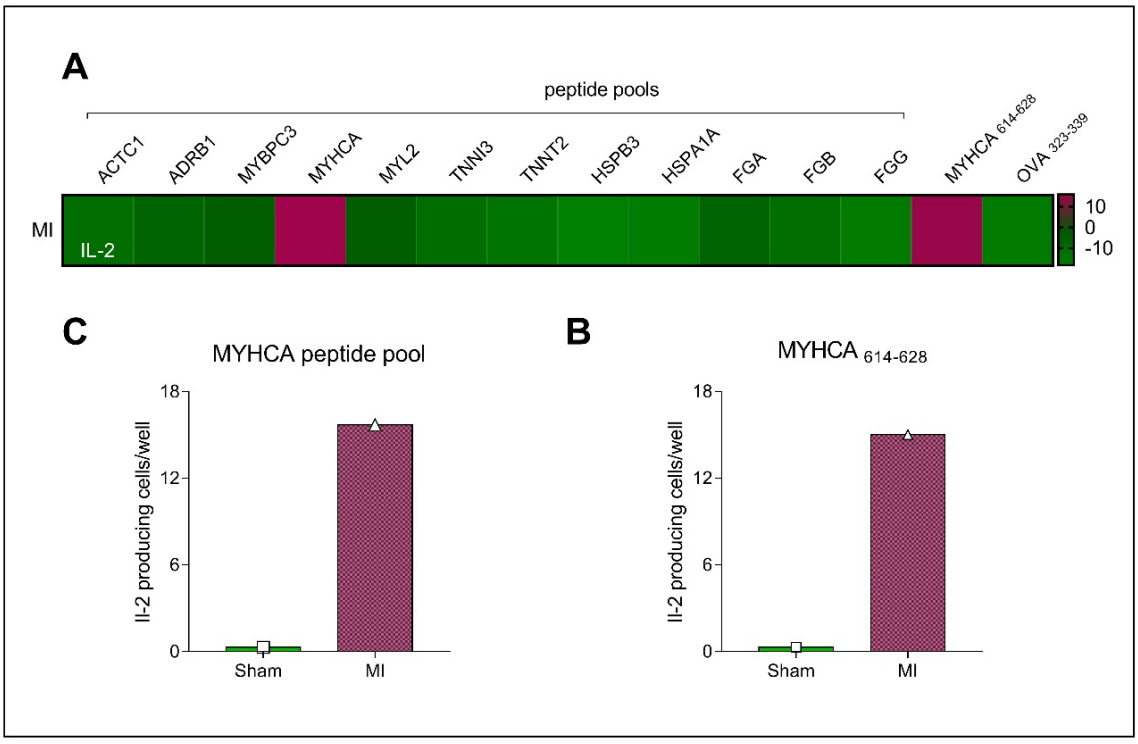

Figure 16 IL-2 response of lymphocytes from med-LNs to antigens 7 days after MI
(**A**) Heatmap illustrating specific T cell responses to predefined putative antigens of interest quantified with elispot assays. (**B** and **C**) Quantification of IL-2–producing cells per well corresponding to the reaction towards (**B**) the MYHCA peptide pool and (**C**) $MYHCA_{614–628}$. (**D** and **E**) Examples of representative elispot well images of the corresponding antigens.

Looking at the IFN-γ response, an already big baseline production in the non-stimulated wells could be noted. Normalization against this higher background followed as previously done before, however this higher IFN-γ background in the mediastinal LN data still distinguishes itself from the obtained data in the spleen, since no IFN-γ reaction at all could be observed there. This big baseline production may be explained by local post-MI inflammatory reactions.

Surprisingly, we found that the same MYHCA peptide pool along with the single peptide $MYHCA_{614–628}$ caused a suppression of that baseline IFN-γ response in the MI group compared to the sham-operated one (**Figure 17**). Studying the scale more closely and comparing the amount of IFN-γ producing cells, a major decrease relative to a rather small increase in the response of splenocytes (**Figure 13**) becomes clear.

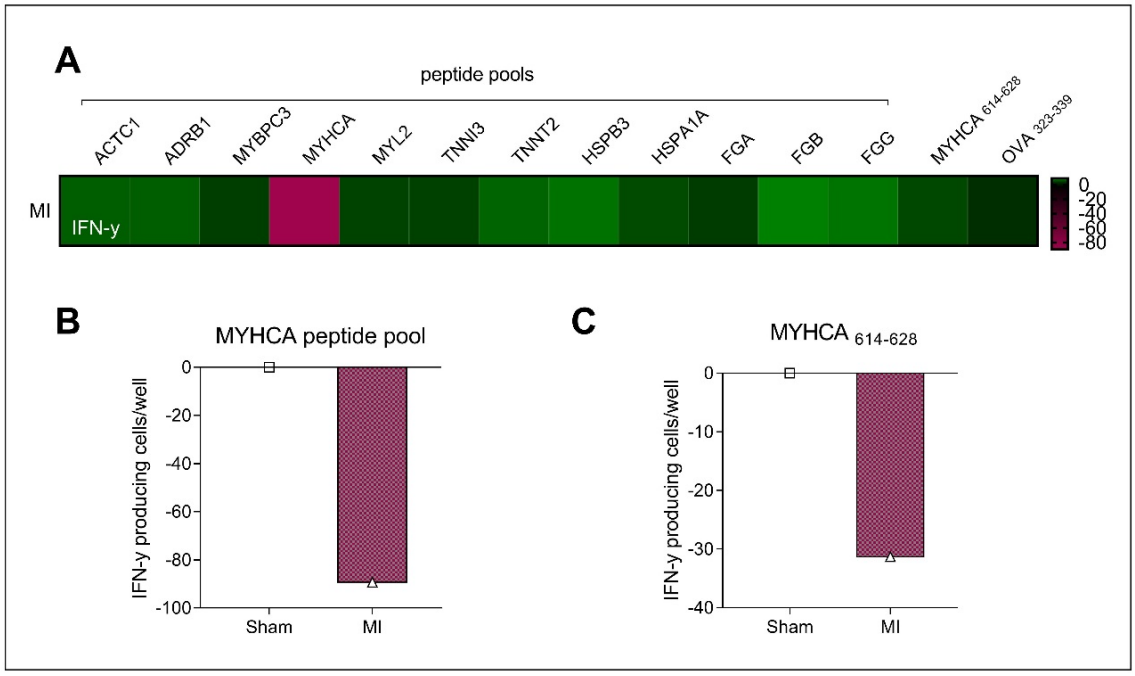

Figure 17 IFN-γ response of lymphocytes from med-LNs to antigens 7 days after MI

(**A**) Heatmap illustrating specific T cell responses to predefined putative antigens of interest quantified with elispot assays. (**B** and **C**) Quantification of IFN-γ–producing cells per well corresponding to the reaction towards (**B**) the MYHCA peptide pool and (**C**) $MYHCA_{614–628}$. (**D** and **E**) Examples of representative elispot well images of the corresponding antigens.

Moreover, a legend-plex assay was conducted with supernatant from the elispot assay of the lymphocytes from the mediastinal lymph nodes of animals seven days after MI (**Figure 18**). Additional to IL-2 and IFN-γ we investigated a broader spectrum of cytokines (IL-2, IL-4, IL-5, IL-6, IL-10, IL-13, IFN-γ, TNF-α) with this assay. The results on IL-2 and IFN-γ can be neglected due to this method being consecutively conducted after the primary Elispot.

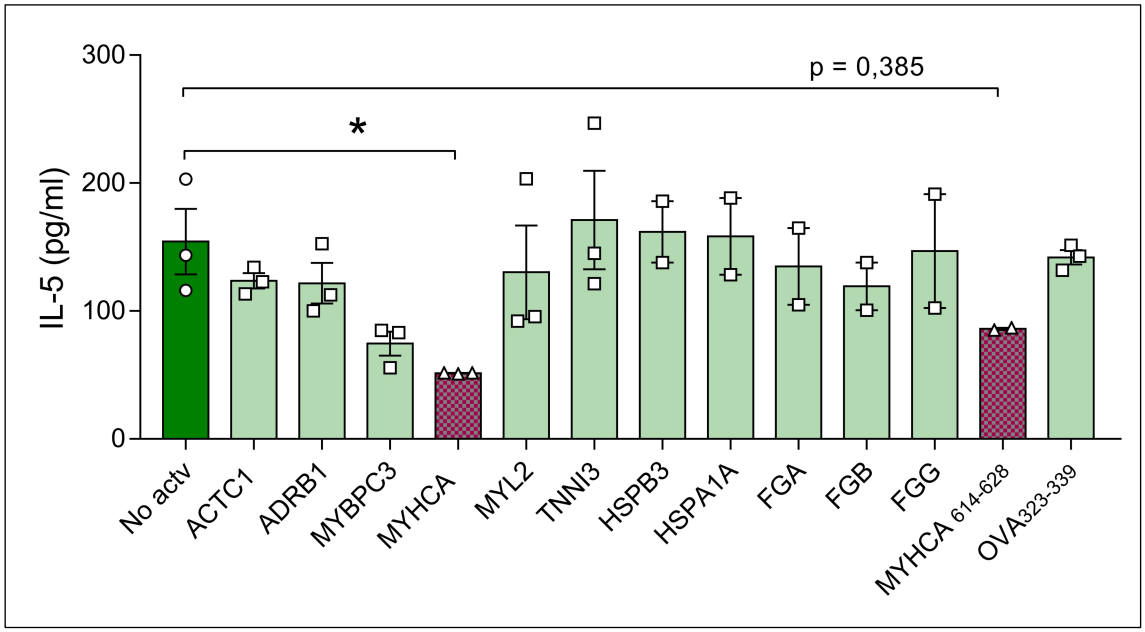

Figure 18 IL-5 response of lymphocytes from med-LNs to antigens 7 days after MI
Bar graph illustrating the IL-5 concentration in the supernatant after cell culture of lymphocytes from mediastinal lymph nodes extracted seven days after MI. These cells were stimulated by predefined putative antigens. The initial supernatant volume of 150 µl was diluted with 80µl. Parameters were adjusted correspondingly. Samples were divided into three technical replicates, originating though from biological replicates pooled into one metamouse.

Examining the supernatant for these other cytokines our results revealed only a clear result for IL-5. All peptide pools and single peptides, as well as negative controls lead to an increased activation of IL-5 producing cells in the MI group resulting in a big baseline production. Conversely, the MYHCA peptide pool shows a significant suppression on comparison with the negative control with no activation. This suppression is the same response we were previously able to observe for IFN-γ (**Figure 17**).

The difference in background activation between MI and Sham group must be noted, highlighting again a probable higher activation in the MI group by local post-MI inflammatory reactions. The MYPBC3 pool also seems to be leading to a slight suppression of IL-5 similar to the one by the single $MYHCA_{614–628}$ peptide. This increases the amount of putative relevant epitopes in the activation of heart specific $CD4^+$ T cells that can be further investigated in the future.

Taken together, the results from the med-LNs confirm that MYHCA is a major dominant antigen, but also suggest that at the local lymph nodes the responder cells seem to acquire a rather undifferentiated (IL-2) or suppressor phenotype (less IFN-γ/IL-5, Th1/Th2).

4.2.1.4. Hybridoma model

The following experiments concerning hybridomas were primarily done with Elena Vogel's technical assistance.

The scarcity of cells is often the limiting factor for proper investigation. The generation of hybridomas, by fusion of lymphoma cells with heart specific $CD4^+$ T cells leads to an unlimited source of cells for further experimentation and in some cases, with only very little cell yield, describes the only possible solution for analysis.

The fusion experiments for hybridoma synthesis have been proved to be more challenging than expected. For the fusion experiments the following cell yields were used, which were generally pooled samples to overcome cell count limitations. From the spleen in total $4{,}0x10^8$ cells in the MI and $1{,}65x10^8$ cells in the Sham group were used, corresponding to an amount of $3{,}4x10^7$ (MI) and $1{,}4x10^7$ (Sham) for the pooled mediastinal LNs. Furthermore, the following cell yield was acquired from the heart by cell sorting: $1{,}0x10^5$ cells for the MI group and $2{,}6x10^4$ for the Sham group. We were able to fuse these specific $CD4^+$ T cells, derived from the mediastinal lymph nodes as well as the spleen of Balb/c mice seven days after EMI, with thymoma cells (BW 5147gal). Our main objective was the generation of a limitless source of specific $CD4^+$ T cells for more thorough testing. The fusion yield differed corresponding to the lymphocyte origin and is summarized in Table 5. We observed more fusions after MI than in the sham-operated

group, reinforcing the notion of an increased activation of T cells after infarction, since only activated cells can create fusions. Nevertheless, the fused cells were unstable, and we could not cultivate them for a long-term period. Given the great challenges of producing hybridomas of non-immunized animals, we decided against pursuing this approach further. In future studies, the specificity of med-LN $CD4^+$ T cells shall be studied using other state-of-the-art methods, such as single-cell TCR-sequencing followed by TCR cloning and testing.

Table 5 Hybridoma fusion yield

	MI	Sham
Spleen	11 pools (5 clones ea.)	—
Med.-LN	4 pools (5 clones ea.)	2 pools (5 clones ea.)
Heart	—	—

4.2.2. T cell specificity in C57BL/6J

4.2.2.1. Early response after myocardial infarction

Additionally to the findings from the experimentation on Balb/c mice we also used our previously defined epitope list for the I-A^b haplotype to investigate T cell specificity after MI against a C57BL/6J background.

Lymphocytes purified from the spleen of infarcted C57BL/6J mice seven days after EMI showed a significant IL-2 response on incubation with several of our proposed antigen pools: α actin, cardiac muscle 1 [ACTC1] (**Figure 19, A-C**), myosin-binding protein C3 [MYBPC3] (**Figure 19, A, D, E**) and myosin heavy chain α [MYHCA] (**Figure 19, A, F, G**). Sham-operated, non-infarcted mice did not show a similar response, but remained inactivated. The significance was proved by a two-way ANOVA followed by turkey post hoc test for multiple comparisons. (**Figure 19**). To the best of our knowledge, this is the first evidence for heart-specific T cell responses in this mouse strain.

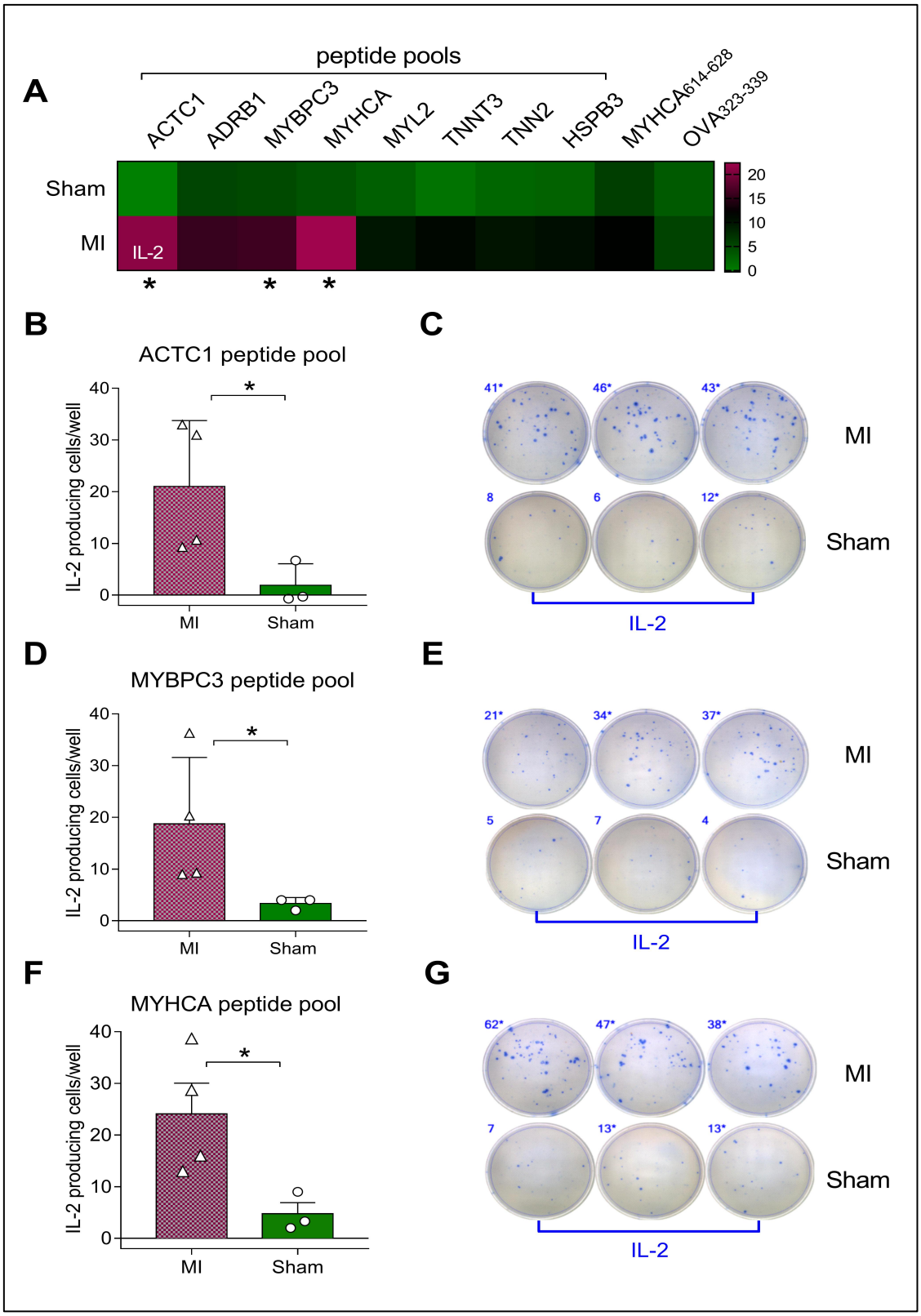

Figure 19 IL-2 response of splenocytes to antigens 7 days after MI in C57BL/6J mice

(**A**) Heatmap illustrating specific T cell responses to predefined putative antigens of interest quantified with elispot assays. (**B**, **D** and **F**) Quantification of IL-2–producing cells per well corresponding to the reaction towards (**B**) the ACTC1 peptide pool, (**D**) the MYBPC3 peptide pool and (**F**) the MYHCA peptide pool. (**C, E** and **G**) Examples of representative elispot well images of the corresponding antigens.

However, no IFN-γ response as sign of activation to any of the peptide pools, including $MYHCA_{614–628}$, could be noted. This data corresponds to our findings obtained from Balb/c mice. Some individual IFN-γ activation was observed, yet by the rare and patternless nature of it we expect this to be due to contamination or other activation of cells by chance (**Figure 20**).

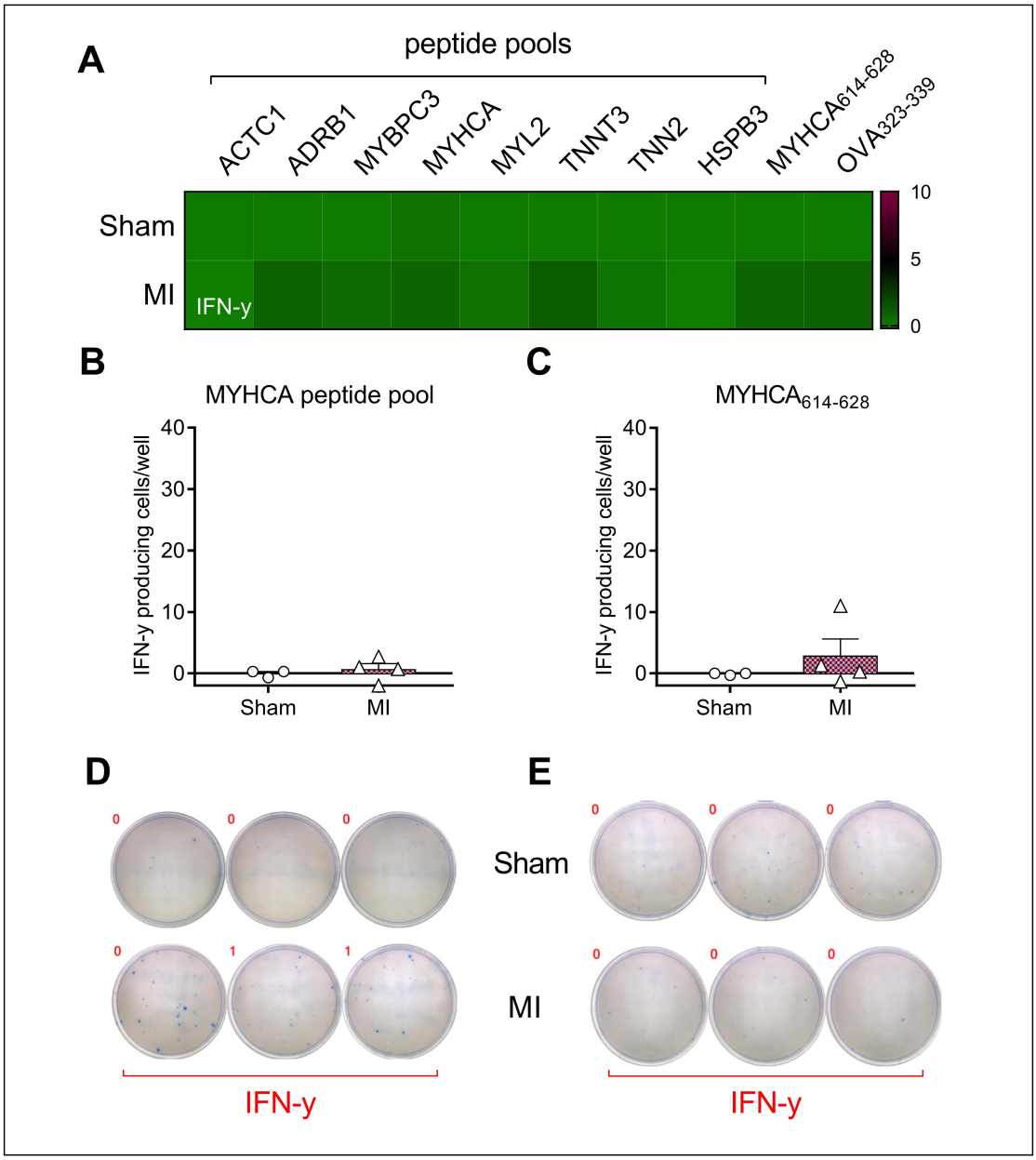

Figure 20 IFN-γ response of splenocytes to antigens 7 days after MI in C57BL/6J mice
(**A**) Heatmap illustrating specific T cell responses to predefined putative antigens of interest quantified with elispot assays. (**B** and **C**) Quantification of IFN-γ–producing cells per well corresponding to the reaction towards (**B**) the MYHCA peptide pool and (**C**) $MYHCA_{614–628}$.

4.2.3. Balb/c vs. C57BL/6J

A different set of putative epitopes was discovered for Balb/c and for C57BL/6J (See **Table 6** and **7**, **Appendix**). On comparison of the early T cell responses after MI Balb/c mice developed specific T cells towards the myosin heavy chain α [MYHCA], whereas in C57BL/6J not only myosin heavy chain α [MYHCA] (**Figure 19, A, F, G**), but also α actin, cardiac muscle 1 [ACTC1] (**Figure 19, A-C**) and myosin-binding protein C3 [MYBPC3] (**Figure 19, A, D, E**) evoked a significant production of antigen specific T cells.

Generally, the overall spots produced, corresponding to the amount of IL-2 producing cells, were higher in C57BL/6J than Balb/c. This could be due to numerous reasons and still remains to be further elaborated in the future.

5. DISCUSSION

5.1. Summary

Within the last decades the field of Immunocardiology emerged. The influence of the immune system on several cardiac mechanisms has been scrutinized, naming some fields of importance: metabolism[110], rhythm[111,112], autoimmune myocarditis[50,113,114], MI[21,22], myocardial aging[115] and heart failure[10,116-118]. Increasingly not only the relevance of the innate[30], but also of the adaptive immune system has been discovered and focussing on MI especially T cells have been shown to play a major role[21,48]. Nowadays many options for the prevention[119,120] of an acute coronary syndrome as well as treatment for possible long-term defects in the form of heart failure[121] have been established. The huge potential for therapeutical interference right after myocardial injury is left totally untouched. The underlying immunological phenomena of early healing after MI are recently being dissected with various views on the salutary[42,45,49,51,53] or detrimental[10,36,115,117] immunological effects. Their specificity, whether featured by a general response to the inflammatory myocardial milieu or driven by specific antigens released by dying cardiomyocytes, has not been addressed so far.

In this thesis we sought to combine a hypothesis driven approach with a broad screening method in order to identify cardiac antigens relevant in the myocardial healing process after infarction. With an in-silico prediction tool, supplied by the website IEDB, a catalogue of 399 antigens, distributed over 12 proteins and two haplotypes was created. Hereby focussing on antigen presentation via MHC-II and only on epitopes with a certain affinity and binding potential. The isolated epitopes were then tested via EMI in mice and subsequent immunological antigen recall assay. Here we could find a relevance for α $(MYHCA)_{614-628}$ as a dominant cardiac antigen triggering post-MI $CD4^+$ T cell activation in Balb/c mice. The in vivo relevance of these findings has been further confirmed by other lab members, who transferred infarcted Balb/c mice with transgenic T cells engineered to express a TCR recognizing the exact same epitope (to be detailed below).[49] The discovery of the specific antigens gives the advantage of allowing us to elaborate more refined tools to track and characterize these specific cells. These experiments advance us

in that direction, and we can foresee to have these tools available not only for Balb/c mice, in the form of TCR-m cells, but also for C57BL/6J.

Deducing from our data an additional significance of several other α (MYHCA) epitopes can be expected but remains to be exactly defined. For further analysis T cell hybridomas have been created to be able to test epitopes on a much larger scale.

These experiments can be a stepstone to further research and may lead to a significant translational meaning in the clinical setting concerning the improvement of cardiac healing and prevention of long-term heart failure by defining new putative pharmacological targets.

5.2. Balb/c versus C57BL/6J difference

For a very long time various autoimmune disease susceptibilities across different mouse strains have been observed.[122,123] Especially a diverged susceptibility to experimental autoimmune myocarditis has been detected very early on.[124,125] Balb/c mice seem to be susceptible to autoimmune myocarditis, whereas C57BL/6J were found to be resistant.[88] Different inter strain disease susceptibilities were also observed in the context of autoimmune encephalomyelitis[126] or diabetes[127].

Our epitope predictions revealed an overall of 193 epitopes for the I-A^d haplotype, corresponding to Balb/c mice (**Table 6, Appendix)**, and 206 for I-A^b, corresponding the C57BL/6J strain (**Table 7**, **Appendix**). Looking at myosin heavy chain α [MYHCA] a shift towards the Balb/c mice becomes apparent: 77 epitopes for I-A^d and 13 epitopes for I-A^b. With an increased amount of putative presentable epitopes, a shift of disease susceptibility towards Balb/c mice may be deduced within our findings. On comparison of the early T cell responses after MI Balb/c mice developed a significant antigen specific T cell response towards MYHCA (**Figure 12**). However, C57BL/6J responded not only towards MYHCA, but also ACTC1 and MYBPC3 significantly (**Figure 19)**.

This response does not match our initial hypothesis concerning disease susceptibility. According to that, Balb/c mice should have presented a more intense activation for MYHCA than C57BL/6J mice. More astonishing is though that C57BL/6J seem to show a

diverse response in contrast to a response dominated by a single dominant antigen in Balb/c mice. Moreover, Balb/c mice recognize a Myh6 peptide that is located exactly in the Myh6/7 diverging site, concluding that a differentiation between the cardiac and the skeletal muscle is made. However, even though C57BL/6J mice can also respond to Myh6 epitopes, the identified epitopes are located in regions that overlap with Myh7 in the skeletal muscle, implying that they are not exactly heart specific epitopes. The functional consequence of having such polyclonal vs. oligoclonal and heart specific vs. muscle specific responses remains unknown and an open point for very interesting future research.

It should be noted that the initially proclaimed vulnerability of Balb/c mice within the context of MI would match the one to experimental autoimmune myocarditis. Genetically predisposed mice can be induced to develop T cell mediated myocarditis by immunization with cardiac myosin. [88] Balb/c mice have been shown to develop autoimmune myocarditis, whereas C57BL/6J mice do not.[89]

Taking a closer look at the myosin heavy chain II protein structure in general two major myosin fragments can be distinguished, each consisting of a larger N-terminal heavy meromyosin (HMM) and a C-terminal light meromyosin (LMM). The former HMM is built of two globular heads (termed sub-fragment S1), which are connected to a hinge structure (S2), thereby building a bridge between the HMM and the long dimeric coiled-coil rod (LMM). When comparing MYHCA alpha and MYHCA beta a 93% homology can be observed. Due to these 7% of nonoverlapping structures, completely different immune responses can be triggered, which confirms the notion that within these nonoverlapping areas important amino acid residues have to be found.[22,88] Pummerer et al. predicted the capacity of MYHCA derived specific peptides to be presented at I-A^d and I-A^b murine MHC-II haplotypes.[88] Another group compared the myosin-reacting autoantibodies produced in mice, rats and humans and recognized epitopes at the S2 regions, whereas the distribution of most T cell MHC-II restricted antigens is rather focused on the S1 region.[22]

Finally the match of the epitopes from our research to some of the epitopes found already back in the 90s within the context of myocarditis[88] enhance the implication of their relevance in MI.

Mouse strains like Balb/c and C57BL/6J are isogenic, specifying that the haplotype of all individuals is expressed exactly the same. Humans on the other hand exhibit thousands of different haplotypes. Thus, corresponding to the findings in the murine model, a different disease susceptibility between individuals can be expected. Tang et al. encouraged with their results the speculation about the prognostic potential of HLA phenotyping and the determination of the TCR repertoire of circulating T cells in chronic heart failure patients.[128]

5.3. Cardiac antigens in myocarditis and myocardial infarction

The relevance of cardiac antigens within the context of autoimmune myocarditis has been thoroughly investigated.[129] The transfer of T cells from diseased mice to healthy recipients leads to the development of cardiac injury, concluding that myosin induced acute myocarditis is a T cell mediated disease.[113] Early on MYHCA has been shown to be constitutively processed and presented to $CD4^+$ T cells by antigen presenting cells in the heart draining mediastinal lymph nodes. Even in healthy mice under steady state conditions, in the absence of cardiac damage, this process was observed.[54,130] According to new findings these healthy mice show specific alterations to the heart draining lymph nodes during physiological aging.[115] Additionally A/J mice derived T cell hybridomas specific for mouse cardiac myosin have been generated and used to demonstrate that endogenous myosin/I-Ak complexes are constitutively expressed on antigen-presenting cells in the heart.[131] In conclusion, all this data is pointing towards myosin as a dominant cardiac antigen.

Focussing on myosin, the heart-specific myosin isoform displays a perfect example as a source for cardiac antigens, since it is selectively expressed only in the myocardial tissue. The major isoform in the myocardium is myosin heavy chain alpha (MYHCA), derived from the gene Myh6. As mentioned before, Pummerer et al. were able to identify relevant epitopes for the development of autoimmune myocarditis within the Myhca gene by

testing the nonoverlapping areas of the cardiac alpha isoform and the skeletal beta isoform. At this point the specific MHC-II-restricted epitope $MYHCA_{614–628}$ has been deemed pathogenically important in experimental autoimmune myocarditis for the first time.[88]

To follow this line of thought a transgenic mouse strain has been developed, exclusively expressing transgenic T cell receptors (TCRs) specific for the immunogenic MYHCA peptide ($MYHCA_{614–629}$) presented in the MHC-II context. Consequently, the high number of MYHCA reactive T cells circulating in the these so called TCR-M mice result in spontaneous development of progressive myocarditis associated with ventricular wall thickening but lacking evident systolic dysfunction. Another approach can be used via non-transgenic mice. They contain physiologically only a low prevalence of MYHCA reactive T cells and for further testing TLR stimulation with CFA or LPS is needed. Via transfer of TCR-M-Cells to Balb/c mice autoimmune myocarditis could be induced. The model of TCR-M mice presents a great model for further investigation, particularly useful to research the development of autoreactive T cells without the influence of exogenous TLR agonists.[117] These experiments demonstrated $MYHCA_{614–629}$ to be an important cardiac antigen in the pathogenesis of autoimmune myocarditis in inbred mice.[117]

Inflammation is widely perceived as a mediator of tissue damage, although it encompasses so much more: a path to healing. Nindl et al. were able to demonstrate the positive influence of pro-inflammatory factors on cardiac disease progression. Interferon gamma (IFN-γ) was depicted as the central player. However, their experiments revealed a worsened exhibition of myocarditis in IFN-γ-deficient mice, thus proving the essential role of this inflammatory arm of the immune system in triggering subsequent anti-inflammatory compensatory responses.[22,117]

An involvement of myosin, especially $MYHCA_{614–629}$, in myocarditis seems thoroughly investigated. The conclusion that they might be relevant in the context of MI as well, has been increasingly discussed. Several independent studies agree on the presence of anti-myosin, anti-actin and anti-troponin autoantibodies in the sera of patients with MI, ischemic heart failure and even under physiological conditions.[132-135] Anti-myosin antibody titres have been also correlated with poorer prognosis, making them a putative

prognostical marker in clinical diagnostics.[136] However, questioning whether these auto antibodies contribute to post-MI remodelling is still highly debated.

Nevertheless, it has to be considered that elevated cardiac antigens, particularly anti-myosin antibody titres, are merely a readout for myocardial injury, without a direct implication to disease progression. In accordance to that, an elevated anti-myosin and anti-troponin titre was found to correlate with higher circulating levels of troponin I, which serves as a biomarker for cardiomyocyte necrosis.[133]

Arguing against this line of thought is experimental data suggesting a key role of anti-myosin antibodies in mediating post-MI remodelling and heart failure.[21,47] Adding specific anti-myosin IgGs purified from patients with ischemic heart disease to cardiomyocytes for instance, leads to in vitro impairment of contractility.[137] Moreover, in susceptible mouse strains MYHCA adsorbed in adjuvants can cause autoimmune myocarditis and foster the deposition of heart-reactive autoantibodies.[138] In alignment to that is the observation that heart failure may be induced in Balb/c mice after transfer of affinity-purified IgGs from myocarditis patients.[139] A cross-reaction between anti-myosin autoantibodies purified from rats and epitopes on beta-1-adrenergic receptors (ADRB1) has been observed, resulting in a stimulation of the downstream signalling pathways.[140] This is especially interesting, since our experiments included the testing of an epitope panel, derived from the beta-1-adrenergic receptor.

As opposed to autoimmune myocarditis, the transfer of lymphocytes obtained from infarcted donors to healthy recipients showed no sign of myocardial injury.[49] Therefore the conclusion, that during the early healing phase after MI the T cell mediated autoimmune response seems not pathogenic, is further stressed.[49]

Finally our experiments were able to identify cardiac myosin (MYHCA) as a dominant cardiac antigen also in the context of MI, by on the one hand showing a significant reaction towards myosin, on the other hand through our “negative” results for all other tested peptide groups. This unbiased method lead to the beginning of the dissection of the role of MYHCA-specific T cell responses in the wounded myocardium.[49]

5.4. Myosin-specific T cell responses triggered by myocardial infarction

Recently experiments of our group were able to identify the in vivo functional relevance of $MYHCA_{614–629}$ for the first time. Generally speaking we investigated whether heart-specific T cells exert salutary or detrimental effects in the context of MI.[49] The hallmark of autoimmune diseases is T cell autoreactivity. Nevertheless, it can also promote self-maintenance and foster tissue repair. The foundation for all further testing was laid by the epitope mapping experiments, naming myosin heavy chain α (MYHCA), especially $MYHCA_{614–628}$, a dominant cardiac antigen involved in triggering $CD4^+$ T cell activation in Balb/c mice after MI. $MYHCA_{614–629}$-specific $CD4^+$ T cells (TCR-M Cells) were transferred to infarcted mice, where they selectively accumulated in the myocardial tissue and mediastinal lymph nodes (med-LNs). Additionally, they acquired a T_{reg} phenotype with a distinct prohealing gene expression profile mediating cardioprotection.[49] Further research revealed myocardial T_{regs} in autopsy samples from patients with a history of MI. By CXCR4 radioligand marking enlarged med-LN with increased cellularity were spotted in PET/CT imaging in patients with MI. The size of med-LN was shown to be proportional to infarct size as well as cardiac function. Summarizing, the results published by Rieckmann et al. present evidence of the induction of pro-healing T cell autoimmunity in mice after MI, at the same time confirming the existence of an analogous heart/med-LN/T cell axis in patients with MI.[49]

5.5. New experimental tools

During this study several experimental tools have been generated that present a potentially meaningful resource for further research in the future.

The murine antigen atlas (see appendix) incorporates a full analysis of the transcriptome of the main 12 proteins deemed relevant as putative cardiac antigens in the context of MI. A compilation of epitopes per protein with high affinity and high probability of presentation have been collected. Our resource were the human antigen atlas for the exact amino acid sequence (FASTA sequence) and expression in the heart, and the IEDB - Immune epitope database and analysis resource - website for epitope sequences,

affinity and presentation probability. After using the IEDB database as source for our experiments, we were thrilled to be able to incorporate our newly generated data in turn into the website. Additional analysis on these epitopes can follow, also conducted by other groups, to complete our still limited understanding of this topic.

Furthermore, one could build on the knowledge from this study to generate new tools to track the responses in C57BL/6J mice, which is the most common strain used in basic research in cardiology.

5.6. Translational considerations

Myosin heavy chain α (MYHCA), especially $MYHCA_{614–628}$, has been deemed a dominant cardiac antigen involved in triggering $CD4^+$ T cell activation after MI in Balb/c mice. The translational potential of MYHCA and the question of whether it presents a relevant peptide also in humans is of crucial interest. Here the disease susceptibility of different mouse strains has to be taken into account as well as the fact that all experiments have been conducted with isogenic mouse strains, whereas humans display a huge HLA polymorphism.

On a further note Gil-Cruz et al. were able to show a relevance of myosin in humans with a specific DQB hablotype.[141] As discussed before, the HLA polymorphism has been connected to a lot of different disease susceptibilities. Certain HLA types are associated with particular diseases. Our experimental findings concerning a relevance of $Myhca_{614-628}$ in MI have been proven on a Balb/c background. C57BL/6J mice did not show the same response. Can we then even deduce a significance in humans? Generally, this is a limitation of all murine models. But also experiments behind a certain HLA type in humans leave the question open, whether this can be applied for all HLA types or only certain ones.

Concluding, our experiments identified the immunological response after MI to be antigen specific and discovered MYHCA as a relevant cardiac antigen source. A lot of follow-up experiments on different immunogenic backgrounds as well as more human studies have to be pursued to understand the full complex picture. However, these

results are first promising potential steps towards influencing the cardiac healing process positively after myocardial injury.

5.7. Outlook and opportunities

As of today, acute MI can be treated with good therapeutic and interventional options and the progression of remodelling can be somewhat attenuated trying to prevent the development of chronic heart failure. Nevertheless, there are no means available to support the myocardial healing process that bridges these two conditions. No biomarkers are currently available to predict or monitor the myocardial healing process. Early interference of adverse healing and remodelling is therefore not possible until a critical, then clinically apparent, heart failure stage is reached. This exhibits the unmet need to better understand the immunological underlying phenomena of myocardial healing. A multidisciplinary approach, bridging cardiology and immunology shows tremendous promise for personalized immunotherapeutic interventions as treatment option. A correlation between the results from our antigen recall assays and the clinical findings (e.g., infarct size) reinforces the clinical relevance of this approach. The identified epitope $MYHCA_{614–628}$ may be a promising target for specific immune therapies, modulating the healing process early on and preventing long term heart failure.

First and foremost, the striking data from the epitope screening on C57BL/6J background opens up many questions. How much is the haplotype involved in cardiac T cell activation after MI? Are there specific epitopes to be identified? What does the differing data between Balb/c and C57BL/6J mean for our translational considerations and the HLA polymorphism in humans? These questions amongst others should be further elaborated, which could lead to a better understanding of the immunological mechanisms after MI.

The generated T cell hybridomas display a great tool for more thorough analysis. We were able to generate several fusions for hybridomas, though the final generation was not completely successful. Typically, hybridomas are generated through several rounds of immunization. In contrast, the MI stimulation is far less potent, explaining the difficulties in the synthetizing process. The scarcity of eligible T cells purified from the Med-LN or the

heart increased the complexity further. So far, we were not yet able to synthesize hybridomas from T cells derived directly from the infarcted heart. In the future, this would give us more insight into the immunological process after MI and supply data to compare and to analyze the heart, mediastinal lymph node and spleen axis. Nevertheless, by having an unlimited supply of cells, in the form of hybridomas, at our disposal many more experiments can be conducted. The discrimination of the myosin related single epitopes. Discovery of even other epitopes of interest by systematic investigation of more cytokines. And therefore finally, the understanding of the heart specific immunological responses relevant for the healing process after myocardial injury.

Previously it was shown that by using MHC class II/IAk tetramers cardiac myosin heavy chain-α-specific $CD4^+$ cells can be detected.[142] MHC tetramers are molecular constructs that mimic the surface of antigen-presenting cells that are loaded with a particular epitope of interest. These constructs can be used to probe specific T cells carrying receptors that are complementary to that specific MHC / peptide. Since these constructs can be conjugated with fluorescent dyes, they can be used to track antigen-specific T cells using flow cytometry. Transferring this approach would give us promising insight into the in vivo distribution and activity of cardiac antigen specific T cells. The acquisition of mouse I-A^d -Myhca tetramers, as originally planned, did not follow through. The team is currently in the process of sourcing similar reagents. Most likely, however, this will take more time and will only lead to experiments being carried out at a later point in time. The team will certainly continue to pursue these experiments.

Another path, now that we know which antigens are relevant in the model of MI, could lead to trying to specifically modulate these responses in vivo, using MYHCA immunization, tolerization or MHC-II blocking protocols. The working group is already planning to employ such approaches, based on our initial findings.

Furthermore, it is important to mention that our lab currently conducts experiments, investigating the question of $CD4^+$ T cell activation after MI in patients. Isolated antigen specific $CD4^+$ T cells are cultivated and tested against a corresponding panel of human epitopes, previously identified using the same tools as for the murine epitope search. These experiments will give an idea of the translational potential and it will be interesting

to compare the upcoming results with the murine findings. Due to the limiting factors in human studies, the experimentation in the animal model with far greater possibilities still displays a useful model for analysis and a better understanding.

6. SUMMARY

Cardiovascular diseases (CVD) are the leading cause of death in the European Union (over 4 million deaths annually), with devastating individual and economic consequences. The most common ones within the various pathologies subsumed as CVD are atherosclerosis of the coronary arteries and subsequent myocardial infarction (MI).

Recent studies revealed that T cells play a crucial role in post-MI inflammation, healing and remodelling processes. Nevertheless, the specificity profile of adaptive immune responses in the infarcted myocardium has not yet been differentiated. The experiments portrayed in this thesis sought to assess whether post-MI $CD4^+$ T cell responses in mice are triggered by heart specific antigens, and eventually identify relevant epitopes.

We were able to create a murine antigen atlas including a list of 206 epitopes for I-A^b and 193 epitopes for I-A^d presented on MHC-II in the context of MI. We sought to consecutively test this panel by in vitro T cell proliferation and antigen recall assays ex vivo. The elispot assay was used as a readout for antigen-specific stimulation by measurement of IL-2 and IFN-γ production, currently the most sensitive approach available to detect even small counts of antigen producing cells. Splenocytes as well as lymphocytes from mediastinal lymph nodes were purified from animals seven days or 56 days after EMI conducted by ligation of the left anterior descending artery.

We were able to provide evidence that post-MI T cell responses in Balb/c mice are triggered by heart-specific antigens and that MYHCA, especially $MYHCA_{614-628}$, is relevant for that response. Moreover, a significant specific T cell response after MI in C57BL/6J mice was observed for α actin, cardiac muscle 1 [ACTC1], myosin-binding protein C3 [MYBPC3] and myosin heavy chain α [MYHCA] derived heart specific antigens. The steps towards a successful generation of specific T cell hybridomas display a promising direction for more thorough analysis.

Generally, the epitopes of interest for Balb/c as well as C57BL/6J could be further investigated and may eventually be modulated in the future.

7. ZUSAMMENFASSUNG

Herz-Kreislauf-Erkrankungen (CVD) sind die häufigste Todesursache in der Europäischen Union (über 4 Millionen Todesfälle pro Jahr) mit verheerenden individuellen und wirtschaftlichen Folgen.[1-3] Die häufigsten, innerhalb der verschiedenen als CVD subsumierten Pathologien sind Arteriosklerose der Koronararterien und der häufig daraus folgende Myokardinfarkt (MI).

Aktuelle Studien haben gezeigt, dass T-Zellen eine entscheidende Rolle bei Entzündungs-, Heilungs- und Umbauprozessen nach einem Myokardinfarkt spielen. Das Spezifitätsprofil adaptiver Immunantworten im infarzierten Myokard konnte bisher jedoch noch nicht differenziert werden. Die in dieser Arbeit dargestellten Experimente gingen der Frage nach, ob $CD4^+$ T-Zellantworten nach einem Myokardinfarkt in Mäusen durch herzspezifische Antigene ausgelöst werden und ob hieraus relevante Epitope identifiziert werden können.

Uns gelang es, einen Maus-Antigen-Atlas zu erstellen, der eine Zusammenstellung von 206 Epitopen für $I\text{-}A^b$ und 193 Epitope für $I\text{-}A^d$ enthält, welche auf MHC-II im Rahmen des Myokardinfarkts präsentiert werden. Dieses Panel wurde nacheinander durch In-vitro-T-Zell-Proliferations- und Antigen-Recall-Assays ex vivo getestet. Der Elispot-Assay wurde zur Quantifizierung der antigen-spezifischen Stimulation durch Messung der IL-2- und IFN-γ-Produktion verwendet. Dies ist derzeit der sensitivste verfügbare Ansatz, um selbst kleine Anzahlen von antigen-produzierenden Zellen nachzuweisen. Splenozyten sowie Lymphozyten aus mediastinalen Lymphknoten der Mäuse wurden sieben Tage bzw. 56 Tage nach einem experimentellen Myokardinfarkt, welcher durch Ligation der linken anterioren absteigenden Arterie durchgeführt wurde, aufgereinigt.

Wir konnten nachweisen, dass Post-MI-T-Zellantworten in Balb/c Mäusen durch herzspezifische Antigene ausgelöst werden, und dass MYHCA, insbesondere $MYHCA_{614\text{-}628}$, für diese Antwort relevant ist. Darüber hinaus konnte eine signifikante spezifische T-

Zell-Antwort nach Myokardinfarkt in C57BL/6J auf aus Alpha-Actin des Herzmuskels 1 [ACTC1], Myosin-bindendes Protein C vom Herztyp [MYBPC3] und der schweren Kette des Myosins α [MYHCA] generierten herzspezifischen Antigenen gezeigt werden. Die Schritte in Richtung einer erfolgreichen Produktion spezifischer T-Zell-Hybridome verweisen auf einen vielversprechenden Kurs für eine gründlichere Analyse.

Schlussendlich können die für Balb/c und C57BL/6J Mäuse als relevant identifizierten Epitope weiter untersucht und möglicherweise in Zukunft moduliert werden.

8. REFERENCES

1 Townsend, N. *et al.* Cardiovascular disease in Europe: epidemiological update 2016. *European Heart Journal* **37**, 3232-3245, doi:10.1093/eurheartj/ehw334 (2016).

2 Yeates, K. *et al.* A Global Perspective on Cardiovascular Disease in Vulnerable Populations. *Can J Cardiol* **31**, 1081-1093, doi:10.1016/j.cjca.2015.06.035 (2015).

3 Ibanez, B. *et al.* 2017 ESC Guidelines for the management of acute myocardial infarction in patients presenting with ST-segment elevation: The Task Force for the management of acute myocardial infarction in patients presenting with ST-segment elevation of the European Society of Cardiology (ESC). *European Heart Journal* **39**, 119-177, doi:10.1093/eurheartj/ehx393 (2017).

4 Yusuf, S. *et al.* Effect of potentially modifiable risk factors associated with myocardial infarction in 52 countries (the INTERHEART study): case-control study. *The Lancet* **364**, 937-952, doi:https://doi.org/10.1016/S0140-6736(04)17018-9 (2004).

5 Ertl, G. & Frantz, S. Wound model of myocardial infarction. *American Journal of Physiology-Heart and Circulatory Physiology* **288**, H981-H983, doi:10.1152/ajpheart.00977.2004 (2005).

6 Fu, Y. *et al.* Time to Treatment Influences the Impact of ST-Segment Resolution on One-Year Prognosis. *Circulation* **104**, 2653-2659, doi:doi:10.1161/hc4701.099731 (2001).

7 Boersma, E. & Group, T. P. C. A. v. T.-T. C. Does time matter? A pooled analysis of randomized clinical trials comparing primary percutaneous coronary intervention and in-hospital fibrinolysis in acute myocardial infarction patients. *European Heart Journal* **27**, 779-788, doi:10.1093/eurheartj/ehi810 (2006).

8 Keeley, E. C., Boura, J. A. & Grines, C. L. Primary angioplasty versus intravenous thrombolytic therapy for acute myocardial infarction: a quantitative review of 23 randomised trials. *The Lancet* **361**, 13-20, doi:https://doi.org/10.1016/S0140-6736(03)12113-7 (2003).

9 Ponikowski, P. *et al.* 2016 ESC Guidelines for the diagnosis and treatment of acute and chronic heart failure. *European Journal of Heart Failure* **18**, 891-975, doi:10.1002/ejhf.592 (2016).

10 Bansal, S. S. *et al.* Activated T Lymphocytes are Essential Drivers of Pathological Remodeling in Ischemic Heart Failure. *Circ Heart Fail* **10**, e003688-e003688, doi:10.1161/CIRCHEARTFAILURE.116.003688 (2017).

11 Benjamin, E. J. *et al.* Heart Disease and Stroke Statistics-2017 Update: A Report From the American Heart Association. *Circulation* **135**, e146-e603, doi:10.1161/CIR.0000000000000485 (2017).

12 Nahrendorf, M., Pittet Mikael, J. & Swirski Filip, K. Monocytes: Protagonists of Infarct Inflammation and Repair After Myocardial Infarction. *Circulation* **121**, 2437-2445, doi:10.1161/CIRCULATIONAHA.109.916346 (2010).

13 McKay, R. G. *et al.* Left ventricular remodeling after myocardial infarction: a corollary to infarct expansion. *Circulation* **74**, 693-702, doi:doi:10.1161/01.CIR.74.4.693 (1986).

14 Ertl, G. & Frantz, S. Healing after myocardial infarction. *Cardiovasc Res* **66**, 22-32, doi:10.1016/j.cardiores.2005.01.011 (2005).

15 Pfeffer, M. A. & Braunwald, E. Ventricular remodeling after myocardial infarction. Experimental observations and clinical implications. *Circulation* **81**, 1161-1172, doi:doi:10.1161/01.CIR.81.4.1161 (1990).

16 Sutton, M. G. & Sharpe, N. Left ventricular remodeling after myocardial infarction: pathophysiology and therapy. *Circulation* **101**, 2981-2988, doi:10.1161/01.cir.101.25.2981 (2000).
17 Cleutjens, J. P. M., Blankesteijn, W. M., Daemen, M. J. A. P. & Smits, J. F. M. The infarcted myocardium: Simply dead tissue, or a lively target for therapeutic interventions. *Cardiovascular Research* **44**, 232-241, doi:10.1016/s0008-6363(99)00212-6 (1999).
18 Smits, J. F. & Daemen, M. J. Insights from animal models of myocardial infarction: do ACE inhibitors limit the structural response? *Br Heart J* **72**, S61-S64, doi:10.1136/hrt.72.3_suppl.s61 (1994).
19 Pfeffer, M. A., Lamas, G. A., Vaughan, D. E., Parisi, A. F. & Braunwald, E. Effect of Captopril on Progressive Ventricular Dilatation after Anterior Myocardial Infarction. *New England Journal of Medicine* **319**, 80-86, doi:10.1056/nejm198807143190204 (1988).
20 Pfeffer, M. A. *et al.* Effect of captopril on mortality and morbidity in patients with left ventricular dysfunction after myocardial infarction. Results of the survival and ventricular enlargement trial. The SAVE Investigators. *N Engl J Med* **327**, 669-677, doi:10.1056/nejm199209033271001 (1992).
21 Hofmann, U. & Frantz, S. Role of Lymphocytes in Myocardial Injury, Healing, and Remodeling After Myocardial Infarction. *Circulation Research* **116**, 354-367, doi:doi:10.1161/CIRCRESAHA.116.304072 (2015).
22 Nunes-Silva, V., Frantz, S. & Ramos, G. C. in *The Immunology of Cardiovascular Homeostasis and Pathology* (eds Susanne Sattler & Teresa Kennedy-Lydon) 225-250 (Springer International Publishing, 2017).
23 Latet, S. C., Hoymans, V. Y., Van Herck, P. L. & Vrints, C. J. The cellular immune system in the post-myocardial infarction repair process. *International Journal of Cardiology* **179**, 240-247, doi:https://doi.org/10.1016/j.ijcard.2014.11.006 (2015).
24 Prabhu, S. D. & Frangogiannis, N. G. The Biological Basis for Cardiac Repair After Myocardial Infarction: From Inflammation to Fibrosis. *Circulation research* **119**, 91-112, doi:10.1161/CIRCRESAHA.116.303577 (2016).
25 Mathes, D. *et al.* CD4+ Foxp3+ T-cells contribute to myocardial ischemia-reperfusion injury. *Journal of Molecular and Cellular Cardiology* **101**, 99-105, doi:https://doi.org/10.1016/j.yjmcc.2016.10.007 (2016).
26 Santos-Zas, I., Lemarié, J., Tedgui, A. & Ait-Oufella, H. Adaptive Immune Responses Contribute to Post-ischemic Cardiac Remodeling. *Front Cardiovasc Med* **5**, 198-198, doi:10.3389/fcvm.2018.00198 (2019).
27 Frantz, S. *et al.* Monocytes/macrophages prevent healing defects and left ventricular thrombus formation after myocardial infarction. *The FASEB Journal* **27**, 871-881, doi:10.1096/fj.12-214049 (2013).
28 Swirski, F. K. *et al.* Identification of Splenic Reservoir Monocytes and Their Deployment to Inflammatory Sites. *Science* **325**, 612-616, doi:10.1126/science.1175202 (2009).
29 Zlatanova, I., Pinto, C. & Silvestre, J.-S. Immune Modulation of Cardiac Repair and Regeneration: The Art of Mending Broken Hearts. *Front Cardiovasc Med* **3**, 40-40, doi:10.3389/fcvm.2016.00040 (2016).
30 Nahrendorf, M. & Swirski, F. K. Monocyte and macrophage heterogeneity in the heart. *Circulation research* **112**, 1624-1633, doi:10.1161/CIRCRESAHA.113.300890 (2013).
31 Nahrendorf, M. *et al.* The healing myocardium sequentially mobilizes two monocyte subsets with divergent and complementary functions. *J Exp Med* **204**, 3037-3047, doi:10.1084/jem.20070885 (2007).
32 Anzai, T. Post-infarction inflammation and left ventricular remodeling: a double-edged sword. *Circ J* **77**, 580-587, doi:10.1253/circj.cj-13-0013 (2013).

33 He, S. *et al.* Lp-PLA2 Antagonizes Left Ventricular Healing After Myocardial Infarction by Impairing the Appearance of Reparative Macrophages. *Circ Heart Fail* **8**, 980-987, doi:10.1161/CIRCHEARTFAILURE.115.002334 (2015).
34 Dutta, P. & Nahrendorf, M. Monocytes in myocardial infarction. *Arterioscler Thromb Vasc Biol* **35**, 1066-1070, doi:10.1161/atvbaha.114.304652 (2015).
35 Bradshaw, A. D. & DeLeon-Pennell, K. Y. T-cell regulation of fibroblasts and cardiac fibrosis. *Matrix Biology*, doi:https://doi.org/10.1016/j.matbio.2020.04.001 (2020).
36 Panizzi, P. *et al.* Impaired Infarct Healing in Atherosclerotic Mice With Ly-6ChiMonocytosis. *Journal of the American College of Cardiology* **55**, 1629-1638, doi:https://doi.org/10.1016/j.jacc.2009.08.089 (2010).
37 Hofmann, U. *et al.* Interleukin-13 Deficiency Aggravates Healing and Remodeling in Male Mice After Experimental Myocardial Infarction. *Circulation: Heart Failure* **7**, 822-830, doi:doi:10.1161/CIRCHEARTFAILURE.113.001020 (2014).
38 Gladow, N. *et al.* Treatment of mice with a ligand binding blocking anti-CD28 monoclonal antibody improves healing after myocardial infarction. *PloS one* **15**, e0227734-e0227734, doi:10.1371/journal.pone.0227734 (2020).
39 Schwartz, M., Moalem, G., Leibowitz-Amit, R. & Cohen, I. R. Innate and adaptive immune responses can be beneficial for CNS repair. *Trends in Neurosciences* **22**, 295-299, doi:https://doi.org/10.1016/S0166-2236(99)01405-8 (1999).
40 Harty, M., Neff, A. W., King, M. W. & Mescher, A. L. Regeneration or scarring: An immunologic perspective. *Developmental Dynamics* **226**, 268-279, doi:10.1002/dvdy.10239 (2003).
41 Burzyn, D. *et al.* A special population of regulatory T cells potentiates muscle repair. *Cell* **155**, 1282-1295, doi:10.1016/j.cell.2013.10.054 (2013).
42 Hui, S. P. *et al.* Zebrafish Regulatory T Cells Mediate Organ-Specific Regenerative Programs. *Developmental Cell* **43**, 659-672.e655, doi:https://doi.org/10.1016/j.devcel.2017.11.010 (2017).
43 Ramos, G., Hofmann, U. & Frantz, S. Myocardial fibrosis seen through the lenses of T-cell biology. *Journal of molecular and cellular cardiology* **92**, 41-45, doi:10.1016/j.yjmcc.2016.01.018 (2016).
44 Ramos, G. C. *et al.* The autoimmune nature of post-infarct myocardial healing: oral tolerance to cardiac antigens as a novel strategy to improve cardiac healing. *Autoimmunity* **45**, 233-244, doi:10.3109/08916934.2011.647134 (2012).
45 Weirather, J. *et al.* Foxp3+ CD4+ T Cells Improve Healing After Myocardial Infarction by Modulating Monocyte/Macrophage Differentiation. *Circulation Research* **115**, 55-67, doi:10.1161/CIRCRESAHA.115.303895 (2014).
46 Hofmann, U. *et al.* A Collagen α2(I) Mutation Impairs Healing after Experimental Myocardial Infarction. *The American Journal of Pathology* **180**, 113-122, doi:https://doi.org/10.1016/j.ajpath.2011.09.033 (2012).
47 Hofmann, U. *et al.* Activation of CD4+ T Lymphocytes Improves Wound Healing and Survival After Experimental Myocardial Infarction in Mice. *Circulation* **125**, 1652-1663, doi:10.1161/CIRCULATIONAHA.111.044164 (2012).
48 Hofmann, U. & Frantz, S. Role of T-cells in myocardial infarction. *European Heart Journal* **37**, 873-879, doi:10.1093/eurheartj/ehv639 (2015).
49 Rieckmann, M. *et al.* Myocardial infarction triggers cardioprotective antigen-specific T helper cell responses. *The Journal of Clinical Investigation* **129**, 4922-4936, doi:10.1172/JCI123859 (2019).
50 Maisel, A. *et al.* Experimental Autoimmune Myocarditis Produced by Adoptive Transfer of Splenocytes After Myocardial Infarction. *Circulation Research* **82**, 458-463, doi:doi:10.1161/01.RES.82.4.458 (1998).

51 Borg, N. *et al.* CD73 on T Cells Orchestrates Cardiac Wound Healing After Myocardial Infarction by Purinergic Metabolic Reprogramming. *Circulation* **136**, 297-313, doi:doi:10.1161/CIRCULATIONAHA.116.023365 (2017).
52 Sobirin, M. A. *et al.* Activation of Natural Killer T Cells Ameliorates Postinfarct Cardiac Remodeling and Failure in Mice. *Circulation Research* **111**, 1037-1047, doi:doi:10.1161/CIRCRESAHA.112.270132 (2012).
53 Saxena, A. *et al.* Regulatory T cells are recruited in the infarcted mouse myocardium and may modulate fibroblast phenotype and function. *Am J Physiol Heart Circ Physiol* **307**, H1233-H1242, doi:10.1152/ajpheart.00328.2014 (2014).
54 Van der Borght, K. *et al.* Myocardial Infarction Primes Autoreactive T Cells through Activation of Dendritic Cells. *Cell Rep* **18**, 3005-3017, doi:10.1016/j.celrep.2017.02.079 (2017).
55 Laroumanie, F. *et al.* CD4+ T Cells Promote the Transition From Hypertrophy to Heart Failure During Chronic Pressure Overload. *Circulation* **129**, 2111-2124, doi:10.1161/CIRCULATIONAHA.113.007101 (2014).
56 Nevers, T. *et al.* Left Ventricular T-Cell Recruitment Contributes to the Pathogenesis of Heart Failure. *Circ Heart Fail* **8**, 776-787, doi:10.1161/CIRCHEARTFAILURE.115.002225 (2015).
57 Kallikourdis, M. *et al.* T cell costimulation blockade blunts pressure overload-induced heart failure. *Nat Commun* **8**, 14680-14680, doi:10.1038/ncomms14680 (2017).
58 Petrie, H. T. Role of thymic organ structure and stromal composition in steady-state postnatal T-cell production. *Immunological Reviews* **189**, 8-20, doi:10.1034/j.1600-065X.2002.18902.x (2002).
59 Janeway, C. *Immunobiology 5 : the immune system in health and disease*. (Garland Pub., 2001).
60 Klein, L., Kyewski, B., Allen, P. M. & Hogquist, K. A. Positive and negative selection of the T cell repertoire: what thymocytes see (and don't see). *Nat Rev Immunol* **14**, 377-391, doi:10.1038/nri3667 (2014).
61 Kyewski, B. & Klein, L. A central role for central tolerance. *Annu Rev Immunol* **24**, 571-606, doi:10.1146/annurev.immunol.23.021704.115601 (2006).
62 Klein, L., Hinterberger, M., Wirnsberger, G. & Kyewski, B. Antigen presentation in the thymus for positive selection and central tolerance induction. *Nat Rev Immunol* **9**, 833-844, doi:10.1038/nri2669 (2009).
63 Nakagawa, T. *et al.* Cathepsin L: critical role in Ii degradation and CD4 T cell selection in the thymus. *Science* **280**, 450-453, doi:10.1126/science.280.5362.450 (1998).
64 Gommeaux, J. *et al.* Thymus-specific serine protease regulates positive selection of a subset of CD4+ thymocytes. *Eur J Immunol* **39**, 956-964, doi:10.1002/eji.200839175 (2009).
65 Nedjic, J., Aichinger, M., Mizushima, N. & Klein, L. Macroautophagy, endogenous MHC II loading and T cell selection: the benefits of breaking the rules. *Curr Opin Immunol* **21**, 92-97, doi:10.1016/j.coi.2009.01.013 (2009).
66 Nedjic, J., Aichinger, M., Emmerich, J., Mizushima, N. & Klein, L. Autophagy in thymic epithelium shapes the T-cell repertoire and is essential for tolerance. *Nature* **455**, 396-400, doi:10.1038/nature07208 (2008).
67 Kedzierska, K. & Koutsakos, M. The ABC of Major Histocompatibility Complexes and T Cell Receptors in Health and Disease. *Viral Immunol* **33**, 160-178, doi:10.1089/vim.2019.0184 (2020).
68 Josefowicz, S. Z., Lu, L.-F. & Rudensky, A. Y. Regulatory T cells: mechanisms of differentiation and function. *Annu Rev Immunol* **30**, 531-564, doi:10.1146/annurev.immunol.25.022106.141623 (2012).

69 Koch, U. & Radtke, F. Mechanisms of T Cell Development and Transformation. *Annual Review of Cell and Developmental Biology* **27**, 539-562, doi:10.1146/annurev-cellbio-092910-154008 (2011).
70 Krueger, A., Ziętara, N. & Łyszkiewicz, M. T Cell Development by the Numbers. *Trends in Immunology* **38**, 128-139, doi:https://doi.org/10.1016/j.it.2016.10.007 (2017).
71 Zinkernagel, R. M. & Doherty, P. C. Restriction of in vitro T cell-mediated cytotoxicity in lymphocytic choriomeningitis within a syngeneic or semiallogeneic system. *Nature* **248**, 701-702, doi:10.1038/248701a0 (1974).
72 Blum, J. S., Wearsch, P. A. & Cresswell, P. Pathways of antigen processing. *Annu Rev Immunol* **31**, 443-473, doi:10.1146/annurev-immunol-032712-095910 (2013).
73 Rock, K. L., Reits, E. & Neefjes, J. Present Yourself! By MHC Class I and MHC Class II Molecules. *Trends Immunol* **37**, 724-737, doi:10.1016/j.it.2016.08.010 (2016).
74 Gaud, G., Lesourne, R. & Love, P. E. Regulatory mechanisms in T cell receptor signalling. *Nat Rev Immunol* **18**, 485-497, doi:10.1038/s41577-018-0020-8 (2018).
75 Ward-Kavanagh, L. K., Lin, W. W., Šedý, J. R. & Ware, C. F. The TNF Receptor Superfamily in Co-stimulating and Co-inhibitory Responses. *Immunity* **44**, 1005-1019, doi:10.1016/j.immuni.2016.04.019 (2016).
76 Cox, M. A., Harrington, L. E. & Zajac, A. J. Cytokines and the inception of CD8 T cell responses. *Trends Immunol* **32**, 180-186, doi:10.1016/j.it.2011.01.004 (2011).
77 Curtsinger, J. M. & Mescher, M. F. Inflammatory cytokines as a third signal for T cell activation. *Curr Opin Immunol* **22**, 333-340, doi:10.1016/j.coi.2010.02.013 (2010).
78 Mempel, T. R., Henrickson, S. E. & von Andrian, U. H. T-cell priming by dendritic cells in lymph nodes occurs in three distinct phases. *Nature* **427**, 154-159, doi:10.1038/nature02238 (2004).
79 Mills, K. H. Regulatory T cells: friend or foe in immunity to infection? *Nat Rev Immunol* **4**, 841-855, doi:10.1038/nri1485 (2004).
80 Sakaguchi, S., Sakaguchi, N., Asano, M., Itoh, M. & Toda, M. Immunologic self-tolerance maintained by activated T cells expressing IL-2 receptor alpha-chains (CD25). Breakdown of a single mechanism of self-tolerance causes various autoimmune diseases. *J Immunol* **155**, 1151-1164 (1995).
81 Hori, S., Nomura, T. & Sakaguchi, S. Control of regulatory T cell development by the transcription factor Foxp3. *Science* **299**, 1057-1061, doi:10.1126/science.1079490 (2003).
82 Fontenot, J. D., Gavin, M. A. & Rudensky, A. Y. Foxp3 programs the development and function of CD4+CD25+ regulatory T cells. *Nature Immunology* **4**, 330-336, doi:10.1038/ni904 (2003).
83 Ohkura, N., Kitagawa, Y. & Sakaguchi, S. Development and maintenance of regulatory T cells. *Immunity* **38**, 414-423, doi:10.1016/j.immuni.2013.03.002 (2013).
84 Chen, W. *et al.* Conversion of peripheral CD4+CD25- naive T cells to CD4+CD25+ regulatory T cells by TGF-beta induction of transcription factor Foxp3. *J Exp Med* **198**, 1875-1886, doi:10.1084/jem.20030152 (2003).
85 Ellis, J. S., Wan, X. & Braley-Mullen, H. Transient depletion of CD4+ CD25+ regulatory T cells results in multiple autoimmune diseases in wild-type and B-cell-deficient NOD mice. *Immunology* **139**, 179-186, doi:10.1111/imm.12065 (2013).
86 Vignali, D. A. A., Collison, L. W. & Workman, C. J. How regulatory T cells work. *Nature Reviews Immunology* **8**, 523-532, doi:10.1038/nri2343 (2008).
87 Collison, L. W. *et al.* The inhibitory cytokine IL-35 contributes to regulatory T-cell function. *Nature* **450**, 566-569, doi:10.1038/nature06306 (2007).

88 Pummerer, C. L. *et al.* Identification of cardiac myosin peptides capable of inducing autoimmune myocarditis in BALB/c mice. *J Clin Invest* **97**, 2057-2062, doi:10.1172/jci118642 (1996).
89 Liao, L., Sindhwani, R., Leinwand, L., Diamond, B. & Factor, S. Cardiac alpha-myosin heavy chains differ in their induction of myocarditis. Identification of pathogenic epitopes. *The Journal of clinical investigation* **92**, 2877-2882, doi:10.1172/JCI116909 (1993).
90 Fagerberg, L. *et al.* Analysis of the human tissue-specific expression by genome-wide integration of transcriptomics and antibody-based proteomics. *Mol Cell Proteomics* **13**, 397-406, doi:10.1074/mcp.M113.035600 (2014).
91 Lindskog, C. *et al.* The human cardiac and skeletal muscle proteomes defined by transcriptomics and antibody-based profiling. *BMC Genomics* **16**, 475, doi:10.1186/s12864-015-1686-y (2015).
92 Uhlen, M. *et al.* Proteomics. Tissue-based map of the human proteome. *Science* **347**, 1260419, doi:10.1126/science.1260419 (2015).
93 Nguyen, H. & James, E. A. Immune recognition of citrullinated epitopes. *Immunology* **149**, 131-138, doi:10.1111/imm.12640 (2016).
94 Hermans, M. P. J. *et al.* Long-term mortality in patients with ST-segment elevation myocardial infarction is associated with anti-citrullinated protein antibodies. *International Journal of Cardiology* **240**, 20-24, doi:10.1016/j.ijcard.2017.04.046 (2017).
95 Sato, T., Satooka, H., Ichioka, S., Maruo, Y. & Hirata, T. Citrullinated fibrinogen is a target of autoantibodies in interstitial lung disease in mice with collagen-induced arthritis. *Int Immunol*, doi:10.1093/intimm/dxaa021 (2020).
96 Yu, N. Y. *et al.* Complementing tissue characterization by integrating transcriptome profiling from the Human Protein Atlas and from the FANTOM5 consortium. *Nucleic Acids Res* **43**, 6787-6798, doi:10.1093/nar/gkv608 (2015).
97 Consortium, T. U. UniProt: a worldwide hub of protein knowledge. *Nucleic Acids Research* **47**, D506-D515, doi:10.1093/nar/gky1049 (2018).
98 Vita, R. *et al.* The Immune Epitope Database (IEDB): 2018 update. *Nucleic Acids Research* **47**, D339-D343, doi:10.1093/nar/gky1006 (2018).
99 Bui, H.-H. *et al.* Automated generation and evaluation of specific MHC binding predictive tools: ARB matrix applications. *Immunogenetics* **57**, 304-314, doi:10.1007/s00251-005-0798-y (2005).
100 Sturniolo, T. *et al.* Generation of tissue-specific and promiscuous HLA ligand databases using DNA microarrays and virtual HLA class II matrices. *Nature Biotechnology* **17**, 555-561, doi:10.1038/9858 (1999).
101 Nielsen, M., Lundegaard, C. & Lund, O. Prediction of MHC class II binding affinity using SMM-align, a novel stabilization matrix alignment method. *BMC Bioinformatics* **8**, 238, doi:10.1186/1471-2105-8-238 (2007).
102 Wang, P. *et al.* A Systematic Assessment of MHC Class II Peptide Binding Predictions and Evaluation of a Consensus Approach. *PLOS Computational Biology* **4**, e1000048, doi:10.1371/journal.pcbi.1000048 (2008).
103 Wang, P. *et al.* Peptide binding predictions for HLA DR, DP and DQ molecules. *BMC Bioinformatics* **11**, 568, doi:10.1186/1471-2105-11-568 (2010).
104 Voipio, H. M., Baneux, P., Gomez de Segura, I. A., Hau, J. & Wolfensohn, S. Guidelines for the veterinary care of laboratory animals: report of the FELASA/ECLAM/ESLAV Joint Working Group on Veterinary Care. *Lab Anim* **42**, 1-11, doi:10.1258/la.2007.007027 (2008).
105 Guillen, J. FELASA guidelines and recommendations. *J Am Assoc Lab Anim Sci* **51**, 311-321 (2012).

106 Vogel, B., Siebert, H., Hofmann, U. & Frantz, S. Determination of collagen content within picrosirius red stained paraffin-embedded tissue sections using fluorescence microscopy. *MethodsX* **2**, 124-134, doi:10.1016/j.mex.2015.02.007 (2015).
107 Song, J. *et al.* PROSPER: An Integrated Feature-Based Tool for Predicting Protease Substrate Cleavage Sites. *PLOS ONE* **7**, e50300, doi:10.1371/journal.pone.0050300 (2012).
108 Neu, N. *et al.* Cardiac myosin induces myocarditis in genetically predisposed mice. *The Journal of Immunology* **139**, 3630-3636 (1987).
109 Krebs, P. *et al.* Molecular mapping of autoimmune B cell responses in experimental myocarditis. *Journal of Autoimmunity* **28**, 224-233, doi:https://doi.org/10.1016/j.jaut.2007.01.003 (2007).
110 Amit, U. *et al.* New Role for Interleukin-13 Receptor α1 in Myocardial Homeostasis and Heart Failure. *J Am Heart Assoc* **6**, e005108, doi:10.1161/JAHA.116.005108 (2017).
111 Monnerat, G. *et al.* Macrophage-dependent IL-1β production induces cardiac arrhythmias in diabetic mice. *Nat Commun* **7**, 13344-13344, doi:10.1038/ncomms13344 (2016).
112 Hulsmans, M. *et al.* Macrophages Facilitate Electrical Conduction in the Heart. *Cell* **169**, 510-522.e520, doi:10.1016/j.cell.2017.03.050 (2017).
113 Smith, S. C. & Allen, P. M. Myosin-induced acute myocarditis is a T cell-mediated disease. *The Journal of Immunology* **147**, 2141-2147 (1991).
114 Kaya, Z., Katus, H. A. & Rose, N. R. Cardiac troponins and autoimmunity: Their role in the pathogenesis of myocarditis and of heart failure. *Clinical Immunology* **134**, 80-88, doi:https://doi.org/10.1016/j.clim.2009.04.008 (2010).
115 Ramos, G. C. *et al.* Myocardial aging as a T-cell–mediated phenomenon. *Proceedings of the National Academy of Sciences* **114**, E2420-E2429, doi:10.1073/pnas.1621047114 (2017).
116 Eriksson, U. *et al.* Dendritic cell–induced autoimmune heart failure requires cooperation between adaptive and innate immunity. *Nature Medicine* **9**, 1484-1490, doi:10.1038/nm960 (2003).
117 Nindl, V. *et al.* Cooperation of Th1 and Th17 cells determines transition from autoimmune myocarditis to dilated cardiomyopathy. *European Journal of Immunology* **42**, 2311-2321, doi:10.1002/eji.201142209 (2012).
118 Ramos, G., Hofmann, U. & Frantz, S. Immune repertoires in the failing heart: the global picture. *European Heart Journal* **40**, 3934-3936, doi:10.1093/eurheartj/ehz548 (2019).
119 Borghi, C. & Ambrosioni, E. Primary and secondary prevention of myocardial infarction. *Clin Exp Hypertens* **18**, 547-558, doi:10.3109/10641969609088984 (1996).
120 Gurfinkel, E. P. & Lernoud, V. S. Prevention of myocardial infarction. *Curr Opin Cardiol* **21**, 503-509, doi:10.1097/01.hco.0000240589.99215.6d (2006).
121 Seferovic, P. M. *et al.* Clinical practice update on heart failure 2019: pharmacotherapy, procedures, devices and patient management. An expert consensus meeting report of the Heart Failure Association of the European Society of Cardiology. *European Journal of Heart Failure* **21**, 1169-1186, doi:10.1002/ejhf.1531 (2019).
122 Handisurya, A. *et al.* Strain-specific properties and T cells regulate the susceptibility to papilloma induction by Mus musculus papillomavirus 1. *PLoS Pathog* **10**, e1004314, doi:10.1371/journal.ppat.1004314 (2014).
123 Oomen, L. C., Van der Valk, M. A. & Den Engelse, L. Tumour susceptibility in mice in relation to H-2 haplotype. *IARC Sci Publ*, 205-221 (1983).
124 Chen, P. *et al.* Susceptibility to autoimmune myocarditis is associated with intrinsic differences in CD4(+) T cells. *Clin Exp Immunol* **169**, 79-88, doi:10.1111/j.1365-2249.2012.04598.x (2012).

125 Neu, N., Beisel, K. W., Traystman, M. D., Rose, N. R. & Craig, S. W. Autoantibodies specific for the cardiac myosin isoform are found in mice susceptible to Coxsackievirus B3-induced myocarditis. *The Journal of Immunology* **138**, 2488 (1987).
126 Teuscher, C., Blankenhorn, E. P. & Hickey, W. F. Differential susceptibility to actively induced experimental allergic encephalomyelitis and experimental allergic orchitis among BALB/c substrains. *Cellular Immunology* **110**, 294-304, doi:https://doi.org/10.1016/0008-8749(87)90124-9 (1987).
127 Podolin, P. L. *et al.* DIFFERENTIAL GLYCOSYLATION OF INTERLEUKIN 2, THE MOLECULAR BASIS FOR THE NOD Idd3 TYPE 1 DIABETES GENE? *Cytokine* **12**, 477-482, doi:https://doi.org/10.1006/cyto.1999.0609 (2000).
128 Tang, T.-T. *et al.* Pathologic T-cell response in ischaemic failing hearts elucidated by T-cell receptor sequencing and phenotypic characterization. *European Heart Journal* **40**, 3924-3933, doi:10.1093/eurheartj/ehz516 (2019).
129 Błyszczuk, P. Myocarditis in Humans and in Experimental Animal Models. *Front Cardiovasc Med* **6**, 64-64, doi:10.3389/fcvm.2019.00064 (2019).
130 Smith, S. C. & Allen, P. M. Expression of myosin-class II major histocompatibility complexes in the normal myocardium occurs before induction of autoimmune myocarditis. *Proc Natl Acad Sci U S A* **89**, 9131-9135, doi:10.1073/pnas.89.19.9131 (1992).
131 Donermeyer, D. L., Beisel, K. W., Allen, P. M. & Smith, S. C. Myocarditis-inducing epitope of myosin binds constitutively and stably to I-Ak on antigen-presenting cells in the heart. *J Exp Med* **182**, 1291-1300, doi:10.1084/jem.182.5.1291 (1995).
132 De Scheerder, I. *et al.* Detection of anti-contractile antibodies after cardiac surgery using ELISA assay. *Clin Exp Immunol* **60**, 403-406 (1985).
133 Dangas, G. *et al.* Prevalence of autoantibodies against contractile proteins in coronary artery disease and their clinical implications. *The American Journal of Cardiology* **85**, 870-872, doi:https://doi.org/10.1016/S0002-9149(99)00883-8 (2000).
134 Merbl, Y., Zucker-Toledano, M., Quintana, F. J. & Cohen, I. R. Newborn humans manifest autoantibodies to defined self molecules detected by antigen microarray informatics. *The Journal of Clinical Investigation* **117**, 712-718, doi:10.1172/JCI29943 (2007).
135 O'Donohoe, T. J., Schrale, R. G. & Ketheesan, N. The role of anti-myosin antibodies in perpetuating cardiac damage following myocardial infarction. *International Journal of Cardiology* **209**, 226-233, doi:https://doi.org/10.1016/j.ijcard.2016.02.035 (2016).
136 Hong, P., Yuhua, L., Zhaohui, W., Jihua, D. & Qing, L. Effect of anti-cardiac myosin antibody on prognosis of patients with acute myocardial infarction. *Journal of Tongji Medical University* **20**, 46-48, doi:10.1007/BF02887674 (2000).
137 Warraich, R. S. *et al.* Human cardiac myosin autoantibodies impair myocyte contractility: a cause-and-effect relationship. *The FASEB Journal* **20**, 651-660, doi:10.1096/fj.04-3001com (2006).
138 Neumann, D. A. *et al.* In vivo deposition of myosin-specific autoantibodies in the hearts of mice with experimental autoimmune myocarditis. *J Immunol* **148**, 3806-3813 (1992).
139 Caforio, A. L. P. *et al.* Passive transfer of affinity-purified anti-heart autoantibodies (AHA) from sera of patients with myocarditis induces experimental myocarditis in mice. *International Journal of Cardiology* **179**, 166-177, doi:10.1016/j.ijcard.2014.10.165 (2015).
140 Li, Y., Heuser, J. S., Cunningham, L. C., Kosanke, S. D. & Cunningham, M. W. Mimicry and Antibody-Mediated Cell Signaling in Autoimmune Myocarditis. *The Journal of Immunology* **177**, 8234, doi:10.4049/jimmunol.177.11.8234 (2006).
141 Gil-Cruz, C. *et al.* Microbiota-derived peptide mimics drive lethal inflammatory cardiomyopathy. *Science* **366**, 881-886, doi:10.1126/science.aav3487 (2019).

142 Massilamany, C., Gangaplara, A., Chapman, N., Rose, N. & Reddy, J. Detection of cardiac myosin heavy chain-α-specific CD4 cells by using MHC class II/IA(k) tetramers in A/J mice. *J Immunol Methods* **372**, 107-118, doi:10.1016/j.jim.2011.07.004 (2011).

9. LIST OF FIGURES AND TABLES

10. APPENDIX

10.1. Murine antigen atlas

10.1.1. Peptide library of murine, I-A^d-restricted cardiac antigens

Table 6 Peptide library of murine, I-A^d-restricted cardiac antigens

Haplotype, peptide sequence, percentile and pool code of each peptide used for the Balb/c experiments.

Haplotype	Protein$_{peptide}$	Sequence	%	Id
ACTC1				
I-A^d	Actc1$_{132-146}$	PAMYVAIQAVLSLYA	0.03	0-01-001
I-A^d	Actc1$_{173-187}$	LPHAIMRLDLAGRDL	2.48	0-01-002
I-A^d	Actc1$_{223-237}$	LDFENEMATAASSSS	8.00	0-01-003
I-A^d	Actc1$_{312-326}$	ADRMQKEITALAPST	1.04	0-01-004
I-A^d	Actc1$_{319-333}$	ITALAPSTMKIKIIA	4.75	0-01-005
I-A^d	Actc1$_{323-337}$	APSTMKIKIIAPPER	4.16	0-01-006
I-A^d	Actc1$_{352-366}$	STFQQMWISKQEYDE	8.23	0-01-007
ADRB1				
I-A^d	Adrb1$_{24-39}$	GAATAARLLVLASPP	1.76	0-02-008
I-A^d	Adrb1$_{95-111}$	FIMSLASADLVMGLL	2.63	0-02-009
I-A^d	Adrb1$_{142-157}$	TASIETLCVIALDRY	3.60	0-02-010
I-A^d	Adrb1$_{144-160}$	SIETLCVIALDRYLA	3.19	0-02-011
I-A^d	Adrb1$_{164-178}$	FRYQSLLTRARARAL	1.22	0-02-012
I-A^d	Adrb1$_{166-181}$	YQSLLTRARARALVC	5.46	0-02-013
I-A^d	Adrb1$_{174-188}$	TRARARALVCTVWAI	4.27	0-02-014
I-A^d	Adrb1$_{177-193}$	RARALVCTVWAISAL	3.10	0-02-015
I-A^d	Adrb1$_{179-194}$	RALVCTVWAISALVS	2.20	0-02-016
I-A^d	Adrb1$_{182-196}$	VCTVWAISALVSFLP	1.35	0-02-017
I-A^d	Adrb1$_{303-318}$	ALREQKALKTLGIIM	0.23	0-02-018
I-A^d	Adrb1$_{380-394}$	CCARRAACRRRAAHG	1.61	0-02-019
MYBPC3				
I-A^d	Mybcp3$_{15-29}$	KPRSAEVTAGSAAVF	6.25	0-03-020
I-A^d	Mybcp3$_{17-31}$	RSAEVTAGSAAVFEA	5.03	0-03-021
I-A^d	Mybcp3$_{18-32}$	SAEVTAGSAAVFEAE	8.47	0-03-022
I-A^d	Mybcp3$_{57-71}$	LAAEGKRHTLTVRDA	3.62	0-03-023
I-A^d	Mybcp3$_{60-74}$	EGKRHTLTVRDASPD	0.86	0-03-024
I-A^d	Mybcp3$_{171-185}$	VFSARVAGASLLKPP	5.34	0-03-025
I-A^d	Mybcp3$_{210-224}$	SYDRASKVYLFELHI	4.57	0-03-026
I-A^d	Mybcp3$_{265-279}$	LRSAFRRTSLAGAGR	7.66	0-03-027
I-A^d	Mybcp3$_{266-281}$	RSAFRRTSLAGAGRRT	3.54	0-03-028
I-A^d	Mybcp3$_{268-283}$	AFRRTSLAGAGRRTSD	5.08	0-03-029
I-A^d	Mybcp3$_{370-384}$	QVNKGHKIRLTVELA	6.66	0-03-030
I-A^d	Mybcp3$_{374-388}$	GHKIRLTVELADPDA	2.27	0-03-031

I-A^d	Mybcp3$_{411-425}$	VGAKRTLTISQCSLA	6.69	0-03-032
I-A^d	Mybcp3$_{412-427}$	GAKRTLTISQCSLADD	8.08	0-03-033
I-A^d	Mybcp3$_{453-467}$	TRSLEDQLVMVGQRV	6.27	0-03-034
I-A^d	Mybcp3$_{916-929}$	LQGLTERRSMLVKDL	1.84	0-03-035
I-A^d	Mybcp3$_{919-933}$	LTERRSMLVKDLPTG	0.30	0-03-036
I-A^d	Mybcp3$_{932-946}$	TGARLLFRVRAHNVA	9.52	0-03-037
I-A^d	Mybcp3$_{834-848}$	EGVAYEMRVYAVNAV	0.98	0-03-038
I-A^d	Mybcp3$_{835-849}$	GVAYEMRVYAVNAVG	1.02	0-03-039
I-A^d	Mybcp3$_{833-847}$	IEGVAYEMRVYAVNA	2.37	0-03-040
I-A^d	Mybcp3$_{827-841}$	HEARRMIEGVAYEMR	4.04	0-03-041
I-A^d	Mybcp3$_{756-770}$	DQVNLTVKVIDVPDA	4.49	0-03-042
I-A^d	Mybcp3$_{757-771}$	QVNLTVKVIDVPDAP	5.03	0-03-043
I-A^d	Mybcp3$_{542-556}$	EVYQSIADLAVGAKD	4.60	0-03-044
I-A^d	Mybcp3$_{537-551}$	QEKKLEVYQSIADLA	4.92	0-03-045
I-A^d	Mybcp3$_{543-557}$	VYQSIADLAVGAKDQ	5.04	0-03-046
I-A^d	Mybcp3$_{533-547}$	ELIVQEKKLEVYQSI	5.19	0-03-047
I-A^d	Mybcp3$_{544-558}$	YQSIADLAVGAKDQA	7.05	0-03-048
I-A^d	Mybcp3$_{624-638}$	KLHFMEVKIDFVPRQ	5.68	0-03-049
I-A^d	Mybcp3$_{973-987}$	RHLRQTIQKKVGEPV	6.92	0-03-050
I-A^d	Mybcp3$_{1047-1061}$	NMEDKATLILQIVDK	4.08	0-03-051
I-A^d	Mybcp3$_{1046-1060}$	ENMEDKATLILQIVD	4.64	0-03-052
I-A^d	Mybcp3$_{1183-1197}$	LANRSIIAGYNAILC	9.15	0-03-053
I-A^d	Mybcp3$_{1223-1237}$	FRMFCKQGVLTLEIR	4.90	0-03-054
MYHCA				
I-A^d	Myh6$_{1-15}$	MTDAQMADFGAAAQY	5.60	0-04-055
I-A^d	Myh6$_{41-56}$	DKEEYVKAKVVSREG	1.79	0-04-056
I-A^d	Myh6$_{86-100}$	KIEDMAMLTFLHEPA	4.06	0-04-057
I-A^d	Myh6$_{105-119}$	LKERYAAWMIYTYSG	6.58	0-04-058
I-A^d	Myh6$_{131-145}$	LPVYNAEVVAAYRGK	5.69	0-04-059
I-A^d	Myh6$_{186-201}$	VNTKRVIQYFASIAA	4.25	0-04-060
I-A^d	Myh6$_{190-204}$	RVIQYFASIAAIGDRS	3.42	0-04-061
I-A^d	Myh6$_{191-205}$	VIQYFASIAAIGDRS	2.73	0-04-062
I-A^d	Myh6$_{216-231}$	LEDQIIQANPALEAF	9.18	0-04-063
I-A^d	Myh6$_{420-434}$	QVYYSIGALAKSVYE	2.46	0-04-064
I-A^d	Myh6$_{605-619}$	TVVGLYQKSSLKLMA	9.10	0-04-065
I-A^d	Myh6$_{608-622}$	GLYQKSSLKLMATLF	1.55	0-04-066
I-A^d	Myh6$_{609-623}$	LYQKSSLKLMATLFS	0.98	0-04-067
I-A^d	Myh6$_{610-624}$	YQKSSLKLMATLFST	1.20	0-04-068
I-A^d	*Myh6$_{614-628}$	SLKLMATLFSTYASA	9.04	0-04-069
I-A^d	Myh6$_{641-655}$	KKGSSFQTVSALHRE	5.64	0-04-070
I-A^d	Myh6$_{642-656}$	KGSSFQTVSALHREN	7.20	0-04-071
I-A^d	Myh6$_{720-734}$	FRQRYRILNPAAIPE	2.13	0-04-072
I-A^d	Myh6$_{721-735}$	RQRYRILNPAAIPEG	4.00	0-04-073
I-A^d	Myh6$_{722-736}$	QRYRILNPAAIPEGQ	2.13	0-04-074
I-A^d	Myh6$_{776-790}$	EEMRDERLSRIITRI	9.91	0-04-075
I-A^d	Myh6$_{777-791}$	EMRDERLSRIITRIQ	7.57	0-04-076
I-A^d	Myh6$_{778-792}$	MRDERLSRIITRIQA	5.05	0-04-077

I-A^d	Myh6$_{781-795}$	ERLSRIITRIQAQAR	7.80	0-04-078
I-A^d	Myh6$_{786-801}$	IITRIQAQARGQLMRI	7.08	0-04-079
I-A^d	Myh6$_{793-807}$	QARGQLMRIEFKKIV	9.50	0-04-080
I-A^d	Myh6$_{810-824}$	RDALLVIQWNIRAFM	8.21	0-04-081
I-A^d	Myh6$_{814-828}$	LVIQWNIRAFMGVKN	4.57	0-04-082
I-A^d	Myh6$_{815-829}$	VIQWNIRAFMGVKNW	3.38	0-04-083
I-A^d	Myh6$_{833-847}$	KLYFKIKPLLKSAET	9.13	0-04-084
I-A^d	Myh6$_{910-924}$	LIKNKIQLEAKVKEM	8.97	0-04-085
I-A^d	Myh6$_{911-925}$	IKNKIQLEAKVKEMT	7.40	0-04-086
I-A^d	Myh6$_{994-1008}$	LTKEKKALQEAHQQA	5.89	0-04-087
I-A^d	Myh6$_{996-1010}$	KEKKALQEAHQQALD	5.26	0-04-088
I-A^d	Myh6$_{1000-1014}$	ALQEAHQQALDDLQA	4.42	0-04-089
I-A^d	Myh6$_{1003-1017}$	EAHQQALDDLQAEED	2.63	0-04-090
I-A^d	Myh6$_{1039-1053}$	SLEQEKKVRMDLERA	4.18	0-04-091
I-A^d	Myh6$_{1040-1054}$	LEQEKKVRMDLERAK	2.54	0-04-092
I-A^d	Myh6$_{1044-1058}$	KKVRMDLERAKRKLE	4.45	0-04-093
I-A^d	Myh6$_{1124-1138}$	LEAERTARAKVEKLR	2.40	0-04-094
I-A^d	Myh6$_{1126-1140}$	AERTARAKVEKLRSD	2.55	0-04-095
I-A^d	Myh6$_{1183-1197}$	ATLQHEATAAALRKK	3.04	0-04-096
I-A^d	Myh6$_{1185-1199}$	LQHEATAAALRKKHA	2.21	0-04-097
I-A^d	Myh6$_{1231-1245}$	DDVTSNMEQIIKAKA	3.20	0-04-098
I-A^d	Myh6$_{1235-1249}$	SNMEQIIKAKANLEK	1.18	0-04-099
I-A^d	Myh6$_{1238-1252}$	EQIIKAKANLEKVSR	7.20	0-04-100
I-A^d	Myh6$_{1258-1272}$	ANEYRVKLEEAQRSL	3.96	0-04-101
I-A^d	Myh6$_{1259-1273}$	NEYRVKLEEAQRSLN	3.67	0-04-102
I-A^d	Myh6$_{1290-1304}$	ARQLEEKEALISQLT	7.55	0-04-103
I-A^d	Myh6$_{1293-1307}$	LEEKEALISQLTRGK	8.74	0-04-104
I-A^d	Myh6$_{1326-1340}$	KAKNALAHALQSSRH	7.27	0-04-105
I-A^d	Myh6$_{1327-1341}$	AKNALAHALQSSRHD	9.00	0-04-106
I-A^d	Myh6$_{1350-1364}$	EEEMEAKAELQRVLS	2.52	0-04-107
I-A^d	Myh6$_{1351-1365}$	EEMEAKAELQRVLSK	2.48	0-04-108
I-A^d	Myh6$_{1388-1402}$	LEEAKKKLAQRLQDA	5.96	0-04-109
I-A^d	Myh6$_{1391-1405}$	AKKKLAQRLQDAEEA	3.10	0-04-110
I-A^d	Myh6$_{1394-1408}$	KLAQRLQDAEEAVEA	5.32	0-04-111
I-A^d	Myh6$_{1397-1411}$	QRLQDAEEAVEAVNA	2.09	0-04-112
I-A^d	Myh6$_{1401-1415}$	DAEEAVEAVNAKCSS	5.43	0-04-113
I-A^d	Myh6$_{1435-1449}$	ERSNAAAAALDKKQR	2.00	0-04-114
I-A^d	Myh6$_{1470-1484}$	ESSQKEARSLSTELF	7.68	0-04-115
I-A^d	Myh6$_{1471-1485}$	SSQKEARSLSTELFK	4.21	0-04-116
I-A^d	Myh6$_{1528-1542}$	EKIRKQLEVEKLELQ	2.97	0-04-117
I-A^d	Myh6$_{1530-1544}$	IRKQLEVEKLELQSA	4.42	0-04-118
I-A^d	Myh6$_{1539-1553}$	VEKLELQSALEEAEA	4.75	0-04-119
I-A^d	Myh6$_{1567-1582}$	NQIKAEIERKLAEKD	6.53	0-04-120
I-A^d	Myh6$_{1589-1605}$	RNHLRMVDSLQTSLD	4.31	0-04-121
I-A^d	Myh6$_{1621-1635}$	GDLNEMEIQLSQANR	0.80	0-04-122
I-A^d	Myh6$_{1623-1637}$	LNEMEIQLSQANRIA	0.59	0-04-123
I-A^d	Myh6$_{1651-1688}$	HLKDTQLQLDDAVHA	7.48	0-04-124
I-A^d	Myh6$_{1652-1686}$	LKDTQLQLDDAVHAN	6.67	0-04-125

I-A^d	Myh6$_{1752-1766}$	NAEEKAKKAITDAAM	2.63	0-04-126
I-A^d	Myh6$_{1782-1796}$	ERMKKNMEQTIKDLQ	7.74	0-04-127
I-A^d	Myh6$_{1783-1797}$	RMKKNMEQTIKDLQH	6.04	0-04-128
I-A^d	Myh6$_{1808-1823}$	GGKKQLQKLEARVRE	2.62	0-04-129
I-A^d	Myh6$_{1809-1824}$	GKKQLQKLEARVREL	5.02	0-04-130
I-A^d	Myh6$_{1868-1882}$	LVDKLQLKVKAYKRQ	1.15	0-04-131
MYL2				
I-A^d	Myl2$_{113-127}$	SLKADYVREMLTTQA	5.24	0-05-132
I-A^d	Myl2$_{118-132}$	DYVREMLTTQAERFS	0.90	0-05-133
I-A^d	Myl2$_{120-134}$	REMLTTQAERFSKEE	5.68	0-05-134
TNNI3				
I-A^d	Tnni3$_{19-33}$	VRRRSSANYRAYATE	6.02	0-06-135
I-A^d	Tnni3$_{32-46}$	TEPHAKKKSKISASR	5.12	0-06-136
I-A^d	Tnni3$_{34-48}$	EPHAKKKSKISASRK	3.40	0-06-137
I-A^d	Tnni3$_{40-54}$	SKISASRKLQLKTLM	3.81	0-06-138
I-A^d	Tnni3$_{44-58}$	ASRKLQLKTLMLQIA	1.20	0-06-139
I-A^d	Tnni3$_{45-59}$	SRKLQLKTLMLQIAK	1.91	0-06-140
I-A^d	Tnni3$_{50-64}$	LKTLMLQIAKQEMER	4.27	0-06-141
I-A^d	Tnni3$_{97-111}$	LCRQLHARVDKVDEE	9.00	0-06-142
I-A^d	Tnni3$_{140-154}$	FKRPTLRRVRISADA	6.71	0-06-143
I-A^d	Tnni3$_{144-158}$	TLRRVRISADAMMQA	0.18	0-06-144
I-A^d	Tnni3$_{146-161}$	RRVRISADAMMQALL	0.10	0-06-145
I-A^d	Tnni3$_{150-165}$	ISADAMMQALLGTRA	0.22	0-06-146
I-A^d	Tnni3$_{152-166}$	ADAMMQALLGTRAKE	1.28	0-06-147
I-A^d	Tnni3$_{160-176}$	LGTRAKESLDLRAHL	1.39	0-06-148
I-A^d	Tnni3$_{163-177}$	RAKESLDLRAHLKQV	7.06	0-06-149
I-A^d	Tnni3$_{164-178}$	AKESLDLRAHLKQVK	6.50	0-06-150
TNNT2				
I-A^d	Tnnt2$_{226-240}$	AERRKALAIDHLNED	1.23	0-07-151
HSPB3				
I-A^d	Hspb3$_{1-15}$	MAKIILRHLIETPVR	7.34	0-08-152
I-A^d	Hspb3$_{71-85}$	GKSRFQILLDVVQFL	4.06	0-08-153
HSPA1A				
I-A^d	Hspa1a $_{117-131}$	EEISSMVLTKMKEIA	7.49	0-09-154
I-A^d	Hspa1a $_{118-132}$	EISSMVLTKMKEIAE	9.09	0-09-155
I-A^d	Hspa1a $_{120-134}$	SSMVLTKMKEIAEAY	7.18	0-09-156
I-A^d	Hspa1a $_{122-136}$	MVLTKMKEIAEAYLG	4.29	0-09-157
I-A^d	Hspa1a $_{137-151}$	HPVTNAVITVPAYFN	4.06	0-09-158
I-A^d	Hspa1a $_{151-165}$	NDSQRQATKDAGVIA	2.62	0-09-159
I-A^d	Hspa1a $_{152-166}$	DSQRQATKDAGVIAG	2.20	0-09-160
I-A^d	Hspa1a $_{153-167}$	SQRQATKDAGVIAGL	2.24	0-09-161
I-A^d	*Hspa1a $_{169-183}$	VLRIINEPTAAAIAY	*18.79	0-09-162

I-A^d	Hspa1a $_{251-265}$	KDISQNKRAVRRLRT	5.47	0-09-163
I-A^d	Hspa1a $_{255-269}$	QNKRAVRRLRTACER	3.42	0-09-164
I-A^d	Hspa1a $_{315-329}$	EPVEKALRDAKMDKA	5.59	0-09-165
I-A^d	Hspa1a $_{321-336}$	LRDAKMDKAQIHDLV	2.21	0-09-166
I-A^d	Hspa1a $_{322-337}$	RDAKMDKAQIHDLVL	2.21	0-09-167
I-A^d	Hspa1a$_{368-382}$	AVAYGAAVQAAILMG	1.02	0-09-168
I-A^d	Hspa1a$_{514-528}$	EIERMVQEAERYKAE	5.46	0-09-169
I-A^d	Hspa1a $_{275-289}$	SSSTQASLEIDSLFE	5.52	0-09-170
I-A^d	Hspa1a $_{598-612}$	ELERVCSPIISGLYQ	6.67	0-09-171
I-A^d	Hspa1a $_{531-545}$	VQRDRVAAKNALESY	4.83	0-09-172
I-A^d	Hspa1a $_{533-547}$	RDRVAAKNALESYAF	3.03	0-09-173
FGA				
I-A^d	*Fiba $_{142-156}$	LRRKVIEKAQQIQAL	1.43	0-10-174
I-A^d	*Fiba $_{144-158}$	RKVIEKAQQIQALQS	1.01	0-10-175
I-A^d	*Fiba $_{148-162}$	EKAQQIQALQSNVRA	0.70	0-10-176
I-A^d	Fiba $_{150-164}$	AQQIQALQSNVRAQL	7.46	0-10-177
I-A^d	Fiba $_{157-171}$	QSNVRAQLIDMKRLE	3.01	0-10-178
I-A^d	Fiba $_{200-214}$	GHQKQLQQVIAKELL	1.60	0-10-179
I-A^d	Fiba $_{202-216}$	QKQLQQVIAKELLPT	5.15	0-10-180
I-A^d	Fiba $_{217-231}$	KDRQYLPALKMSPVP	3.23	0-10-181
I-A^d	Fiba $_{249-263}$	WKALTEMRQMRMELE	1.79	0-10-182
I-A^d	Fiba $_{252-266}$	LTEMRQMRMELERPG	0.35	0-10-183
FGB				
I-A^d	Fibb $_{107-121}$	LNQERPIKSSIAELN	4.79	0-11-184
I-A^d	Fibb $_{179-193}$	DNIPLNLRVLRSILE	9.13	0-11-185
I-A^d	Fibb $_{353-367}$	NEASKYQVSVNKYKG	7.91	0-11-186
I-A^d	Fibb $_{463-477}$	SWYSMRRMSMKIRPF	0.04	0-11-187
FGG				
I-A^d	Fibg $_{124-138}$	LLLTHETSIRYLQEI	7.34	0-12-188
I-A^d	Fibg $_{147-161}$	TNLKQKVAQLEAQCQ	8.72	0-12-189
I-A^d	Fibg $_{253-267}$	LGNEKIHLISMQSTI	8.34	0-12-190
I-A^d	Fibg $_{258-272}$	IHLISMQSTIPYALR	0.51	0-12-191
I-A^d	Fibg $_{260-274}$	LISMQSTIPYALRIQ	1.10	0-12-192
I-A^d	Fibg $_{399-413}$	SRWYSMKETTMKIIP	3.66	0-12-193

* Experimental evidence

10.1.2. Peptide library of murine, I-A^b-restricted cardiac antigens

Table 7 Peptide library of murine, I-A^b-restricted cardiac antigens

Haplotype, peptide sequence, percentile and pool code of each peptide used for the C57BL/6J experiments.

Haplotype	Protein$_{peptide}$	Sequence	%	Id
ACTC1				
I-A^b	Actc1$_{103-117}$	HPTLL**TEAPLNPKA**N	8.42	0-01-001
I-A^b	Actc1$_{105-119}$	TLLT**EAPLNPKAN**RE	7.94	0-01-002
I-A^b	Actc1$_{124-138}$	IM**FETFNVPAM**YVAI	6.00	0-01-003
I-A^b	Actc1$_{125-139}$	MFET**FNVPAMYVA**IQ	8.36	0-01-004
I-A^b	Actc1$_{129-143}$	FNVP**AMYVAIQAV**LS	5.45	0-01-005
I-A^b	Actc1$_{130-144}$	NVPAM**YVAIQAVLS**L	6.79	0-01-006
I-A^b	Actc1$_{141-155}$	AVL**SLYASGRTT**GIV	8.24	0-01-007
I-A^b	Actc1$_{163-177}$	HNVPI**YEGYALPHA**I	3.01	0-01-008
I-A^b	Actc1$_{166-180}$	PIY**EGYALPHAI**MRL	2.00	0-01-009
I-A^b	Actc1$_{196-210}$	TE**RGYSFVTTA**EREI	6.96	0-01-010
I-A^b	Actc1$_{219-233}$	CYVA**LDFENEMAT**AA	6.25	0-01-011
I-A^b	Actc1$_{222-236}$	ALD**FENEMATAA**SSS	4.12	0-01-012
I-A^b	Actc1$_{225-239}$	FENEM**ATAASSSSL**E	5.42	0-01-013
I-A^b	Actc1$_{313-327}$	DRMQ**KEITALAPS**TM	9.40	0-01-014
I-A^b	Actc1$_{316-330}$	QKE**ITALAPSTM**KIK	6.63	0-01-015
I-A^b	Actc1$_{318-332}$	EIT**ALAPSTMKI**KII	9.39	0-01-016
I-A^b	Actc1$_{336-350}$	ERKY**SVWIGGSIL**AS	6.03	0-01-017
I-A^b	Actc1$_{339-353}$	YSV**WIGGSILAS**LST	8.56	0-01-018
I-A^b	Actc1$_{358-372}$	WISK**QEYDEAGPS**IV	2.08	0-01-019
I-A^b	Actc1$_{361-375}$	KQE**YDEAGPSIV**HRK	1.62	0-01-020
ADRB1				
I-A^b	Adrb1$_{30-53}$	RL**LVLASPPASLLPPA**SEGSAPL	1.65	0-02-021
I-A^b	Adrb1$_{105-125}$	VMGLL**VVPFGATIV**VWGRW	2.38	0-02-022
I-A^b	Adrb1$_{218-236}$	VTN**RAYAIASSVVS**FYVP	1.45	0-02-023
I-A^b	Adrb1$_{261-282}$	CE**RRFLGGPARPPSP**EPSPSPG	0.72	0-02-024
I-A^b	Adrb1$_{400-420}$	SGC**LARAGPPPSPGAP**SDDD	1.69	0-02-025
MYBPC3				
I-A^b	Mybcp3$_{14-28}$	KKPRS**AEVTAGSAA**V	8.94	0-03-026
I-A^b	Mybcp3$_{17-31}$	RSA**EVTAGSAAV**FEA	8.02	0-03-027
I-A^b	Mybcp3$_{76-90}$	QGSY**AVIAGSSKV**K(F)	9.32	0-03-028
I-A^b	Mybcp3$_{89-103}$	KFDL**KVTEPAPPE**KA	4.80	0-03-029
I-A^b	Mybcp3$_{90-104}$	FDLKV**TEPAPPEKA**E	4.79	0-03-030
I-A^b	Mybcp3$_{101-115}$	EKAES**EVAPGAPEE**V	9.90	0-03-031
I-A^b	Mybcp3$_{104-118}$	ESE**VAPGAPEEV**PAP	8.20	0-03-032
I-A^b	Mybcp3$_{108-122}$	AP**GAPEEVPAP**ATEL	8.25	0-03-033
I-A^b	Mybcp3$_{109-124}$	PGAPE**EVPAPATEL**EE	8.84	0-03-034
I-A^b	Mybcp3$_{166-180}$	VGG**SIVFSARVA**GAS	5.53	0-03-035

I-A^b	Mybcp3$_{168-182}$	GSIV**FSARVAGAS**LL	3.73	0-03-036
I-A^b	Mybcp3$_{169-183}$	SIVFS**ARVAGASLL**K	3.73	0-03-037
I-A^b	Mybcp3$_{403-417}$	GSK**YIFESVGAK**RTL	8.27	0-03-038
I-A^b	Mybcp3$_{404-418}$	SKYI**FESVGAKRT**LT	8.16	0-03-039
I-A^b	Mybcp3$_{682-696}$	TVTQG**KKASAGPHP**D	9.06	0-03-040
I-A^b	Mybcp3$_{685-699}$	QGK**KASAGPHPD**APE	5.99	0-03-041
I-A^b	Mybcp3$_{739-753}$	KEDE**GVYTVTVKN**PV	6.99	0-03-042
I-A^b	Mybcp3$_{741-755}$	DEGV**YTVTVKNPV**GE	6.38	0-03-043
I-A^b	Mybcp3$_{763-777}$	KV**IDVPDAPAA**PKIS	4.91	0-03-044
I-A^b	Mybcp3$_{765-779}$	IDVP**DAPAAPKIS**NV	5.26	0-03-045
I-A^b	Mybcp3$_{788-802}$	WEP**PAYDGGQPV**LGY	6.90	0-03-046
I-A^b	Mybcp3$_{838-852}$	YE**MRVYAVNAV**G(MSR)	9.66	0-03-047
I-A^b	Mybcp3$_{840-854}$	MRV**YAVNAVGMS**RPS	8.05	0-03-048
I-A^b	Mybcp3$_{842-856}$	VYAV**NAVGMSRPS**PA	4.37	0-03-049
I-A^b	Mybcp3$_{845-859}$	VNA**VGMSRPSPA**SQP	2.51	0-03-050
I-A^b	Mybcp3$_{849-863}$	GM**SRPSPASQP**FMPI	8.45	0-03-051
I-A^b	Mybcp3$_{854-868}$	SPAS**QPFMPIGPP**GE	4.86	0-03-052
I-A^b	Mybcp3$_{857-871}$	SQP**FMPIGPPGE**PTH	4.04	0-03-053
I-A^b	Mybcp3$_{940-954}$	VRAHN**VAGPGGPIV**T	5.96	0-03-054
I-A^b	Mybcp3$_{1158-1172}$	RPGIT**YEPPKYKAL**D	9.62	0-03-055
I-A^b	Mybcp3$_{1157-1171}$	PRPG**ITYEPPKYK**AL	9.67	0-03-056
I-A^b	Mybcp3$_{1173-1187}$	FSEA**PSFTQPLAN**RS	1.40	0-03-057
I-A^b	Mybcp3$_{1169-1183}$	KALD**FSEAPSFTQ**PL	9.30	0-03-058
I-A^b	Mybcp3$_{1170-1184}$	ALDFS**EAPSFTQPL**A	9.73	0-03-059
I-A^b	Mybcp3$_{1176-1190}$	APS**FTQPLANRS**IIA	2.29	0-03-060
MYHCA				
I-A^b	Myh6$_{109-127}$	AAW**MIYTYSGLFCVTV**NP	6.64	0-04-061
I-A^b	Myh6$_{122-142}$	VTVNP**YKWLPVYNA**EVVAAY	7.45	0-04-062
I-A^b	Myh6$_{186-206}$	VNTKRV**IQYFASIAA**IGDRSK	4.16	0-04-063
I-A^b	Myh6$_{216-233}$	TLED**QIIQANPAL**EAFGN	7.14	0-04-064
I-A^b	Myh6$_{247-265}$	FIRIH**FGATGKLAS**ADIE	5.98	0-04-065
I-A^b	Myh6$_{305-323}$	NNP**YDYAFVSQGEVSV**AS	6.72	0-04-066
I-A^b	Myh6$_{345-369}$	EKA**GVYKLTGAI**MHYGNM	6.79	0-04-067
I-A^b	Myh6$_{416-435}$	SVQQV**YYSIGALAK**SVYEK	3.24	0-04-068
I-A^b	Myh6$_{431-451}$	SVYEKM**FNWMVTRIN**ATLETK	4.47	0-04-069
I-A^b	Myh6$_{718-732}$	GDFR**QRYRILNPA**AI	2.13	0-04-070
I-A^b	Myh6$_{719-738}$	DFRQR**YRILNPAAI**PEGQFI	1.77	0-04-071
I-A^b	Myh6$_{1430-1444}$	LM**VDVERSNAA**AAAL	9.37	0-04-072
I-A^b	Myh6$_{1431-1445}$	MVDV**ERSNAAAAA**LD	9.72	0-04-073
MYL2				
I-A^b	Myl2$_{133-147}$	EEIDQ**MFAAFPPDV**T	7.42	0-05-174
I-A^b	Myl2$_{133-151}$	EEIDQM**FAAFPPDVT**GNL	6.17	0-05-175
TNNI3				
I-A^b	Tnni3$_{4-18}$	ESS**DAAGEPQPA**PAP	8.64	0-06-176

I-A^b	Tnni3$_{5-22}$	SSDAA**GEPQPAPAP**VRRR	6.34	0-06-177
I-A^b	Tnni3$_{22-36}$	RSSAN**YRAYATEPH**A	5.21	0-06-178
I-A^b	Tnni3$_{23-41}$	SSANY**RAYATEPHA**KKKSK	3.72	0-06-179
TNNT2				
I-A^b	Tnnt2$_{77-91}$	PKP**SRLFMPNLV**PPK	3.48	0-07-180
I-A^b	Tnnt2$_{78-92}$	KPSRL**FMPNLVPPK**I	3.51	0-07-181
HSPB3				
I-A^b	Hspb3$_{28-61}$	C**RLDHTLYALPGPTIE**DLSK	0.91	0-08-182
HSPA1A				
I-A^b	Hspa1a $_{129-147}$	EI**AEAYLGHPVTNAV**ITVP	3.79	0-09-182
I-A^b	Hspa1a $_{169-186}$	V**LRIINEPTAAAIA**YGLD	2.50	0-09-183
I-A^b	Hspa1a $_{365-380}$	PDE**AVAYGAAVQAAI**L	2.33	0-09-184
I-A^b	Hspa1a $_{438-452}$	VLI**QVYEGERAM**TRD	9.55	0-09-185
I-A^b	Hspa1a $_{453-474}$	NNLL**GRFELSGIPPAPRGV**PQI	1.47	0-09-186
I-A^b	Hspa1a $_{539-555}$	KNALE**SYAFNMKSAV**ED	2.66	0-09-187
I-A^b	Hspa1a $_{605-621}$	PIIS**GLYQGAGAPGA**GG	0.43	0-09-188
I-A^b	Hspa1a $_{616-638}$	APG**AGGFGAQAPKGASGSGPT**IE	5.88	0-09-189
FGA				
I-A^b	Fiba $_{110-124}$	IMEY**LRGDFANAN**NF	8.85	
I-A^b	Fiba $_{217-231}$	KD**RQYLPALKMSP**VP	8.15	
I-A^b	Fiba $_{284-298}$	RGD**FATRGPGSKAE**N	8.45	
I-A^b	Fiba $_{345-359}$	SDS**GNFRPANPN**WGV	3.45	
I-A^b	Fiba $_{358-372}$	GV**FSEFGDSSSPAT**R	7.35	
I-A^b	Fiba $_{370-384}$	ATR**KEYHTGKAV**TSK	5.25	
I-A^b	Fiba $_{500-514}$	SS**HVPEFSSSS**KTST	8.80	
I-A^b	Fiba $_{568-582}$	NGI**FSIKPPGSSKV**F	3.96	
I-A^b	Fiba $_{727-741}$	GGG**WWYNSCQAA**NLN	7.05	
FGB				
I-A^b	Fibb $_{44-58}$	EEPP**SLRPAPPPIS**G	2.15	
I-A^b	Fibb $_{57-71}$	S**GGGYRARPAKATAN**	0.10	
I-A^b	Fibb $_{285-299}$	KWDP**YKKGFGNIA**TN	8.20	
I-A^b	Fibb $_{360-374}$	VSV**NKYKGTAGNAL**M	2.40	
I-A^b	Fibb $_{420-434}$	GG**WWYNRCHAA**NPNG	9.95	
FGG				
I-A^b	Fibg $_{14-28}$	CLL**LLFSPTGLAYV**A	8.40	
I-A^b	Fibg $_{188-202}$	ESG**LYFIRPLKA**KQQ	9.10	
I-A^b	Fibg $_{373-387}$	**YHQGGTYSKSSTT**NG	8.95	

* Experimental evidence

10.2. Abbreviations

°C	Degrees Celsius
Ab	Antibody
ACTC1	Actin alpha 1, cardiac isoform
ADRB1	Adrenoceptor Beta 1
Ag	Antigen
ANOVA	Analysis of variance
APC	Antigen presenting cell
BSA	Bovine Serum albumin
BSS	Balanced salt solution
CD	Cluster of differentiation
CFA	Freud's complete adjuvant
DC	Dendritic Cell
DZHI	Deutsches Zentrum für Herzinsuffizienz
ELISA	Enzyme-linked immunosorbent assay
EMI	Experimetal myocardial infarction
et al.	et alteri
FACS	Fluorescence activated cell sorting
FC	Fragment crystallizable
FCS	Fetal Calf Serum
Fga	Fibrinogen-alpha chain
Fgb	Fibrinogen-beta chain
Fgg	Fibrinogen-gamma chain
Fig.	Figure
FoxP3	Forkhead Box Protein 3
h	Hour
HE	Hematoxylin and Eosin
HRP	Horseradish peroxidase streptavidin
HSC	Hematopoietic stem cell
Hsp	Heat shock protein
Hspb3	Heat-shock protein 27
Hspa1a	Heat-shock protein 72
Ig	Immunoglobulin
IL	Interleukin
INF-γ	Interferon Gamma
IU	International units
L	ligand
LN	Lymph node
Log	Logarithm
LPS	Lipopolysaccharide
Ly6C	Lymphocyte antigen 6 complex, locus C
Ly6G	Lymphocyte antigen 6 complex, locus G
med	Mediastinal
mg	Milligram

MHC	Major histocompatibility complex
Mhl2	Myosin light chain 2 (ventricular)
MI	Myocardial infarction
min	Minute
ml	Milliliter
mM	Milli Mol
MYBPC3	Myosin binding protein C. cardiac
Myh6	Myosin heavy chain 6, cardiac muscle isoform
Myh7	Myosin heavy chain 7, skeletal muscle isoform
Myhc	Myosin heavy chain
OVA	Ovalbumin
PBS	Phosphate buffered saline
pTreg	Peripheral, induced regulatory T cell
sec	Seconds
SEM	Standard Error of mean
SPF	Specific pathogen free
TCM	Central memory T cell
Tconv	Conventional T cell
TCR	T cell receptor
TEM	Effector memory T cell
TGF-β	Transforming growth factor beta (β)
Th	T helper cell
TLR	Toll-like Receptor
TNFα	Tumor necrosis factor α
Tnni3	Troponin I type 3, cardiac isoform
Tnnt2	Troponin T type 2, cardiac isoform
Treg	Regulatory T cell
TRM	Tissue resident memory T cell
tTreg	Thymus derived, naturally occurring, regulatory T cell
TVA	Tierversuchsantrag
U.S.	United states
vs.	Versus
WT	Wild type
µg	Microgram
µl	Microliter

10.3. Acknowledgements

The development of this thesis was conducted in the University Hospital Würzburg and the Comprehensive Heart Failure Center Würzburg and would not have been possible without the help and support of the following people.

First, I am very thankful to my doctoral supervisor Professor Dr. Stefan Frantz, who was the first one to motivate me to explore my interest in research and the field of immunocardiology. Thank you also to Dr. Gustavo Ramos, who was there from the first to the last minute, showing me that finding joy in my work is the best motivation to reach a successful outcome, especially when it comes to research.

Thank you to the members of my lab, particularly Elena Vogel, Andrea Leupold, Murilo Delgobo and Nils Hapke. With the latter, having a similar working field, we developed the standard methods used in this thesis while constantly exchanging about our data.

Thank you also to the DZHI and the Med I, giving me the possibility and the structural background for my thesis.

Many thanks go out to PD Dr. Ulrich Hofmann, who was there when I needed any advice.

A great support was also the Deutsche Herzstiftung e.V., who endorsed me financially with the “Kaltenbach Doktorandenstipendium“.

Finally, I want to thank my family. Without them, constantly encouraging me, this thesis would not have been finished successfully. Especially my mother, Klaudia Gaal, a passionate pharmacologist, who basically started my research career by bringing me to her lab when I was just a baby, deserves a huge credit. Always having my back, being there for me no matter the cost, giving me the possibility of going to university and convincing me that there is nothing impossible for me to achieve. I also want to thank my late father, PD Dr. Johannes Gaal, who sparked the desire to become a doctor in me, and, who I would really wish to still be here with us today to enjoy moments like these. Last but not least I want to thank my partner Dominik, who no matter how many long hours I spent in the lab and how wrong some experiments went, always knew how to cheer me up and encourage me to continue and focus.

Again, thank you to all the numerous people involved with the development of this thesis, it would not have been possible without you.

10.4. Publications

Cardiac epitope mapping in the frame of myocardial infarction

***Gaal, C.**, Hapke, N., Heinrichs, M., Hofmann, U., Frantz, S., Ramos, G.C.*

(Abstract - DGK Jahrestagung 2019)

Myocardial infarction triggers cardioprotective antigen-specific T helper cell responses

*Rieckmann, M., **Gaal, C.**, …, Frantz, S., Hofmann, U., Ramos, G.C.*

(Journal of Clinical Investigation - 2019)

Defining a synovial fluid white blood cell count threshold to predict periprosthetic infection after shoulder arthroplasaty

*Streck, L.E., **Gaal, C.**, …, von Hertzberg-Bölch, S.P., Rueckl, K.*

(Journal of Clinical Medicine – December 23rd 2021)

Patient specific articulating spacer for the two stage exchange at the shoulder

*Streck, L.E., Rueckl, K., **Gaal, C.**, Achenbach, L. Dines, D., Rudert, M.*

(In Submission at Journal for Operative techniques: Orthopaedic traumatology)

Identification of a novel I-A(b)-restricted myosin antigen

***Gaal, C.,** …, Frantz, S., Ramos, G.C.*

(Just before Submission to European Journal of Immunology)

10.5. Oral presentations

The Kami Study – Kardiale Antigene nach MI

***Gaal, C.**, Hapke, N., Ramos, G.*

(Med. Klinik I Retreat, Universitätsklinikum Würzburg 2018)

Cardiac antigens in MI

***Gaal, C.**, Hapke, N.*

(Med. Klinik I Retreat, Universitätsklinikum Würzburg 2019)

10.6. Poster presentations

Mapping cardiac antigens after myocardial infarction

***Gaal, C.**, Hapke, N.*

(DZHI Retreat 2018)

Cardiac epitope mapping in the frame of myocardial infarction

***Gaal, C.**, Hapke, N., Heinrichs, M., Hofmann, U., Frantz, S., Ramos, G.*

(DGK Jahrestagung 2019)